Cable-Stay Strand Residual Strength Related to Security Threats

U.S. Department of Transportation
Federal Highway Administration

Research, Development, and Technology
Turner-Fairbank Highway Research Center
6300 Georgetown Pike
McLean, VA 22101-2296

FOREWORD

This report documents tensile testing of selected seven-wire strands and individual wires of strands that were damaged during cable-stay bundle protection system qualification. The qualification testing was performed to assess the adequacy of protection systems applied over the stay bundle against terroristic threats of blast and thermal cutting. The qualification used a primary acceptance criterion of 75 percent survival of wires. After the testing was performed, it was questioned if certain wires survived sufficiently despite being intact and, in particular, whether wires with nicks, gouges, kinks, or untwisted strands should be considered fully or partially damaged. The tensile testing assessed the residual capacity of strands and wires in various states of damage, attempting to answer these questions while evaluating the qualification results. The results showed that, in terms of blast, the residual strength was not correlated to magnitude of damage (e.g., degree of curvature, impact gouges, or untwisting), and rather the overall strength of the strands uniformly decreased by 5 percent. In terms of thermal cutting, the residual strength was greatly affected by the amount of heat to which the strand was subjected.

The results attained were useful to the bridge owner who performed the qualification testing, and it is expected these results will be very beneficial to other bridge owners who must define protection scheme qualification acceptance criteria for future cable-supported structures. This report will benefit those who oversee qualification testing of cables used on cable-supported bridges, including State transportation departments, bridge design consultants, and cable suppliers who manufacture suspension cables and stays and their protection measures.

<div align="right">

Cheryl Allen Richter, Ph.D., P.E.
Director, Office of Infrastructure
Research and Development

</div>

TECHNICAL REPORT DOCUMENTATION PAGE

1. Report No. FHWA-HRT-17-109	2. Government Accession No.	3. Recipient's Catalog No.	
4. Title and Subtitle Cable-Stay Strand Residual Strength Related to Security Threats		5. Report Date January 2018	
		6. Performing Organization Code:	
7. Author(s) Justin Ocel, Ph.D, P.E.; Jason Provines, P.E.; Vince Charito, P.E.		8. Performing Organization Report No.	
9. Performing Organization Name and Address Bridge and Foundation Engineering Team Office of Infrastructure Research and Development Federal Highway Administration 6300 Georgetown Pike McLean, VA 22101-2296		10. Work Unit No.	
		11. Contract or Grant No. DTFH61-10-D-00017	
12. Sponsoring Agency Name and Address Office of Infrastructure Research and Development Federal Highway Administration 6300 Georgetown Pike McLean, VA 22101-2296		13. Type of Report and Period Covered Final Report; June 2016–May 2017	
		14. Sponsoring Agency Code HRDI-40	
15. Supplementary Notes This project was undertaken as part of an Accident and Terrorist Vulnerability Assessment (ATVA) of a particular bridge partially paid for under the Federal-Aid Program. The U.S. Army Corps of Engineers was a consultant to the bridge owner and devised this research project in support of the ATVA. The testing was conducted in Federal Highway Administration's Turner–Fairbank Highway Research Center Structures Laboratory. The Contracting Officer's Representative for work performed by the contractors was Fassil Beshah (HRDI-40).			
16. Abstract Cable-stay bridge designs are an economical bridge type for long spans. However, long-span bridges also tend to be signature spans and often serve as critical freight corridors and/or critical lifeline structures. As such, it is prudent to consider terroristic threats against these assets and strengthen cable-stay bridges to minimize vulnerabilities. The stays are a critical element in the cable-stay design that should be protected if they are easily accessible from roadways or walkways. The protection schemes applied over cable stays must be qualified based on performance criteria and judged to pass or fail based on agreed-upon acceptance criteria. This project was conducted in support of a particular bridge project where questions were raised after qualification testing regarding the acceptance criteria. One of the criteria was 75 percent survival of wires against blast and thermal-cutting threats. After the qualification testing, it became questionable whether a wire that was gouged, nicked, or bent should be considered to have survived. The testing reported in this report assessed the residual strength of individual wires and strands in various states of damage. For blast, no correlation in strength could be identified against any of the damage metrics, though generally the entire population tested had an overall reduction in strength of 5 percent over new strands. As for the thermal cutting, gouges were quite detrimental, along with exposure to heat. The exposure to heat could easily be visually inspected based on the presence of the polyethylene coating or grease on the strands, though this was a coarse measure. A better means of assessing heat damage was through destructive hardness testing. It was found that strength did not degrade unless the strands were exposed to temperatures of more than 900 °F.			
17. Key Words Cable bundles, cable-stay bridge, terrorist threats, thermal cutting, blast design, threat protection		18. Distribution Statement No restrictions. This document is available through the National Technical Information Service, Springfield, VA 22161. http://www.ntis.gov	
19. Security Classif. (of this report) Unclassified	20. Security Classif. (of this page) Unclassified	21. No. of Pages 100	22. Price N/A

Form DOT F 1700.7 (8–72)   Reproduction of completed page authorized.

SI* (MODERN METRIC) CONVERSION FACTORS

APPROXIMATE CONVERSIONS TO SI UNITS

Symbol	When You Know	Multiply By	To Find	Symbol
LENGTH				
in	inches	25.4	millimeters	mm
ft	feet	0.305	meters	m
yd	yards	0.914	meters	m
mi	miles	1.61	kilometers	km
AREA				
in^2	square inches	645.2	square millimeters	mm^2
ft^2	square feet	0.093	square meters	m^2
yd^2	square yard	0.836	square meters	m^2
ac	acres	0.405	hectares	ha
mi^2	square miles	2.59	square kilometers	km^2
VOLUME				
fl oz	fluid ounces	29.57	milliliters	mL
gal	gallons	3.785	liters	L
ft^3	cubic feet	0.028	cubic meters	m^3
yd^3	cubic yards	0.765	cubic meters	m^3
NOTE: volumes greater than 1000 L shall be shown in m^3				
MASS				
oz	ounces	28.35	grams	g
lb	pounds	0.454	kilograms	kg
T	short tons (2000 lb)	0.907	megagrams (or "metric ton")	Mg (or "t")
TEMPERATURE (exact degrees)				
^oF	Fahrenheit	5 (F-32)/9 or (F-32)/1.8	Celsius	^oC
ILLUMINATION				
fc	foot-candles	10.76	lux	lx
fl	foot-Lamberts	3.426	candela/m^2	cd/m^2
FORCE and PRESSURE or STRESS				
lbf	poundforce	4.45	newtons	N
lbf/in^2	poundforce per square inch	6.89	kilopascals	kPa

APPROXIMATE CONVERSIONS FROM SI UNITS

Symbol	When You Know	Multiply By	To Find	Symbol
LENGTH				
mm	millimeters	0.039	inches	in
m	meters	3.28	feet	ft
m	meters	1.09	yards	yd
km	kilometers	0.621	miles	mi
AREA				
mm^2	square millimeters	0.0016	square inches	in^2
m^2	square meters	10.764	square feet	ft^2
m^2	square meters	1.195	square yards	yd^2
ha	hectares	2.47	acres	ac
km^2	square kilometers	0.386	square miles	mi^2
VOLUME				
mL	milliliters	0.034	fluid ounces	fl oz
L	liters	0.264	gallons	gal
m^3	cubic meters	35.314	cubic feet	ft^3
m^3	cubic meters	1.307	cubic yards	yd^3
MASS				
g	grams	0.035	ounces	oz
kg	kilograms	2.202	pounds	lb
Mg (or "t")	megagrams (or "metric ton")	1.103	short tons (2000 lb)	T
TEMPERATURE (exact degrees)				
^oC	Celsius	1.8C+32	Fahrenheit	^oF
ILLUMINATION				
lx	lux	0.0929	foot-candles	fc
cd/m^2	candela/m^2	0.2919	foot-Lamberts	fl
FORCE and PRESSURE or STRESS				
N	newtons	0.225	poundforce	lbf
kPa	kilopascals	0.145	poundforce per square inch	lbf/in^2

* SI is the symbol for the International System of Units. Appropriate rounding should be made to comply with Section 4 of ASTM E380.
(Revised March 2003)

TABLE OF CONTENTS

LIST OF FIGURES

LIST OF TABLES

LIST OF ABBREVIATIONS

ATVA	Accident and Terrorist Vulnerability Assessment
AUTS	actual ultimate tensile strength
COV	coefficient of variation
DIC	digital image correlation
FBC	full birdcage
FHWA	Federal Highway Administration
HAZ	heat-affected zone
HDPE	high-density polyethylene
HV	Vickers hardness
IBC	incipient birdcage
PTI	Post-Tensioning Institute

INTRODUCTION

The terrorist threat to U.S. bridges is believed to be very credible, and costs for reconstruction and socioeconomic losses from these threats are potentially in the billions of dollars.[1] The time to address protection measures, especially for new bridges, is during the design stage to produce cost-effective protection, as this is more economical than retrofitting later. Cables of cable-supported bridge designs are subject to extra scrutiny because the cable bundles supporting the bridges can come close to the roadways or pedestrian walkways and may be easily accessible. An Accident and Terrorist Vulnerability Assessment (ATVA) is usually part of the planning and design process for these types of important structures to understand how to best incorporate effective strategies. Part of the ATVA includes establishing performance criteria for protection measures against various threats. However, to date, these performance measures have been developed in an ad hoc fashion based on group consensus with limited uniformity across the nation.

In the summer of 2016, the Federal Highway Administration (FHWA) received numerous mockup cable-stay bundles that were subjected to various threats as part of the qualification of a cable protection system. This report does not discuss the specific bridge project for which this qualification testing was performed, nor does it discuss the design of the protection system that was applied over the cable bundles. However, the qualification testing was performed against the threats of fire, ballistics, blast, and cutting tests. Based on the consensus of subject matter experts and the bridge owner, it was determined that acceptance of these performance tests would be 75 percent survival of wires within a bundle using just visual assessment. After observing the various qualification tests, it became obvious there were some challenges with the agreed-upon acceptance criteria, including the following:

- The evaluation of visual damage. A wire was considered ineffective if, in addition to being completely severed, it had any abrasions, nicks, or gouges. Strands that had started to untwist were considered completely damaged. This was based on conservative assumptions, but it was recognized that wires or strands in these partially damaged states may have some reserve strength.

- The evaluation of heat damage. The fire testing subjected cable bundles to heat without a tension load in the bundle. Visual inspection of the cables does not identify the possible changes to material properties that may have occurred due to heat exposure.

OBJECTIVE

The objective of this project was to conduct tensile testing of individual strands from cable-stay bundle qualification tests to assess the change in mechanical properties that may have occurred as a result of the various types of threats. Additionally, assessments of deformation, hardness, and metallography were conducted to determine if these simpler measurement parameters could be correlated to a change in material properties.

BUNDLE DESCRIPTION

Qualification tests were completed on 43-strand and 109-strand bundles. Subsequently, the bundles were provided to FHWA for supplemental testing. All bundles were constructed from 0.62-inch-diameter strands meeting the ASTM A416 specification.[2] All the strands were greased and sheathed in high-density polyethylene (HDPE). While multiple threats were considered for the qualification testing, only bundles that were subjected to certain blast and thermal-cutting scenarios were assessed through the supplemental testing described in this report.

Blast-Tested Bundles

Four bundles subjected to blast were used in this project. Each bundle size (43-strand and 109-strand) was tested at two different standoff distances. Three of the bundles were no longer intact after the blast event; thus, only boxes of individual strands were received. Though the last bundle did remain intact, as pictured in figure 1, it was significantly deformed, and numerous wires were severed.

Source: FHWA.

Figure 1. Photo. Bundle subjected to a blast charge.

Thermal Lance Cut Bundle

One 43-strand bundle that had three different thermal-cutting tests applied to it was delivered. Two tests were performed with a thermal lance and one with an oxyacetylene torch. The notion behind the qualification test was to see how much damage could be done in a set amount of time. Very little damage was caused by the oxyacetylene torch; thus, only the thermal lance cuts were of interest. Figure 2 shows a picture of the bundle with closeups of the two individual thermal lance cuts, labeled "Cut A" and "Cut B."
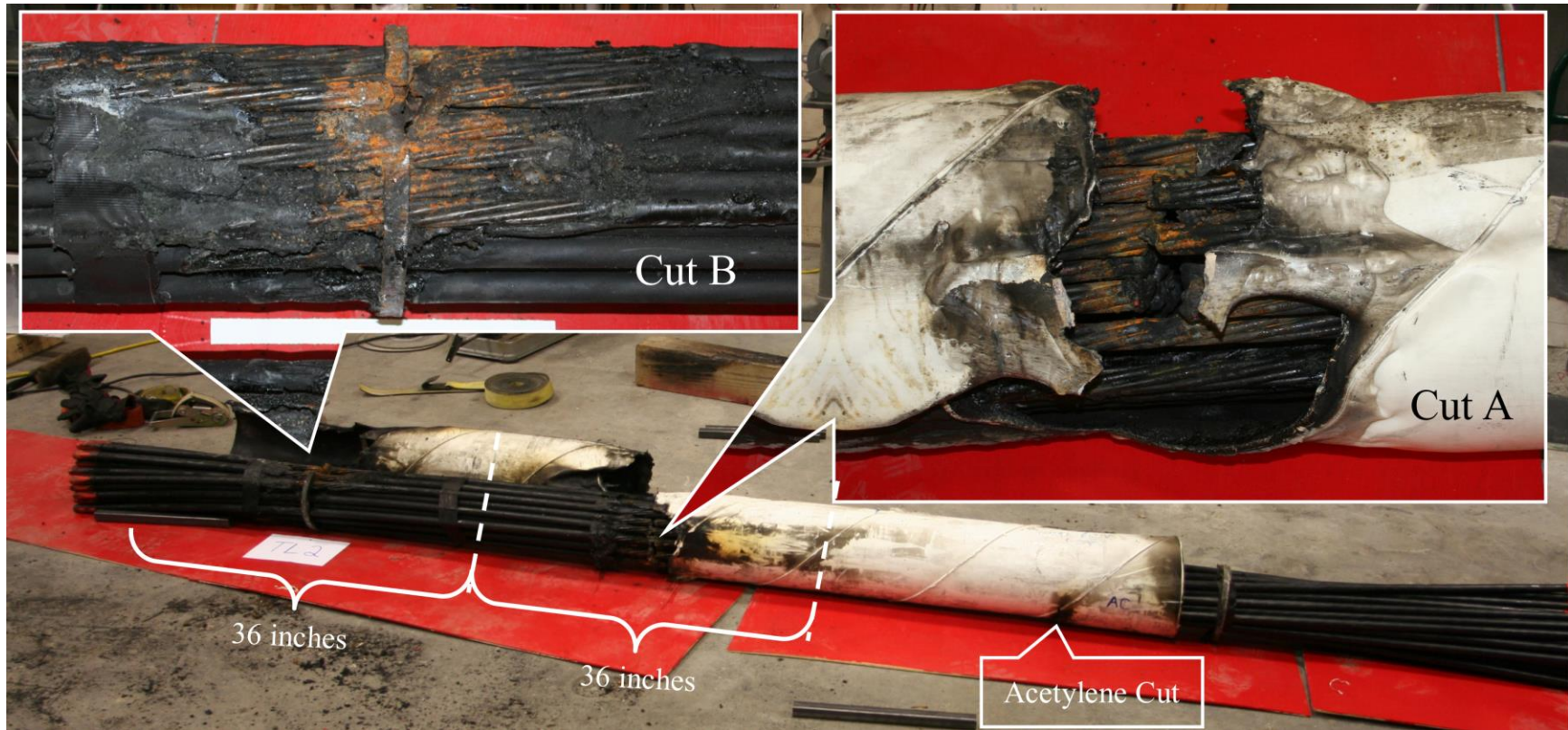
Source: FHWA.

Figure 2. Photo. Bundle subjected to thermal lance tests.

DOCUMENTATION

The condition of each individual strand was documented before any destructive testing was performed. This included disassembling the bundles if they were intact, recording the type and severity of visual damage, and photographing the strands from the blast bundles. This chapter discusses the methods used to document the visual condition of strands retrieved from the thermal lance bundle and select blast bundles of interest and the data that were collected from that effort.

THERMAL LANCE CUT BUNDLE

The bundle was cut into three sections that isolated each of the two thermal lance cuts into roughly 36-inch-long segments. Each segment was centered around each of the two thermal lance zones, as noted in figure 2. The strand ends were numbered to facilitate mapping damage throughout the cross section of the bundle. Due to the large amount of heat input from cutting with the thermal lance, the bundle became a fused mass of melted steel and HDPE, and thus individual strands did not separate easily from the bundle. Separating the strands required effort using crowbars, utility knives, and reciprocating saws.

Figure 3 and figure 4 provide a map of the damage throughout the cross section for cut A. In both figures, each circle represents an individual strand, and the overall arrangement of circles represents the cross-sectional shape of the bundle. The top of each circle has an underlined alphanumeric code designating the strand and will be used to reference individual strands throughout this report. The letter in the alphanumeric code refers to a particular qualification test applied to a bundle, while the number refers to a strand within that bundle. In figure 3, the number shown at the bottom of each circle represents the number of cut wire(s) within that strand, and the color shading of each circle is also keyed to this value. A cut wire is defined as one that has been physically severed into two pieces. In figure 4, the number at the bottom of each circle represents the number of wire(s) with observed damage. In this case, damage is defined as a nick or gouge in an individual wire and not severed. Likewise, color shading of these circles is also linked to a color scale based on the number of damaged wires. Circles shaded black in figure 4 indicate strands that are completely severed and do not contribute separately to the total number of damaged wires. The damage distribution in figure 3 and figure 4 suggests that the thermal lance likely entered the right side of the bundle as depicted in the damage map and moved right to left as it cut through more and more strands.

Figure 5 and figure 6 present similar maps of severed and damaged wires for cut B. The extents of cut and damaged wires were much less for this cut, particularly as evident in figure 6. As shown in figure 2, cut B happened to coincide with the location of a bundle retaining plate, and this greatly impeded the thermal lance operator's ability to compromise the bundle. The same data on cut and damaged wires are replicated with histograms in figure 7 and figure 8, respectively, for cut A and cut B.

Tabulated data represented in figure 3 through figure 6 can be found in appendix A.
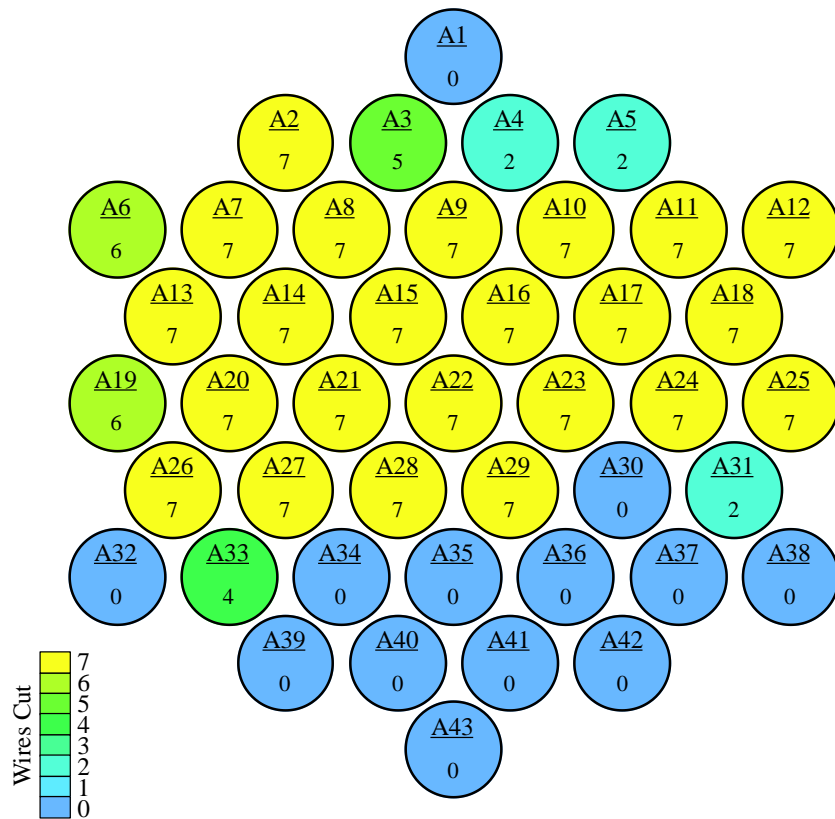
Figure 3. Bubble plot. Map of the number of cut wires in the cross section of thermal lance cut A.
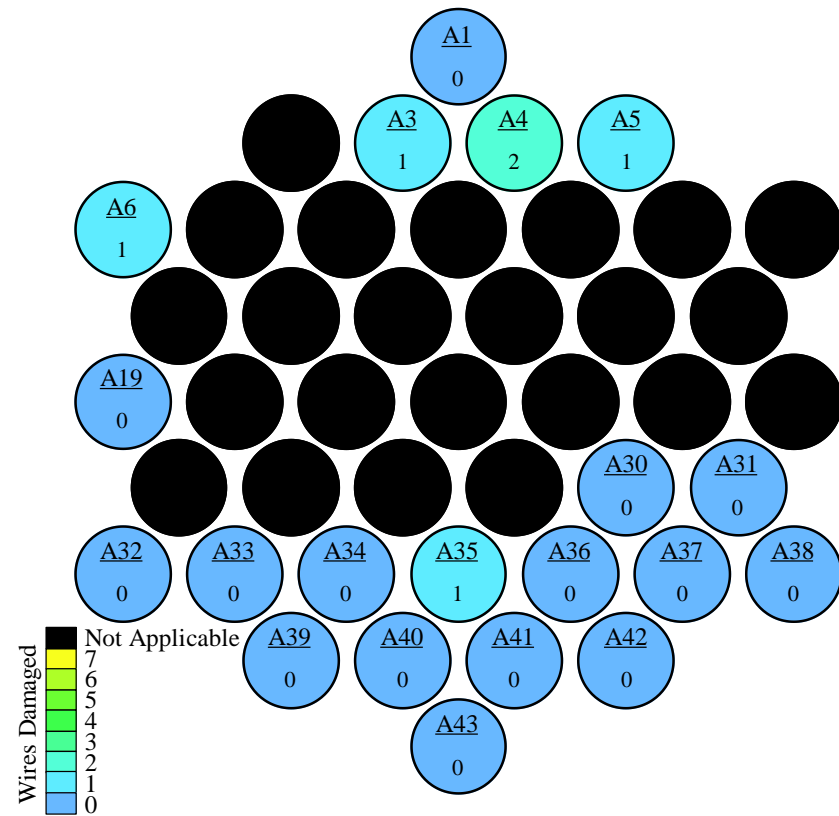
Figure 4. Bubble plot. Map of the number of damaged wires in the cross section of thermal lance cut A.
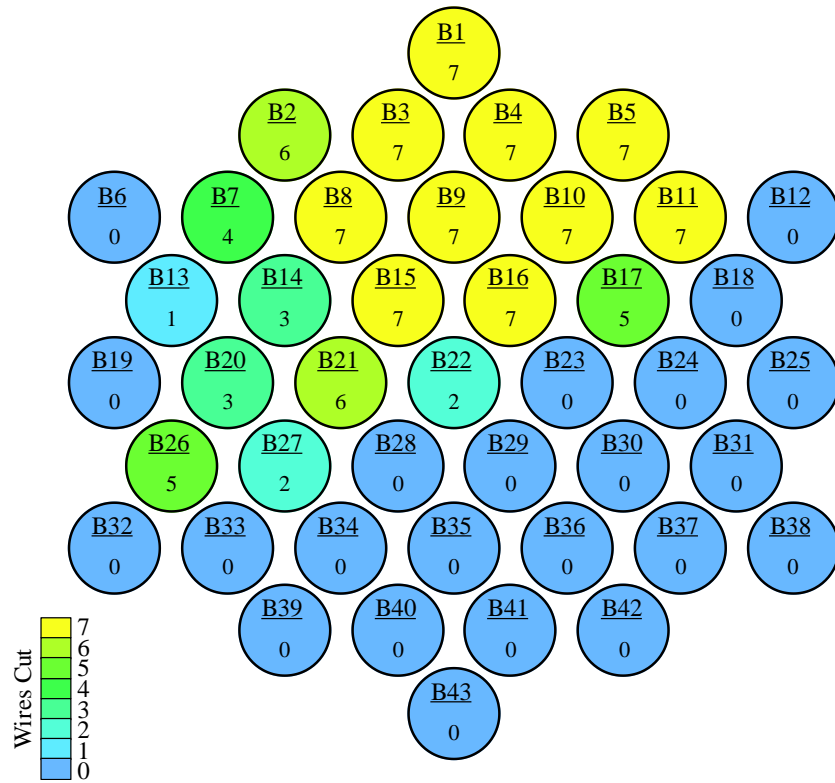
Figure 5. Bubble plot. Map of the number of cut wires in the cross section of thermal lance cut B.
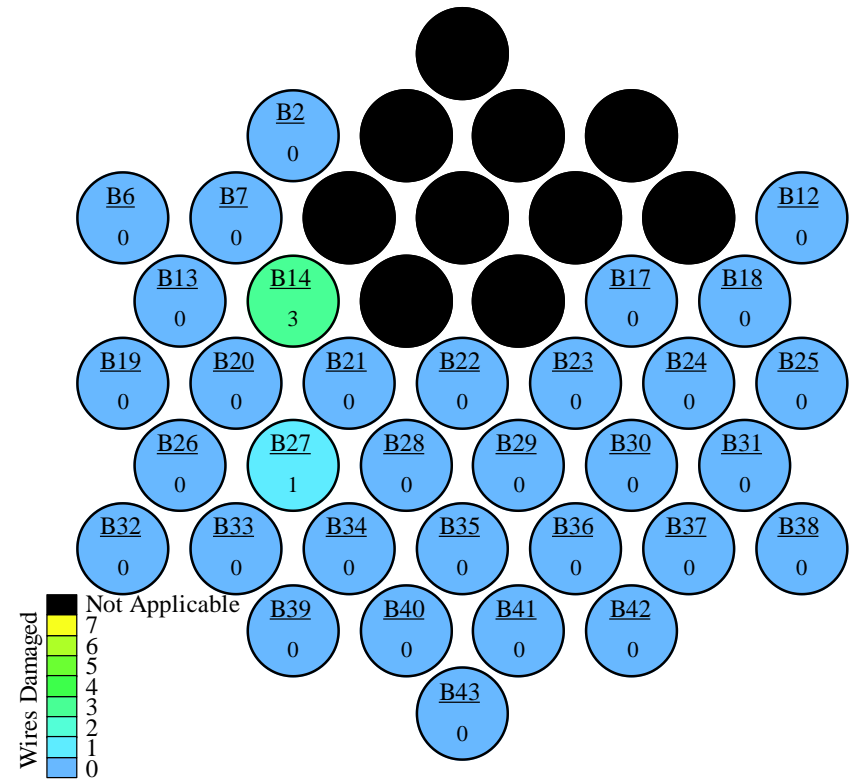
Figure 6. Bubble plot. Map of the number of damaged wires in the cross section of thermal lance cut B.
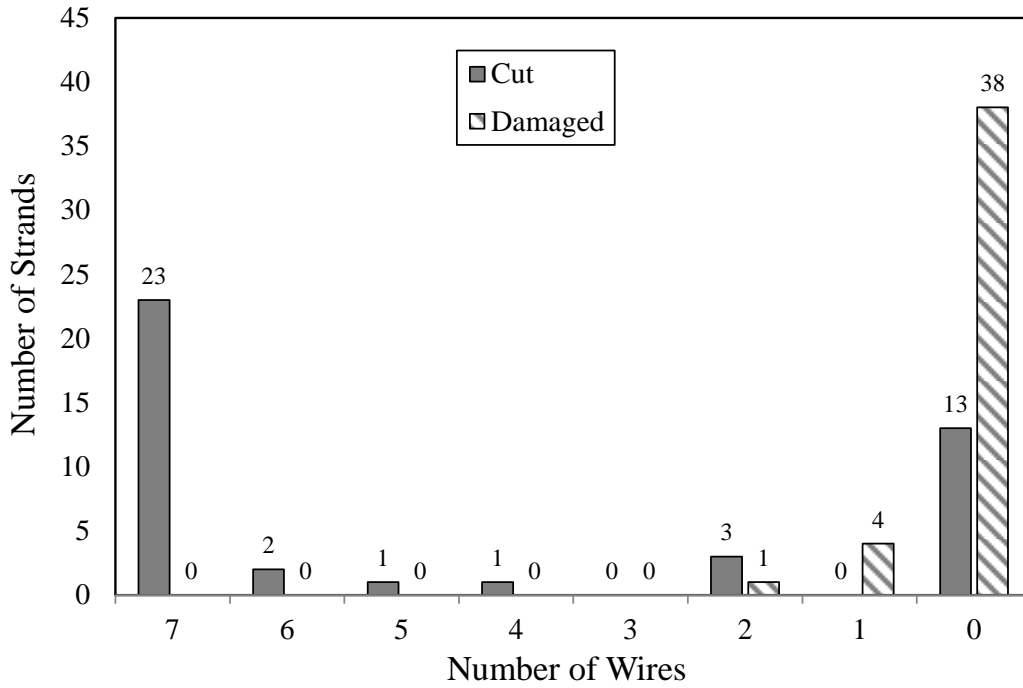
Source: FHWA.

Source: FHWA.

Figure 7. Histogram. Enumerated strands categorized by the number of cut and damaged wires in thermal lance cut A.
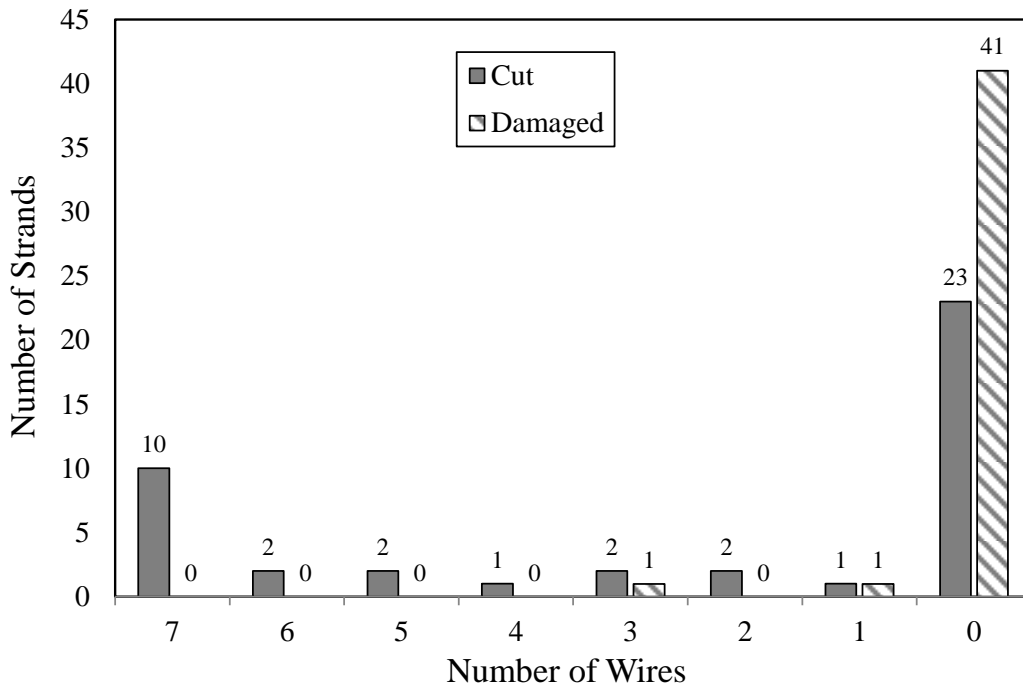
Source: FHWA.

Figure 8. Histogram. Enumerated strands categorized by the number of cut and damaged wires in thermal lance cut B.

BLAST BUNDLES

The four bundles subjected to blast are called "D," "E," "F," and "G." Bundles D and E were 43-strand bundles, and F and G were 109-strand bundles. The strands from bundles D, F, and G were not received as an intact bundle, so it was not possible to create a map of damage relative to the as-constructed bundle. Therefore, for these three bundles, only a histogram can be presented for cut and damaged wires. The term "cut" wires refers to those individual wires that were completely severed into two pieces from the blast event. This is consistent with the definition of cut wires identified after the thermal lance tests. Strands with cut wires were not of interest for further testing (because tension testing them would be difficult), and only strands with all seven wires intact were further categorized for damage. For strands with no wires cut, two levels of damage were assigned: incipient birdcage (IBC) and full birdcage (FBC). The term "birdcaging" refers to a general untwisting of the strand to the point where some wires are not touching each other. An IBC is when one wire has some visible separation from the others; an example is shown in figure 9. An FBC strand is when two or more wires have visible separation from the others; an extreme case is shown in figure 10 where all wires are not touching. If a strand had no cut wires and no signs of birdcaging, it was referred to as an "intact" strand.
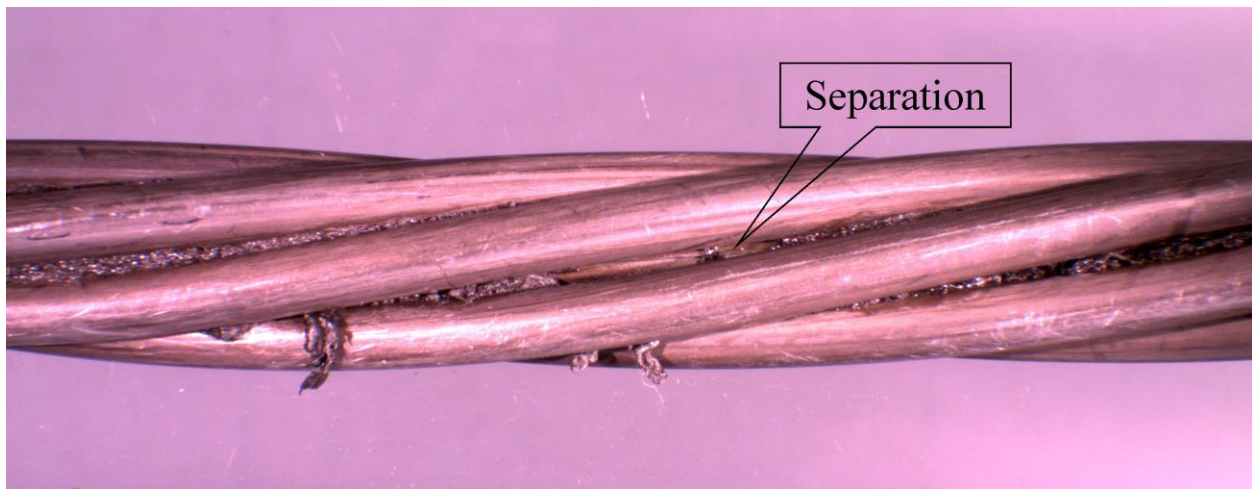
Source: FHWA.

Figure 9. Photo. Strand F38 showing IBC.

Source: FHWA.

Figure 10. Photo. Strand G2 showing FBC.

Figure 11 through figure 14 show histograms of cut and damaged wires for bundles D, E, F, and G, respectively. The number of intact strands is not shown in the bar charts, but it would merely be the number of strands with zero cut wires, minus all those with FBCs and IBCs. It must be

noted that bundle G was a 109-strand bundle, though adding up all the strands in figure 14 sums to only 107 because 2 strands were missing from the delivered bundle.
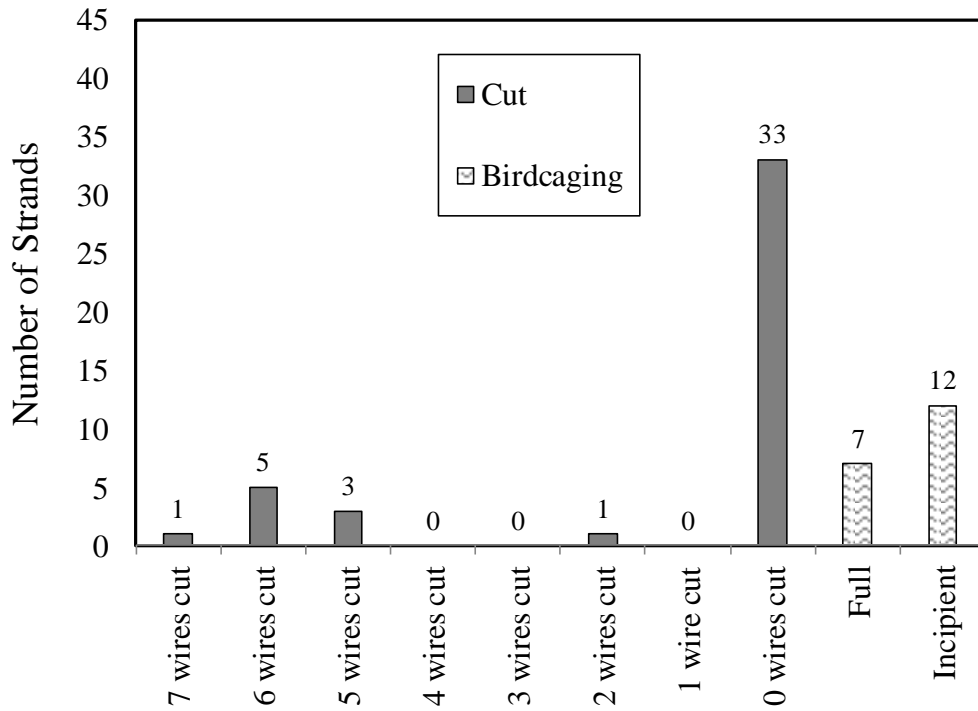
Source: FHWA.

Figure 11. Histogram. Enumerated strands categorized by the number of cut wires and number of birdcaged strands in blast test D.
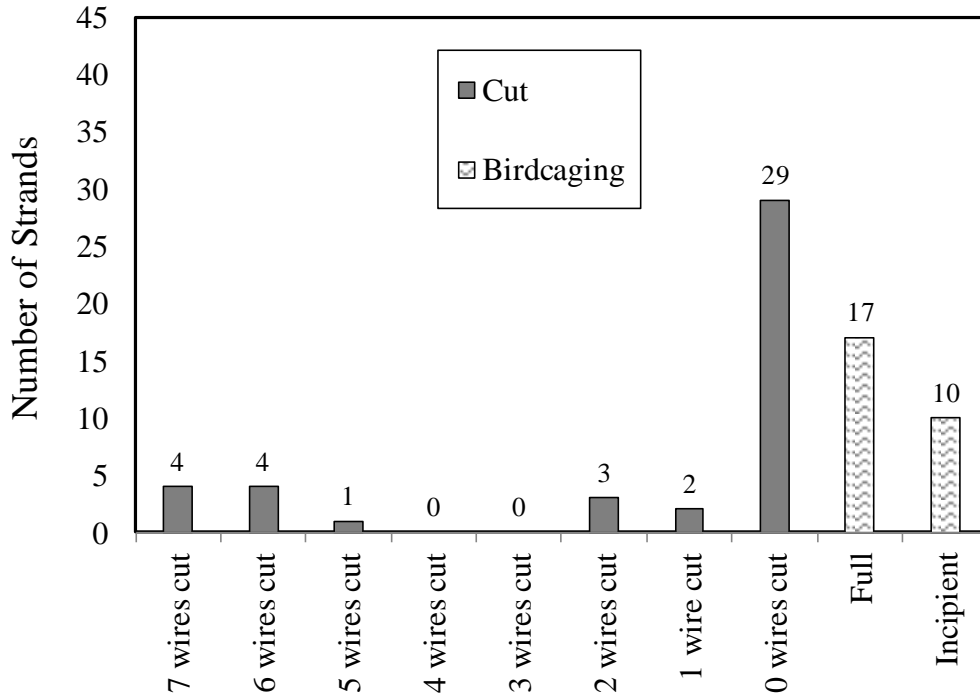
Figure 12. Histogram. Enumerated strands categorized by the number of cut wires and birdcaged strands of the bundle from blast test E.
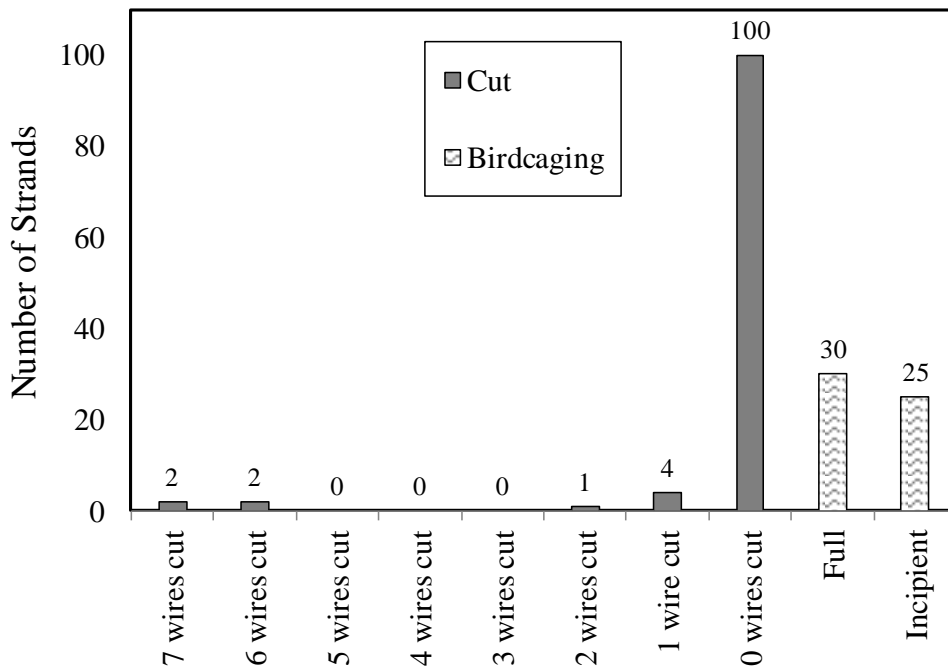
Figure 13. Histogram. Enumerated strands categorized by the number of cut wires and number of birdcaged strands in blast test F.
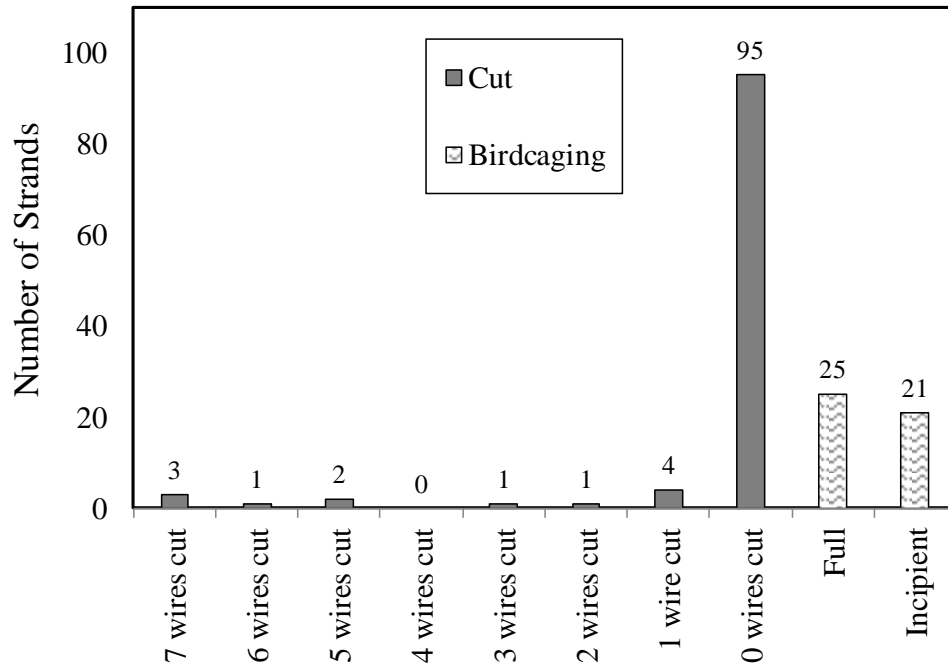
Figure 14. Histogram. Enumerated strands categorized by the number of cut wires and number of birdcaged strands in blast test G.

Bundle E remained intact after the blast event such that cut wires and strand damage could be mapped through the bundle cross section. Figure 15 and figure 16 show the maps of cut and damaged wires from bundle E; the maps were formed in the same manner as described in the "Thermal Lance Cut Bundle" section. Based on the cut wire map, it appears the explosive was centered above strand E1, since all cut wires were isolated within the top half of the bundle. The damaged strand map in figure 16 shades all strands that had cut wires with black, as further damage evaluation was not of concern. However, there was no clear trend on birdcage damage, as full and incipient strands seemed to occur throughout the remaining bundle cross section.
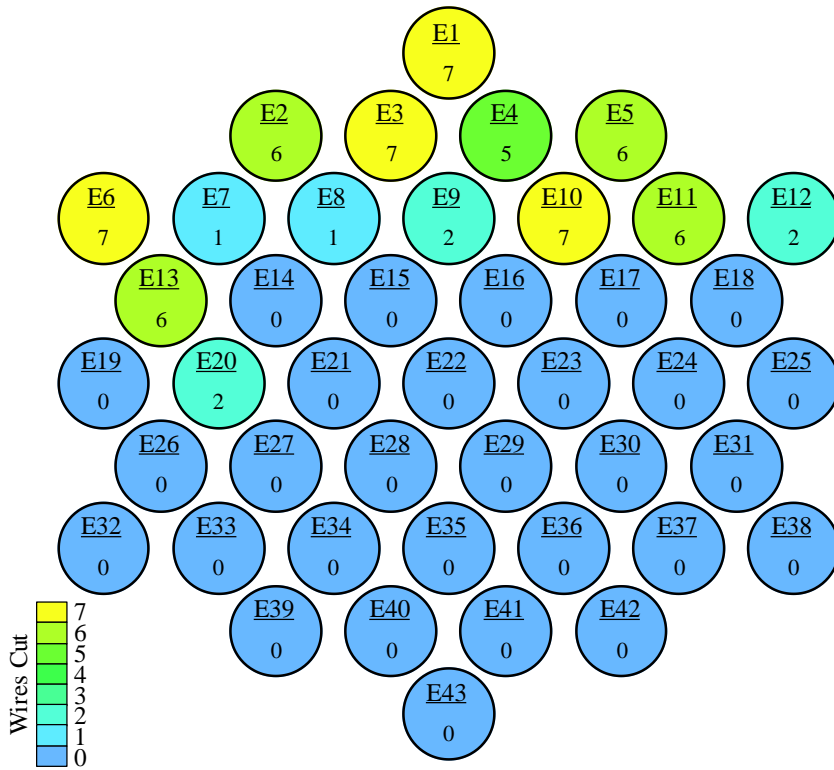
Figure 15. Bubble plot. Map of the number of cut wires near the center of the bundle from blast test E.
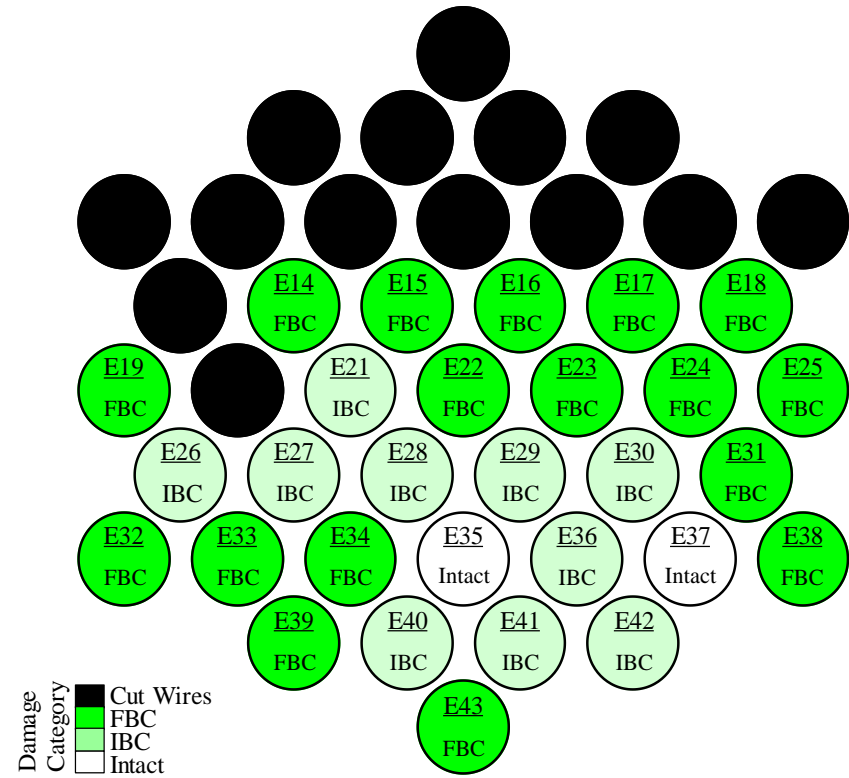
Source: FHWA.

Figure 16. Bubble plot. Map of the number of damaged strands near the center of the bundle from blast test E.

Source: FHWA.

As determined prior to the qualification testing, acceptance of these tests was based on no more than 25 percent loss of wires in a bundle. On a percentage basis, the number of cut wires in bundles D, E, F, and G was 17.9, 21.6, 4.2, and 6.1 percent, respectively, so based solely on these criteria, each of the blast bundles passed the qualification tests. However, after the testing was complete, the question arose as to whether or not a birdcaged strand should be considered to have full capacity. If birdcaging does indicate a reduction of strength, it is possible that the tests may not pass the qualification criteria, since some of the bundles contain a large population of birdcaged strands.

Curvature and Diameter of Strands

The photo of bundle E in figure 1 shows that, after the blast event, the strands are certainly left in a residual bent or kinked shape. One of the primary questions to be explored is, Does this additional cold working from the strand being bent, along with birdcaging, affect the residual strength of the strand? To answer this question, the deformations (curvature and diameter of the strand) of each strand were measured. To characterize curvature, a jig was fabricated to consistently measure the lateral and vertical deformation of the strand relative to a fixed plane along a 24-inch-long chord distance. As illustrated in figure 17, two aluminum angles, spaced with an out-to-out distance of 24 inches, were attached to a piece of plywood. A bent strand was laid on the plywood and put into contact with these two angles. In each blast test, a charge was placed near the center of the bundle along its length, around the outermost surface of a protection device encasing the strand bundle. Thus, assuming the maximum damage was most likely aligned with the charge position, the center of each individual strand was aligned to the middle of the 24-inch-chord distance. In the plane of the plywood, the lateral deformation was measured as the distance normal to the 24-inch chord to the strand (depicted in the plan view of figure 17). The vertical deformation was measured as the distance from the plywood to the center of the strand (depicted in the elevation view of figure 17).
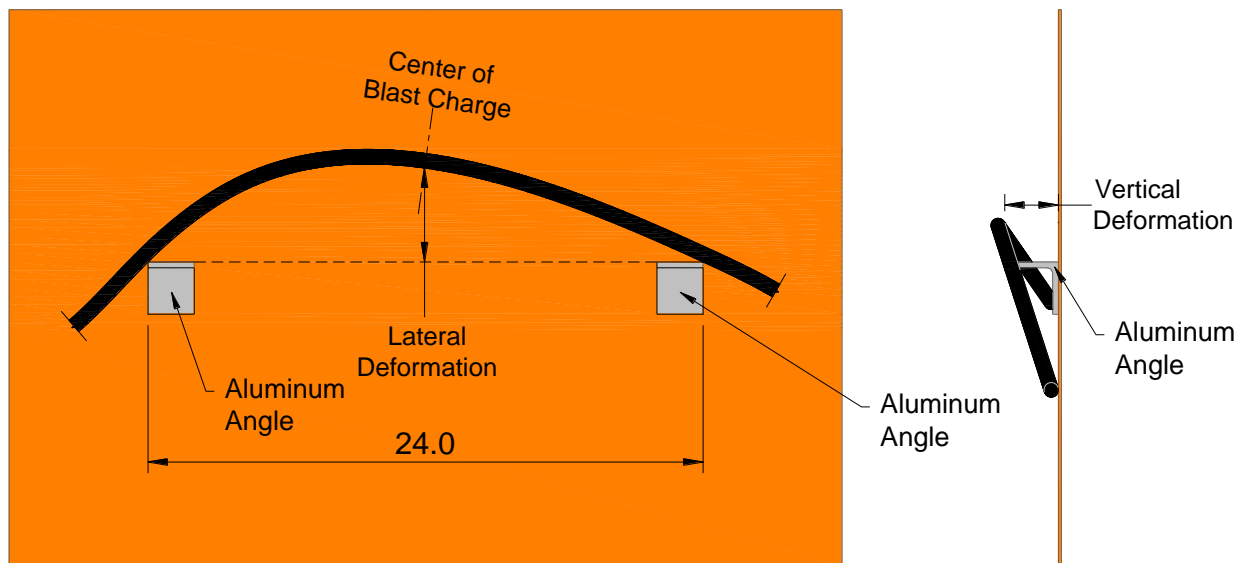
Source: FHWA.
Note: Units = inches.

Figure 17. Illustration. Measuring jig for strand curvature.

14

Unlike the lateral deformation, the vertical deformation did not necessarily capture vertical curvature within the 24-inch-chord distance. In some cases, the strand supported itself up off the plywood within the 24-inch chord, and in other cases, it supported itself at points completely off the plywood. Therefore, the vertical deformation does not depend on a specific length over which the overall deformation occurred, and the usefulness of this measurement may have little or no value in assessing strand damage; it is reported herein for completeness.

If a birdcaged strand was identified, the diameter at the midlength of that strand was measured with a circumferential tape. Since the birdcage did not necessarily occur at the exact center of the strand, the maximum observable diameter within the strand central region (not necessarily within the 24-inch-chord distance) was also measured. Typically, the blast event removed the HDPE cover from around the middle of the strand, revealing if a birdcage condition existed. No further effort was made to remove more of the HDPE cover, so it is possible that the maximum birdcage diameter could have been missed if it occurred elsewhere along the strand within intact portions of the HDPE cover. The likeliness of this was considered low, as the blast events tended to strip most of the HDPE from the center of the strand sampled for tension testing. The raw measurement data for both deformation and diameter are reported in appendix B for each bundle.

Each bundle investigated a different bundle size and standoff distance for evaluating the performance of the protection system. Damage that occurred from each test ranged from no visible damage to any wires in a strand to the severing of all seven wires in a strand. So, for this project, it was not necessary to categorize strand damage as a function of blast test—only to assess the residual strengths based on observed damage. Therefore, all the uncut (i.e., no wires cut) strands from tests D, E, F, and G were lumped together for selection of further testing. This is shown in figure 18 and figure 19. These plots show the variation between vertical deformation, lateral deformation, and birdcaging of strands. In general, FBC strands exhibited larger vertical and lateral deformations, with a maximum value of 3.5 inches. Intact strands showed the least amount of lateral deformation, generally not exceeding 1.5 inches. The IBC strands exhibited lateral deformations in between the measured deformations from the other two sets of categorical damage. The maximum measured diameter of a strand only indicated the severity of FBC. A virgin strand had a measured diameter of $^{40}/_{64}$ inch, and all intact and IBC strands had approximately this value. Most FBC strands had diameters ranging from $^{43}/_{64}$ to $^{68}/_{64}$ inch.
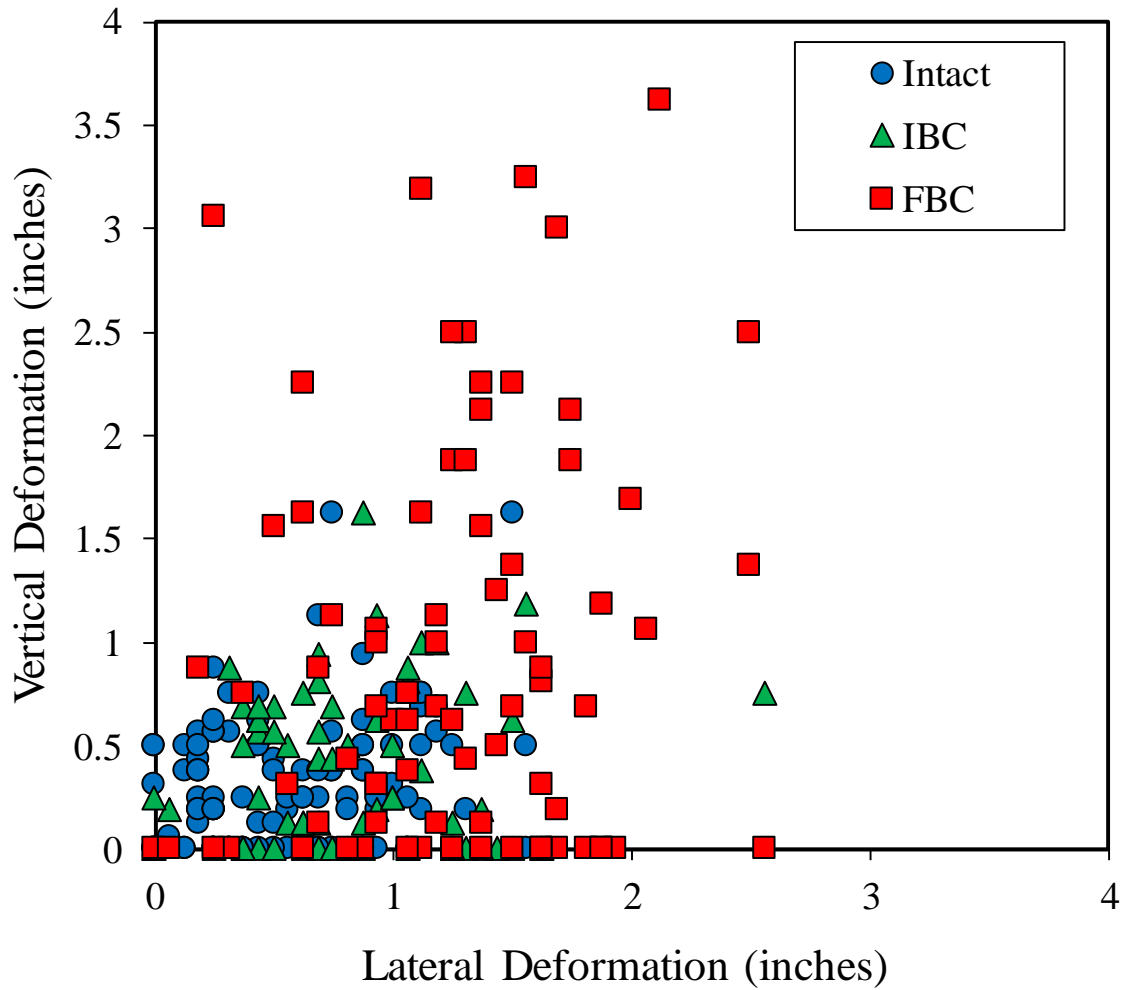
Source: FHWA.

Figure 18. Scatterplot. Variation of vertical deformation, lateral deformation, and strand damage among strands from selected blast tests.
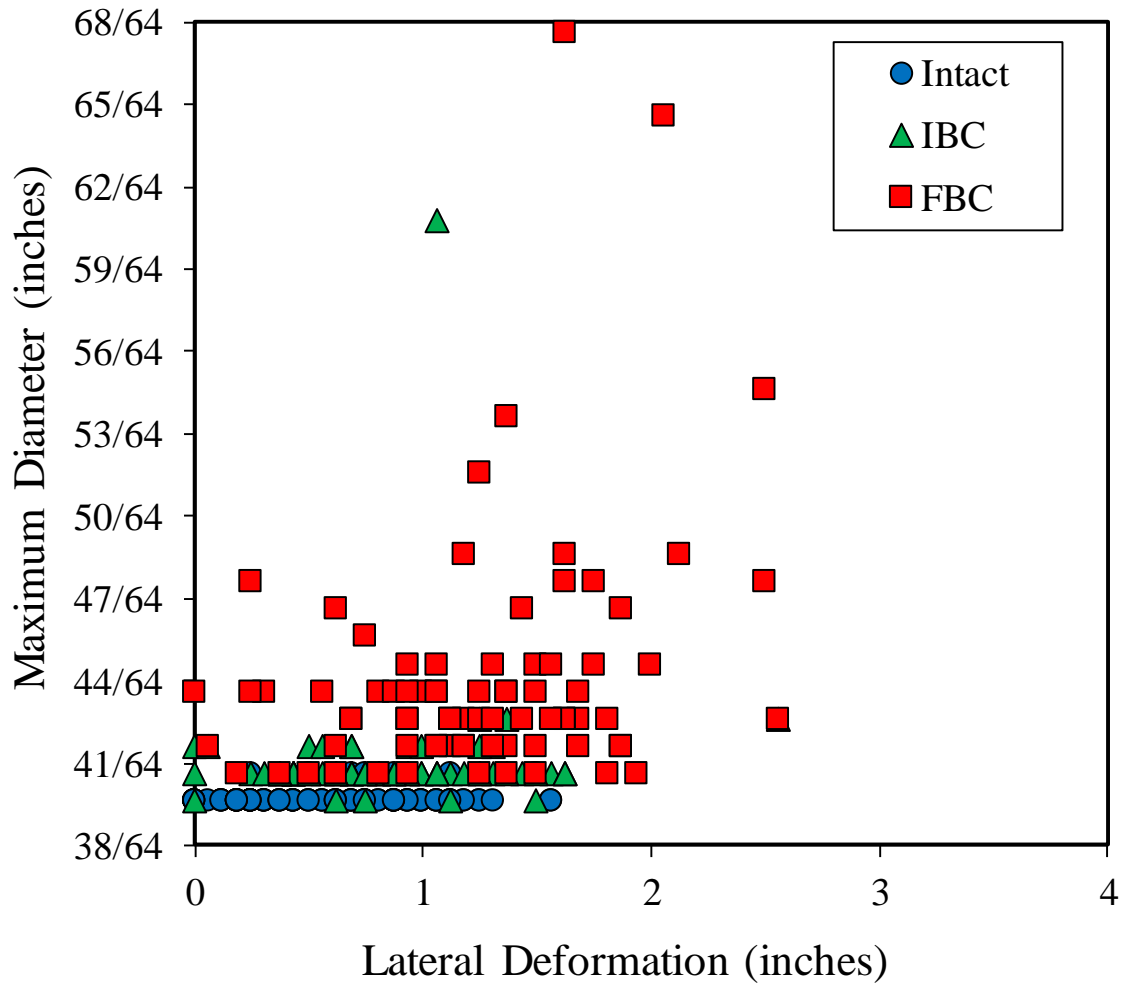
Source: FHWA.

Figure 19. Scatterplot. Variation of maximum diameter, lateral deformation, and strand damage among strands from selected blast tests.

TENSION TESTING

The primary means of evaluating capacity in this project was to tensile test strands and individual wires to failure. Then, residual capacity of strands and wires subjected to blast or thermal cutting was compared to that of virgin strands or virgin wires. This chapter describes the methods of conducting tension tests and the results of that testing.

METHODS

The tension testing of strands was performed in accordance to ASTM A1061.[3] The analysis of results per ASTM A1061 was deviated from at times because ASTM A1061 is meant for testing a new strand, not a strand in a damaged condition. All testing was performed in a 220-kip[1] capacity, servo-valve hydraulic-controlled, four-post universal testing machine. The machine is equipped with hydraulic grips for clamping specimens. The lower grip of this machine is able to freely spin about the hydraulic cylinder's axis, which is a detriment when testing a seven-wire strand. A seven-wire strand has six wires wrapped in a single direction around a central king wire, and when placed under tension, the outer wires will naturally untwist the strand. Therefore, the lower grip required modification to prevent free rotation and resist the torque the strand produces under tension. This is illustrated in figure 20 showing an overall view of the load frame. A steel angle that connects between two of the load frame's posts crosses in front of the lower hydraulic grip. Behind the angle at its midpoint are two roller bearings spaced such that a rectangular block bolted to the grip is restrained to only move up and down within the bearings. This system reacts the torque generated by the strand through a force couple into the load frame posts.

---

[1]1 kip equals 1,000 lb.
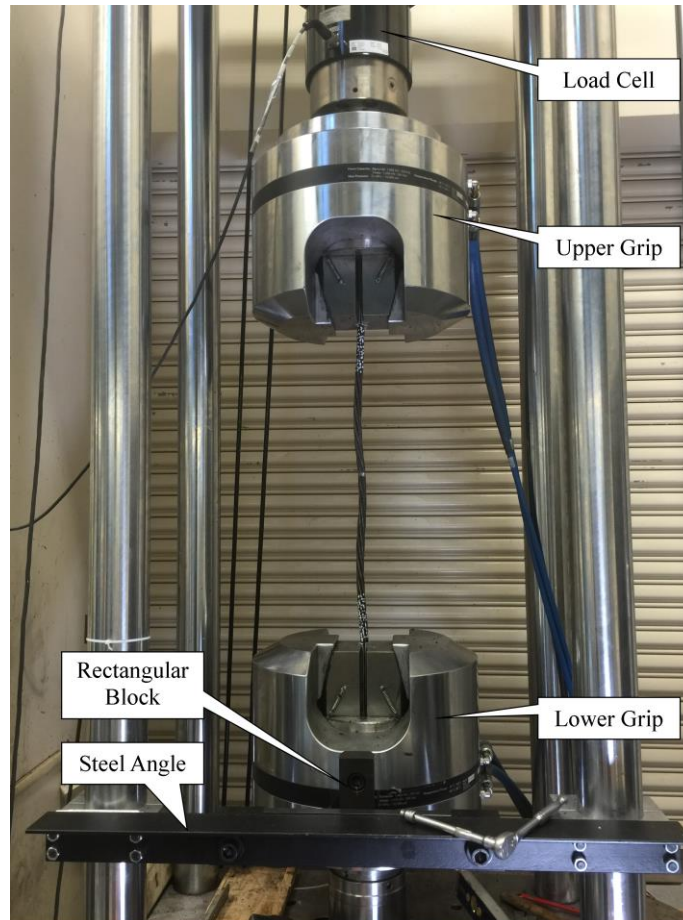
Source: FHWA.

Figure 20. Photo. Load frame with strand D38 installed.

Figure 21 shows a closeup view of the lower grip with the grip, wedges, and padding labeled. The wedges were a typical V-wedge used for gripping round products. The aluminum padding was used so the serrated teeth in the wedges did not gouge the strand itself and to ensure that strand was being gripped through friction only. This gripping method is one of three that are outlined in the ASTM A1061 specification.[3] The aluminum padding was an off-the-shelf extruded angle with dimensions of ¾- by ¾- by $^1/_8$-inch thick. The desired grip pressure was determined to be 3,500 psi—less than this and the strands would slip; greater than this and the propensity of shear failures in the grip increased. This arrangement of wedge, padding, and grip pressure was refined via numerous trial tension tests and seemed to provide the most consistent results. While the method of gripping seemed to have been optimized, virgin strands always failed near one of the grips. As described in ASTM A1061, failures outside the gauge length should be ignored; however, they may be considered valid provided the strand meets the material specification (ASTM A416 in this case) and the fracture was a tensile failure. If the grip is influencing the test results, the fracture surface is oriented at 45°. This is referred to as a "shear failure," and the results were generally ignored. This will be discussed more in the sections that follow.

20

Figure 21. Photo. Raised view of lower grip with strand installed.

Strain was measured with a video extensometer that worked on the principle of two-dimensional digital image correlation (DIC). DIC works by tracking the motion of a high-contrast pattern applied to the specimen with a digital video camera. In this case, the pattern comprised random dots applied with a white paint marker. This is shown in figure 21. The video extensometer could provide class B accuracy from the beginning of the test all the way through fracture. This is mentioned because ASTM A1061 assumes a class B extensometer is used up to the strand yield strength, and a lower accuracy class D extensometer is used post yield through fracture.[3] Likewise, the procedures used to calculate yield strength and elongation assume that the grips will have seating losses, and assumed strain values are used at set ratios of the minimum breaking strength. The use of hydraulic grips and the video extensometer negates some of the calculation assumptions of ASTM A1061, but for this project, ASTM A1061 calculations were strictly followed.[3]

Strands were cut to an approximate 36-inch length, and given the 5-inch depth of the wedges, this left approximately 26 inches from wedge face to wedge face. The wedge-to-wedge distance could not increase more than this, as the crosshead was positioned at its extent. This allowed for a 24-inch-gauge length over which the video extensometer could measure. The 24-inch-gauge length is the minimum allowed by ASTM A1061.[3] The specimens were loaded at a strain rate of 0.015/min over the 24-inch-gauge length. This equated to a crosshead displacement rate of 0.36 inch/min. Generally, failure would occur within a 5-min period.

Strand Preparation

Since the original strands were greased and sheathed, certain difficulties in testing were posed. The HDPE covering on the strand was easily removed with a utility knife; however, the grease was more problematic. It was found that a tension test could only be successfully run when the grease was completely removed from the strand. Once the strand was cut to length, a hose clamp was placed about 10 inches away from each end, and the six outer wires were untwisted away from the king wire, splaying them outward. Then, a pressure washer with conventional dish soap was used to blast away the grease and, once dried, pliers were used to twist the outer wires back into position around the king wire.

VIRGIN STRAND

Virgin strands were used as a baseline to assess the level of damage to the bundles subjected to thermal cuts and blasts. The virgin strands were taken from other qualification tests not described in this report. These qualification tests all produced little to no visual damage within the middle 4 ft of the bundles where the specified procedures of each test were applied. Since the bundles were nominally 12 ft long for each qualification test, virgin strands were taken from the outer 4 ft of these bundles. Numerous strands were used as practice to ensure the testing machine and control software were working as expected and to refine the grip pressure and padding. Ultimately, 16 official virgin strand tension tests were used to define the baseline strength of the strands.

Of the 16 tests on virgin strands, 3 failed in shear within the grips. Figure 22 shows a typical shear failure of a wire from the virgin 2 specimen with the characteristic inclined fracture plane. Shear failures in or at the grips may artificially reduce the strength of the strands, and thus these results were not part of statistical calculations or plotted in any figures shown. The desired fracture pattern is a tension failure that is normal to the applied stress; figure 23 shows a tension failure of five wires in virgin 4, and the remaining two intact wires are noticeably necked.
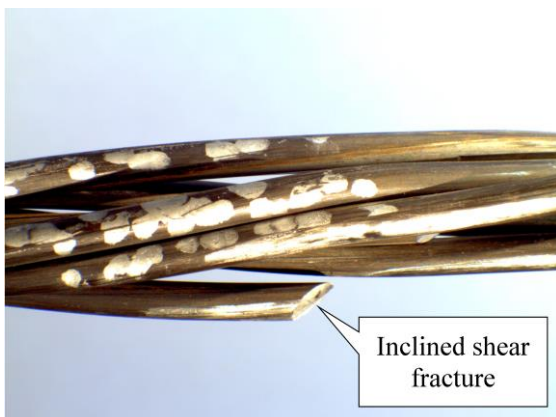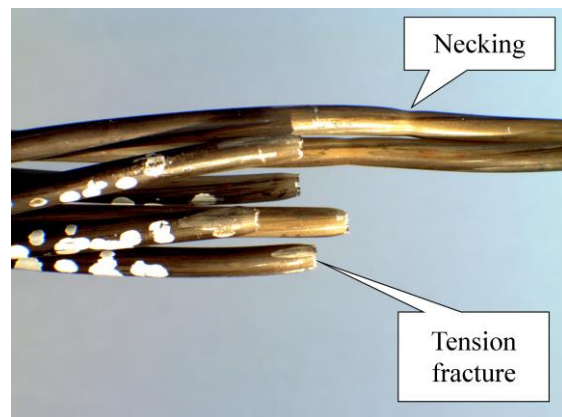
Source: FHWA.

Figure 22. Photo. Shear failure of virgin 2.

Source: FHWA.

Figure 23. Photo. Tension failure of virgin 4.

All pertinent results for each test are reported in table 1. This table lists the modulus, yield load, strain at yield, actual ultimate tensile strength (AUTS), strain at AUTS, and elongation. The

modulus was calculated as the best-fit slope between 20 and 65 percent of the maximum breaking strength. Yield load was calculated using the preload method described in the ASTM A1061 test specification.[3] Often, elongation values were less than the strain at AUTS because the method to calculate elongation in ASTM A1061 defines the zero strain level to be at 10 percent of the maximum breaking strength.

The results listed in table 1 show, on average, the virgin strand did meet the minimum requirements of ASTM A416.[2] The minimum yield and AUTS results were repeatable with coefficients of variation (COVs) less than 1 percent. Plots of load versus strain for the 13 valid virgin specimens are presented in figure 24. All plots nearly overlay each other and show a distinct bilinear behavior. However, elongation values varied much more with a COV nearing 10 percent. The variation of the elongation values is observable in figure 24 from the range of strains over which fracture occurred.

Table 1. Virgin strand results.

Specimen	Modulus (ksi)	Yield Load (kips)	Strain at Yield	AUTS (kips)	Strain at AUTS	Elongation (percent)	Notes
Virgin 1	29,244	58.00	0.0097	64.83	0.0437	4.30	3 tension fractures at grip
Virgin 2[a]	27,434	57.05	0.0099	63.24	0.0322	3.13	2 shear fractures at grip
Virgin 3	28,753	57.96	0.0098	64.99	0.0457	4.49	No fractures, slipped in grip
Virgin 4	27,541	57.52	0.0099	64.36	0.0388	3.78	5 tension fractures at grip
Virgin 5[a]	28,158	57.19	0.0100	63.41	0.0348	3.39	4 tension fractures at grip
Virgin 6	29,027	57.31	0.0098	63.98	0.0387	3.79	3 tension fractures at grip
Virgin 9[a]	28,240	56.90	0.0099	59.67	0.0137	1.29	1 shear fracture at grip
Virgin 10	28,687	57.43	0.0098	63.94	0.0378	3.69	2 tension fractures at grip
Virgin 11	29,530	57.69	0.0097	64.18	0.0384	3.77	3 tension fractures at grip
Virgin 12	28,478	57.31	0.0099	64.37	0.0427	4.18	2 tension fractures at grip
Virgin 13	28,420	57.54	0.0098	64.27	0.0384	3.76	2 tension fractures at grip
Virgin 14	29,003	57.70	0.0097	64.62	0.0421	4.14	3 tension fractures at grip
Virgin 15	28,102	57.14	0.0100	63.79	0.0369	3.59	2 tension fractures at grip
Virgin 16[a]	29,030	57.87	0.0098	63.49	0.0331	3.23	3 tension fractures at grip
Virgin 17[a]	28,787	56.73	0.0097	61.68	0.0257	2.50	1 shear fracture at grip
Virgin 18[a]	28,431	57.29	0.0098	63.54	0.0349	3.41	1 tension fracture at grip
Average[b]	28,646	57.53	0.0098	64.14	0.0389	3.81	—
COV[b] (percent)	1.87	0.50	1.04	0.79	9.57	9.86	—
ASTM A416	—	56.52[c]	—	62.80[c]	—	3.50[c]	—

—Not a requirement.
[a]Specimen failed to meet at least one ASTM A416 requirement.[(2)]
[b]Calculation of average and COV ignores specimens with shear failure in grips.
[c]Represents a minimum value.
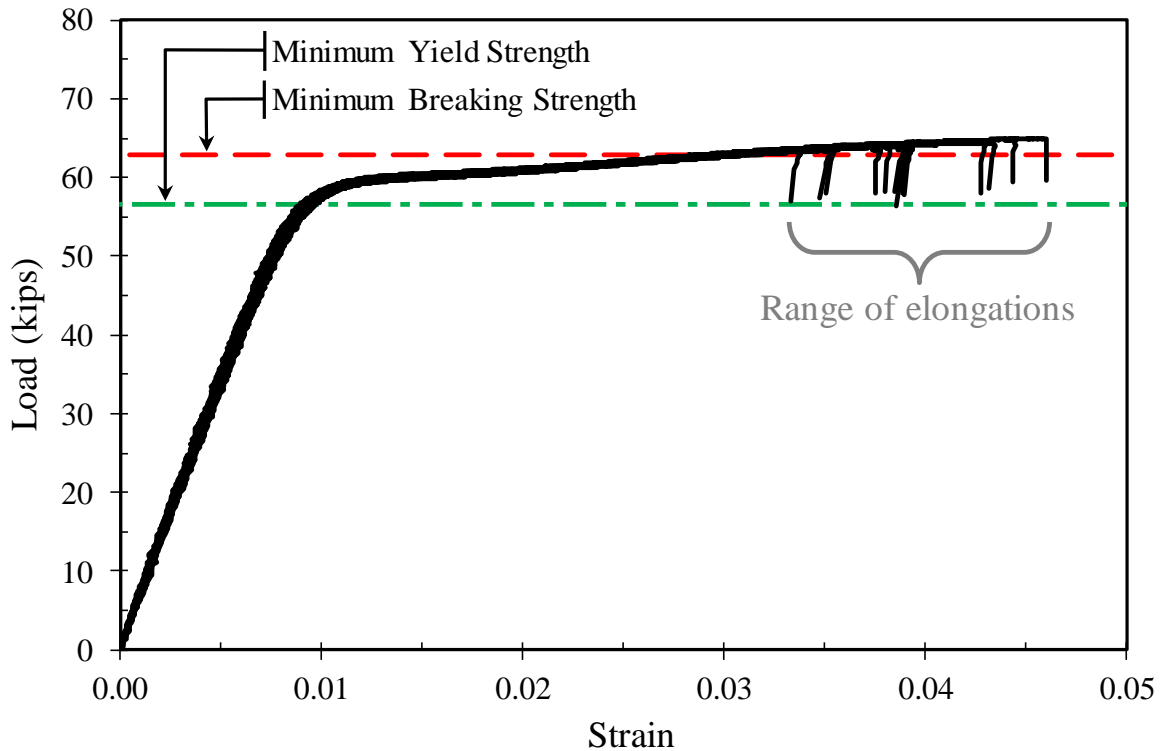
Source: FHWA.

Figure 24. Graph. Load versus strain for all virgin strands not exhibiting shear failure in grips.

VIRGIN WIRE

Individual wires of strand were also tension tested to establish a baseline. Six additional, untested virgin strands were cut to approximately 33 inches in length and then were each separated into six outer wires and one king wire. The king wire has a slightly larger diameter (0.210 inch) than the six outer wires (0.202 inch). Therefore, a population of king and outer wires was tested to establish the baseline for each.

Wires were tested in a different servo-valve hydraulic-controlled load frame (from the one shown in figure 20); it also had hydraulic wedge grips but an overall lower force capacity. Wires had to be tested on this machine because it had wedges capable of gripping wire with a diameter that small. These wedges were only 4 inches deep (in contrast to 5 inches in the other machine), and the wire was directly gripped without padding. The same DIC system was used to measure strain over a 24-inch-gauge length so the results would commensurate with the virgin strand testing. The loading rate was specified as 0.36 inch/min, again, to commensurate with the strand testing.

The king wire and two randomly selected outer wires were tested from each strand. The results in terms of AUTS, strain at AUTS, and total elongation are presented in table 2 and table 3,

25

respectively, for outer and king wires. Only results from wires that fractured within the gauge length are reported in the tables.

Table 2. Virgin outer wire results.

Specimen	AUTS (kips)	Strain at AUTS	Elongation[a] (percent)
Strand B, wire 5	9.42	0.0552	5.67
Strand C, wire 1	9.19	0.0498	5.28
Strand C, wire 2	9.40	0.0568	5.88
Strand D, wire 1	9.31	0.0574	6.43
Strand D, wire 2	9.41	0.0579	6.18
Strand E, wire 1	9.42	0.0585	5.95
Strand E, wire 2	9.37	0.0555	6.03
Strand F, wire 2	9.41	0.0564	6.06
Average	9.37	0.0559	5.93
COV (percent)	0.86	4.86	5.81

[a]Used elongation at fracture criterion in ASTM E8, not the elongation criteria in ASTM A416.[2,4]

Table 3. Virgin king wire results.

Specimen	AUTS (kips)	Strain at AUTS	Elongation[a] (percent)
Strand A, king	10.22	0.0558	6.15
Strand B, king	10.10	0.0547	6.04
Strand C, king	10.10	0.0550	5.96
Strand D, king	10.14	0.0554	6.25
Strand E, king	10.17	0.0560	6.41
Strand F, king	10.13	0.0534	6.47
Average	10.15	0.0551	6.21
COV (percent)	0.43	1.71	3.27

[a]Used elongation at fracture criterion in ASTM E8, not the elongation criteria in ASTM A416.[2,4]

Plots of all the outer wire specimens are shown in figure 25 and for the king wires in figure 26. Because the outer wires have an initial helical shape, there is an initial low stiffness response at low load as the wire is straightened out. Because of this effect, each curve has been offset by a certain strain value such that the elastic portion of the curve intercepts the origin of the plot. This was also done with the king wires; however, since they were mostly straight to begin with, they did not demonstrate the same initial low stiffness behavior.
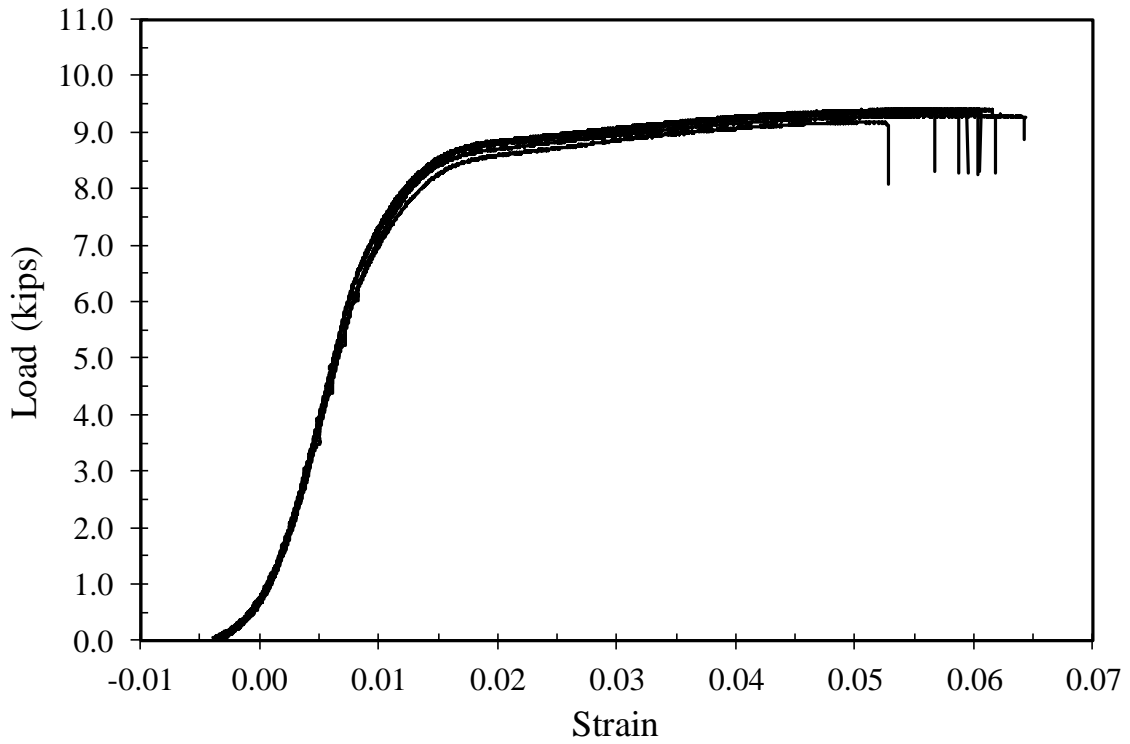
Figure 25. Graph. Load versus strain response of virgin outer wires.
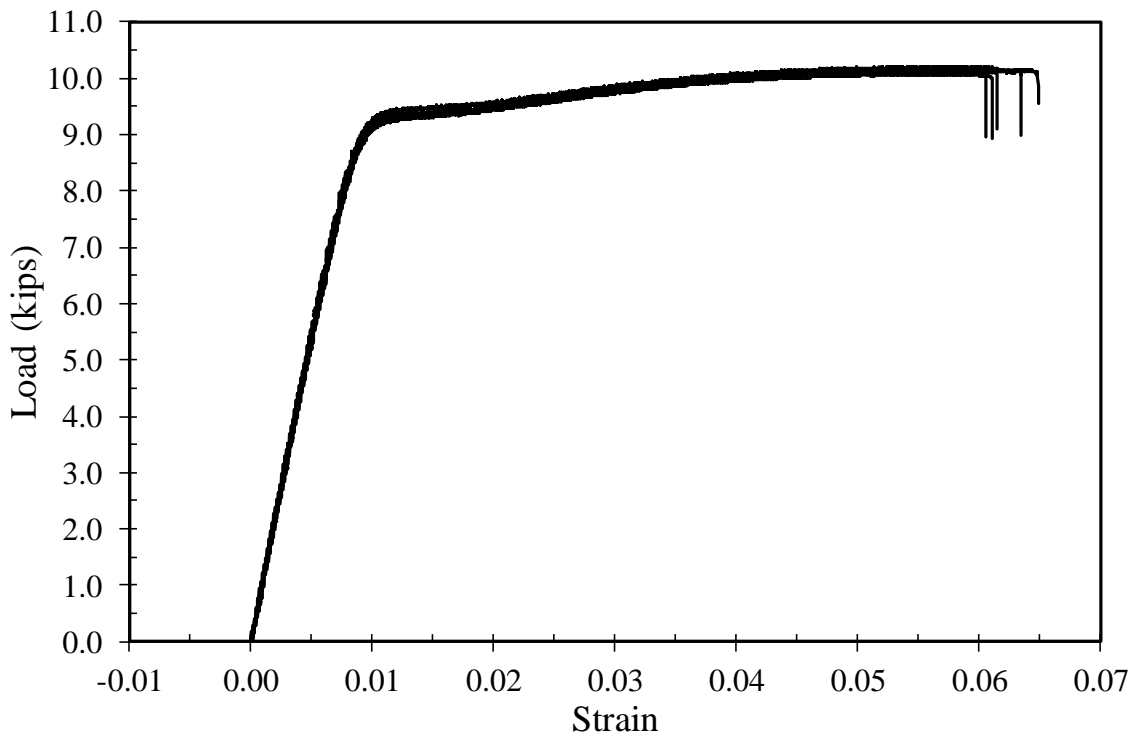
Figure 26. Graph. Load versus strain response of virgin king wires.

THERMAL LANCE TESTS

Strands were selected from a protected bundle subjected to two thermal lance qualification tests for residual capacity tension tests. The selected intact strands (no wires cut) were separated into two categories: One group represented strands assumed closest to the heat source (neighbor to strands completely cut by the tip of the penetrating thermal lance), and another group represented strands assumed to be farthest from the heat source. The decision to select strands for these two categorical groups was made by inspecting the location of the intact strands relative to the location of the strands with all seven wires cut as seen in figure 3 through figure 6. For example, in cut A, strand A30 neighbors three strands with all wires cut by the thermal lance (strands A29, A23, and A24). Thus, strand A30 is close to the heat source and survived with no wires cut. But perhaps the wires in strand A30 were affected by heat (the hypothesis to test). For the second categorical group, strand A43 is located as far as possible from the same heat source as strand A30, with no wires cut and hypothetically less heat exposure. The results from the residual capacity tension tests are reported separately for cuts A and B.

Depending on the thermal cycle applied to strands, microstructural changes might have occurred in the steel wires. These microstructural changes could affect the residual tensile strength in the steel wires. The thermal lance qualification tests did not employ thermocouples to measure magnitude or duration of temperature. However, prior to conducting the tension tests, a visual inspection of the strand (relative to other strands) might provide a qualitative measure of the maximum temperature reached in a steel wire. All strands were originally greased and sheathed, and it is recognized that these coatings will change under sufficiently high heat. The HDPE cover on the majority of the strands selected from the thermal lance test groups was melted. It was also noticed that the grease was either partially or completely burned away from some of the selected strands. Figure 27 shows a picture of the untested B23 strand, considered representative, which shows the HDPE has burned away for a few inches, and the dull appearance at the center of the strand indicates that the grease was possibly burned away on the outer wires. The shinier appearance near the melted HDPE indicates intact grease on the outer wires. After the strands were tested in tension, it was easier to observe the condition of the HDPE and grease both on the outer six wires and around the king wire. Using the information describing the condition of the HDPE and grease might help provide a qualitative measure of the temperature the strand may have experienced.
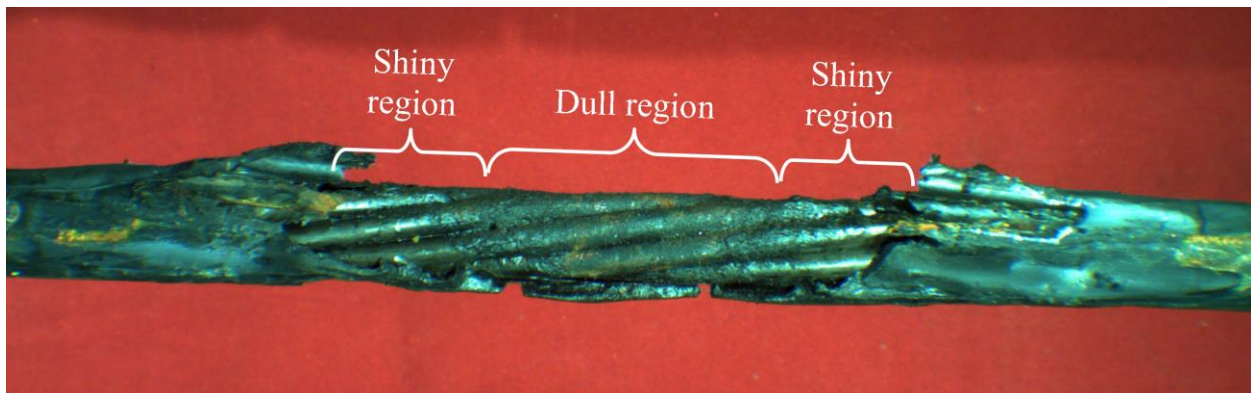
Source: FHWA.

Figure 27. Photo. Untested strand B23 with burned HDPE and grease.

Results

Data from the tensile test results from thermal lance cuts A and B are listed in table 4. The table presents the same mechanical data as listed for the results of virgin strand tension tests in table 1. Additional columns are provided to denote how many wires fractured, the location of the fractures, and the condition of the HDPE and grease. The condition of the HDPE was either melted or not. The grease could have three condition states: completely burned away, burned away only on the outer wires, or not burned at all.

Table 4. Thermal lance cut results.

Specimen	AUTS (kips)	AUTS Ratio[i]	Strain at AUTS	Elongation (percent)	Wires Fractured	In Gauge Length?	HDPE Melted?	Grease Burned Away?
A1	46.92	0.73	0.0086	0.77	2	Yes	Yes	Completely
A30	45.79	0.71	0.0088	0.79	2	Yes	Yes	Only outer wires
A32[a]	57.08	0.89	0.0099	0.90	2	Yes	Yes	Only outer wires
A34[b]	44.28	0.69	0.0073	0.64	2	Yes	Yes	Only outer wires
A35[c]	31.58	0.49	0.0065	0.57	4	Yes	Yes	Completely
A36[d]	62.27	0.97	0.0280	2.71	1	No	Yes	Only outer wires
A37	62.73	0.98	0.0309	3.02	1	No	Yes	Only outer wires
A38[e]	60.76	0.95	0.0242	2.32	0	—	Yes	Only outer wires
A40	63.98	1.00	0.0375	3.67	5	No	Yes	No
A41	62.88	0.98	0.0310	3.01	2	No	Yes	No
A42	63.65	0.99	0.0372	3.64	1	No	Yes	No
A43[f]	59.77	0.93	0.0124	1.16	1	Yes	Yes	Only outer wires
B6	57.37	0.89	0.0105	0.95	1	Yes	Yes	Completely
B12[g]	42.57	0.66	0.0081	0.72	3	Yes	Yes	Completely
B18	49.50	0.77	0.0082	0.74	2	Yes	Yes	Completely
B19	64.55	1.01	0.0458	4.49	4	No	Yes	No
B23	59.42	0.93	0.0120	1.10	1	Yes	Yes	Only outer wires
B24	62.29	0.97	0.0293	2.85	1	No	Yes	No
B25	63.72	0.99	0.0370	3.63	2	No	Yes	Only outer wires
B28	64.51	1.01	0.0422	4.14	1	No	Yes	Only outer wires
B29[h]	62.84	0.98	0.0304	2.95	2	No	Yes	No
B31	63.60	0.99	0.0355	3.44	3	No	Yes	No

Specimen	AUTS (kips)	AUTS Ratio[i]	Strain at AUTS	Elongation (percent)	Wires Fractured	In Gauge Length?	HDPE Melted?	Grease Burned Away?
B32[e]	58.96	0.92	0.0108	1.00	0	—	Yes	No
B33[h]	63.39	0.99	0.0288	2.78	5	No	Yes	No
B37[d]	62.95	0.98	0.0309	3.00	1	No	Yes	No
B38	63.80	0.99	0.0394	3.86	2	No	Yes	No
B39[h]	62.80	0.98	0.0244	2.36	3	No	No	No
B40[d]	58.32	0.91	0.0111	1.03	1	No	No	No
B41	63.34	0.99	0.0270	2.62	2	No	No	No
B42[d]	60.85	0.95	0.0150	1.42	1	No	Yes	No
B43[d]	61.79	0.96	0.0170	1.62	1	No	Yes	No

—No data to report.

[a]Two wires were nicked by the reciprocating saw blade while dismantling the bundle. Fracture did not initiate near saw nicks.

[b]One wire was nicked by the thermal lance. Fracture did not initiate near thermal lance nick.

[c]Two wires were nicked by the thermal lance. Fracture initiated at each nick.

[d]Shear failure in grip.

[e]Slipped in grip and never failed.

[f]One wire was nicked by the reciprocating saw blade while dismantling the bundle. Fracture initiated at saw-cut nick.

[g]No evidence of thermal lance nicks, though fracture in one wire initiated at slag ball fused to a wire.

[h]Video showed slipping at grip, and first fracture was a shear failure of the king wire.

[i]Calculated by dividing AUTS by 64.14 kip, the average AUTS of virgin strands.

Table 4 footnotes add important commentary to explain posttest observations not known a priori. First, according to the map of damaged wires presented in figure 4, the only strand with seven wires intact with damage was A35; this strand was originally documented as having one wire damaged. Visual examination of the fractured strand after testing (shown in figure 28) clearly shows that fractures on two wires initiated from nicks on each wire from the thermal lance. This indicates that the damage mapping presented in figure 3 through figure 6 is subject to some error, as melted HDPE and/or burned grease may have masked damage to wires, though this damage became more apparent after pressure washing to remove grease before testing. Similarly, strand A34 had no reportable damage, but posttest inspection did reveal one nick on a wire. Note, also, that during the dismantling of the bundle, wires in strands A32 and A43 received nicks from the reciprocating saw blade during the cutting operation to remove the melted HDPE cover. The nicks on wires in strand A32 did not appear to affect the residual capacity test results. However, the nicks on wires in strand A43 did appear to affect the residual capacity test results. A posttest view after the tension test on strand B12 is shown in figure 29, and no obvious nicks are visible around the fracture. However, a slag ball fused to one wire coincided with a fracture in one wire, but since two other wires simultaneously fractured, the low strength was likely the result of microstructural changes due to excessive heat, not necessarily the fused slag ball.
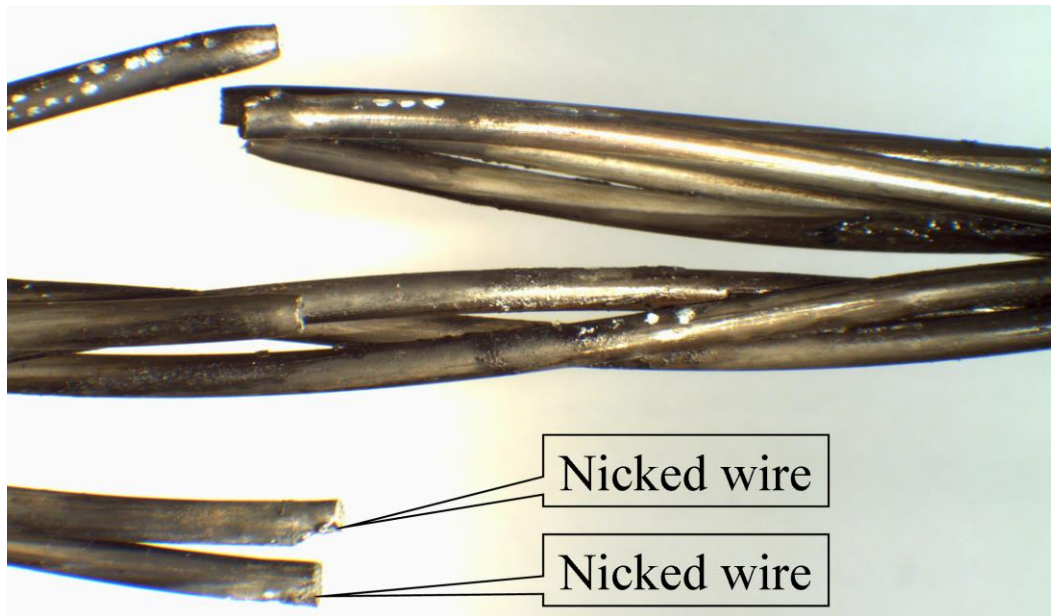
Source: FHWA.

Figure 28. Photo. Fracture of A35.
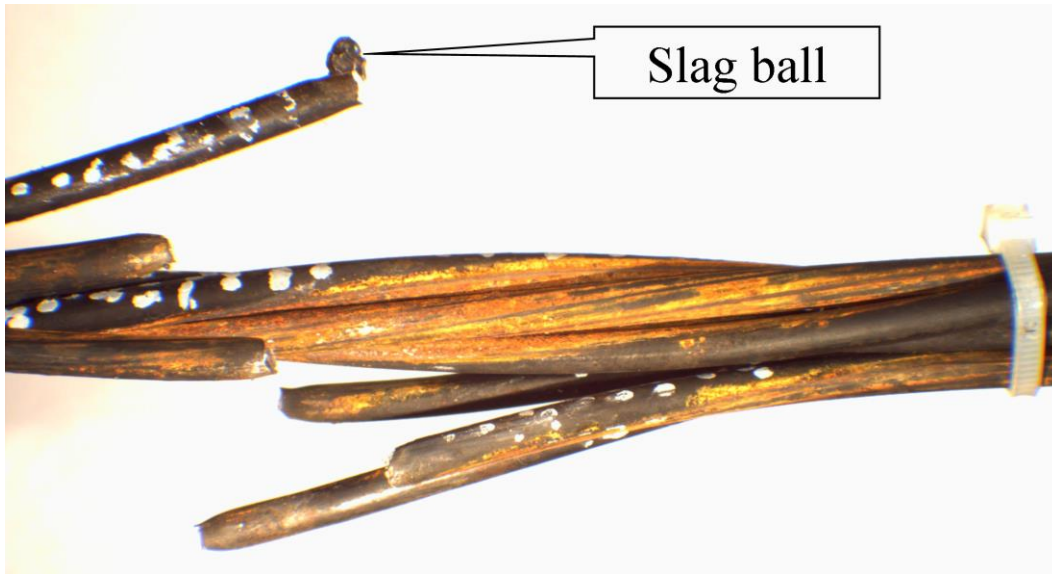
Source: FHWA.

Figure 29. Photo. Fracture of B12.

Statistical measures of the data are not presented in table 4 because the data are subject to the influence of varied heat conditions not readily assessed. Plots of the load versus strain of all the tested thermal lance strands without shear failures are presented in figure 30 and figure 31, respectively, for strands farthest and closest to the heat source. Examining figure 30 for strands farthest from the heat source (A37, A40, A41, A42, B25, B31, B38, and B41) shows curves that follow the reference curve of virgin strands with little deviation. The data from only these eight strands result in an average AUTS of 63.5 kip and 3.4 percent elongation; the average results from the virgin strand were 64.1 kip and 3.8 percent elongation. A null hypothesis test considering the two means to be equal was conducted using a Wilcoxon rank-sum test. The hypothesis was acceptable at the two-tailed 0.01 significance level but rejectable at the two-tailed 0.05 significance level. It was concluded from this that the average virgin results were not statistically different from the average results from the eight strands farthest from the heat.
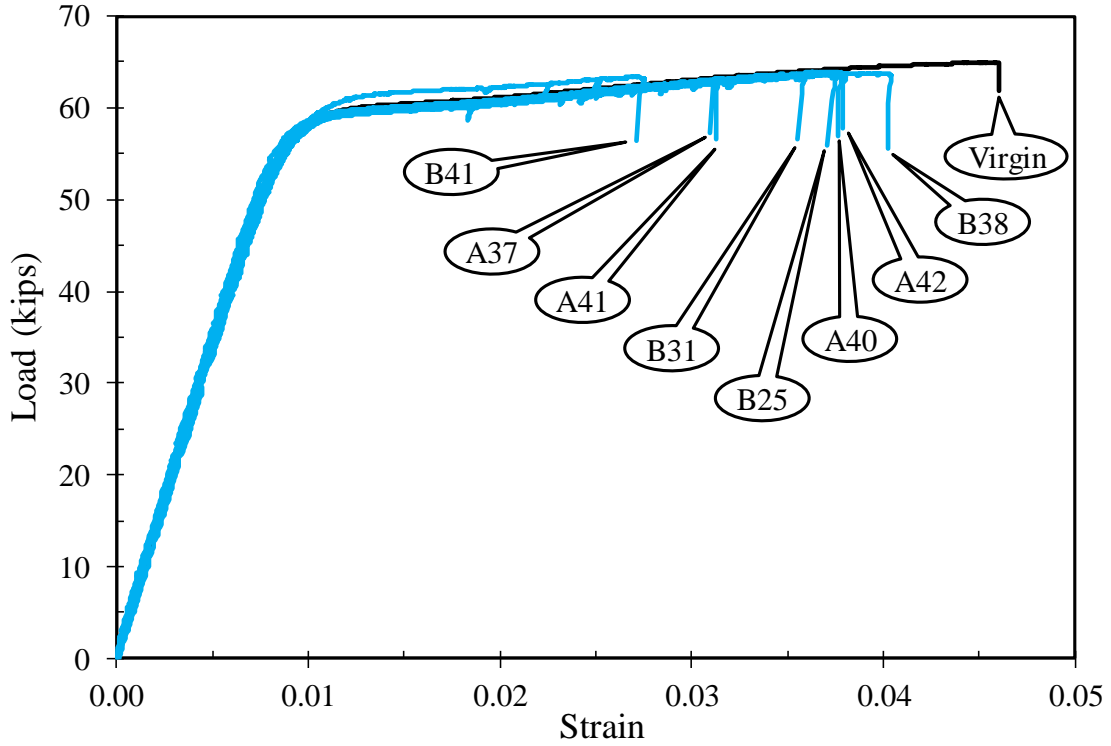
Figure 30. Graph. Load versus strain of thermal lance strands farthest from heat.
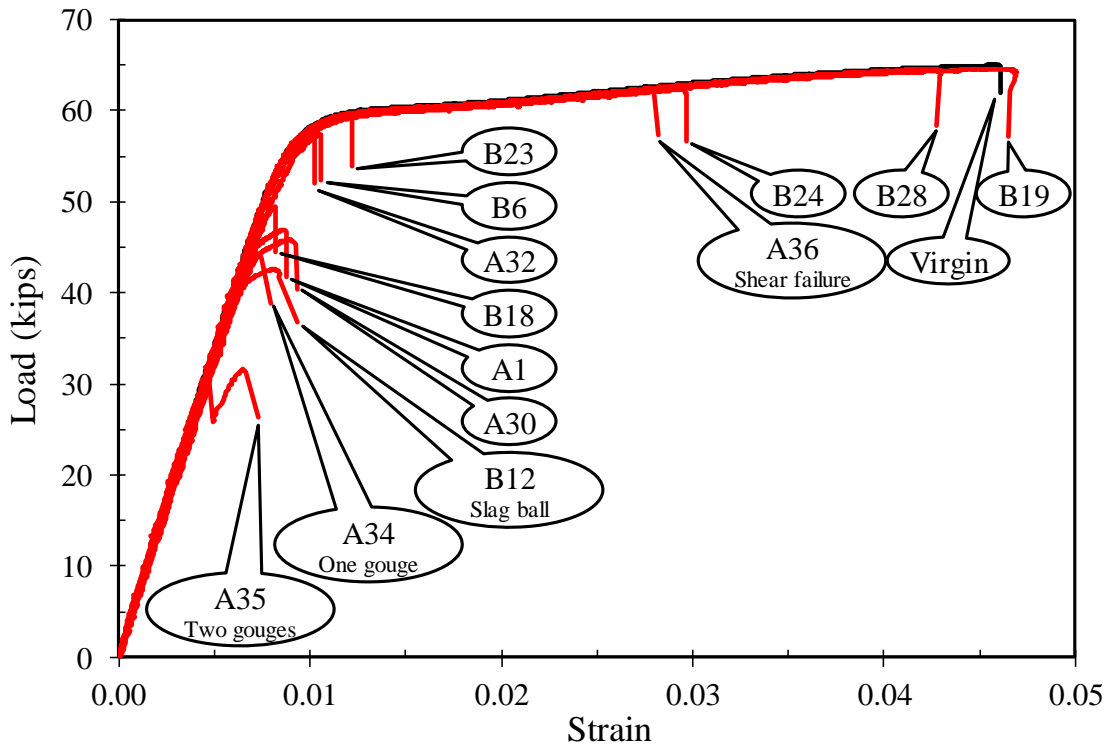
Figure 31. Graph. Load versus strain of thermal lance strands closest to heat.

The results of load versus strain for 13 strands closest to the heat source (i.e., adjacent to strands that were cut or damaged) are presented in figure 31. The results for 4 of 11 strands (A36, B19, B24, and B28) align with load versus strain curves for a virgin strand. Therefore, the proximity of a strand to the thermal cut is not a direct indicator of strength reduction. The HDPE cover of all four of these strands was melted, but the grease was intact around the king wire. The lowest residual capacities were observed after the tension tests of strands exhibiting a form of obvious heat-affected zone (HAZ) within one of the wires, like a gouge or slag ball (e.g., strands A34, A35, and B12). Despite the HAZ defects, these affected strands had residual capacities at least half the maximum load reported for the virgin strand. But the fracture was observed to occur on the elastic portion of the virgin strand reference curve. The residual capacities of remaining strands closest to the heat (A1, A30, A32, B6, B18, and B23) were between half and full capacity of the virgin strand. Similarly, the fracture was observed to occur on the elastic portion of the virgin reference curve. Of these six strands, the grease was completely burned away on four.

It is undesirable for the load–strain behavior of strands during the tension test to exhibit a fracture during the elastic response. However, defining an exact criterion to screen for this is difficult, as the design of stay cable bundles is based on ultimate tensile strength and does not necessarily rely on a certain level of ductility beyond the minimum elongation requirements in ASTM A416.[2] The Post-Tensioning Institute (PTI) does publish a specification covering the design, testing, and installation of bridge stay cables.[5] The fatigue strength of stay cables must be qualified by test according to this specification, and after the fatigue test is complete, the stay cable must be loaded and demonstrate a static strength of at least 92 percent AUTS. The static portion of this test ensures stay cables with fatigued wires have a minimum amount of residual strength in service. Understandably, the results reported herein were not performed in support of fatigue testing; however, the 92-percent criterion is an established bar for residual tensile strength of stay bundles. Table 4 reports the AUTS ratio for each thermal lance strand, and this could be compared to PTI's 92 percent criterion. Using this criterion, strands A1, A30, A32, A34, A35, B6, B12, and B18 are considered to have failed. Therefore, based on the characteristics of these strands, it is conservatively recommended to visually inspect any strands for evidence of nicks, gouges, fused slag, or lacking any grease. If the visual inspection identifies any of these flaws, the strand is assumed to have no residual tensile strength.

Finally, in figure 30, it is seen that the load–strain response of strand B41 has higher offset response overall compared to the load–strain response of the virgin strands. This was seen with other thermal lance strand tests, though deleted from the plots due to shear failures. All test bundles were constructed from two different production lots of strand, and it is suspected that strands in the bundle used in the thermal lance cutting qualification test may have come from both production lots. This may explain the results from testing strand B41 (which may have come from the production lot with uncharacterized virgin strand tensile strength properties).

BLAST STRAND TESTS

Strands selected from protected bundles subjected to specific blast events for residual capacity were chosen to represent three damage categories: across the spectrum of lateral deformation, maximum diameter, and intactness of the strand wires (i.e., intact, FBC, or IBC). Strands were first selected on the basis of the largest measured birdcage diameters and largest lateral measured deformations. Strands with this type of damage are thought to have the largest amount of cold

working. Then, sampling selected strands representing a blend of all three damage categories, but selection focused primarily on identifying strands with the largest lateral deformation.

Installation

The strands recovered after the blast tests were obviously quite deformed, evident from the lateral deformation data presented in the Documentation chapter. The photo in figure 32 shows a view of the D38 strand before installation into the lower or upper grips of the tension test frame. This view shows the extreme bent shape of the strand. To grip the bottom portion of such a bent strand required a strong effort to bend it straight. This same strand is depicted in figure 20 once it was completely installed. The strong efforts included technicians bending the strand by hand and hitting the strand with a dead-blow hammer. Evidence that the installation stresses imposed were elastic was observed when the strand would spring back to its original bent shape after being removed from the grips. When installing birdcaged strands, the dead-blow hammer impacts tended to walk the birdcage up or down the strand or sometimes exacerbate its diameter slightly, but this was necessary to get the strand installed. Figure 33 shows strand G2 installed in the test machine. Strand G2 represented a test sample with one of the largest birdcage diameters.

Source: FHWA.

Figure 32. Photo. Strand D38 before installation.

Source: FHWA.

Figure 33. Photo. Strand G2 after installation.

Results

The results from all the selected blast strands are presented in table 5 through table 7 for FBC, IBC, and intact strands, respectively. The load versus strain plots for all these strands are presented in figure 34 through figure 36, again, respectively for FBC, IBC, and intact strands. The trends in the data are easier to see in the three plots, and they will be discussed individually. Because of the curvature of the strands and presence of birdcages, some strands exhibited a softer response in the test compared to virgin strands, particularly at low loads. The soft displacement response was due to the force required to straighten the strand out or twist the strand back tight. To better compare the results, all data were shifted on the Strain axis such that the elastic portion of the curve would theoretically intersect zero strain. This was done by fitting a line through the data between a load of 10 and 40 kip and using the intercept with the Strain axis, as the offset shift applied to all the data.

Table 5. Residual tensile capacity results of strands selected from bundles from the blast tests: strands with FBC damage.

Specimen	AUTS (kips)	AUTS Ratio[a]	Strain at AUTS	Elongation (percent)	Wires Fractured	In Gauge Length?
G87	63.47	0.99	0.0312	2.98	3	No
F87[b]	58.18	0.91	0.0110	1.00	3	No
E19	61.27	0.96	0.0262	2.48	1	Yes
G2	62.37	0.97	0.0331	3.23	1	Yes
D41[c]	59.91	0.93	0.0257	2.43	1	Yes
F20	64.63	1.01	0.0343	3.30	3	No
G20	63.18	0.99	0.0320	3.09	2	No
D35	63.37	0.99	0.0327	3.17	1	No
F103[c]	63.75	0.99	0.0327	3.13	2	Yes
G99[c]	61.07	0.95	0.0234	2.21	1	Yes
F14	62.57	0.98	0.0279	2.65	1	Yes
G77[c]	60.21	0.94	0.0190	1.80	1	Yes
G19	63.19	0.99	0.0331	3.21	3	No
F27[c]	64.12	1.00	0.0301	2.89	1	Yes
E39	63.10	0.98	0.0348	3.35	1	No
Average[d]	62.59	0.98	0.0297	2.85	—	—
COV[d] (percent)	2.31	2.31	15.67	16.41	—	—

—No data to report.
[a]Calculated by dividing AUTS by 64.14 kip, the average AUTS of virgin strand.
[b]Shear failure in grip.
[c]Impact damage initiated the fracture.
[d]Statistical calculations ignore specimens with shear failures.

Table 6. Residual tensile capacity results of strands selected from bundles from the blast tests: strands with IBC damage.

Specimen	AUTS (kips)	AUTS Ratio[a]	Strain at AUTS	Elongation (percent)	Wires Fractured	In Gauge Length?
E28	62.74	0.98	0.0302	2.88	1	No
E40	62.90	0.98	0.0302	2.92	3	No
E41	63.98	1.00	0.0356	3.45	3	No
E42	62.51	0.97	0.0287	2.76	3	No
D36	63.46	0.99	0.0352	3.41	2	No
G76	63.08	0.98	0.0348	3.35	2	No
F38	65.29	1.02	0.0414	4.02	2	No
D42	63.89	1.00	0.0341	3.29	1	No
D21	63.60	0.99	0.0348	3.39	2	No
G61	63.16	0.98	0.0322	3.12	2	No
F11[b]	62.70	0.98	0.0254	2.45	1	No
E37	62.49	0.97	0.0280	2.73	4	No
G30	63.40	0.99	0.0340	3.30	3	No
Average[c]	63.38	0.99	0.0333	3.22	—	—
COV[c] (percent)	1.23	1.23	11.08	11.30	—	—

—No data to report.
[a]Calculated by dividing AUTS by 64.14 kip, the average AUTS of virgin strand.
[b]Shear failure in grip.
[c]Statistical calculations ignore specimens with shear failures.

Table 7. Residual tensile capacity results of strands selected from bundles from the blast tests: intact strands.

Specimen	AUTS (kips)	AUTS Ratio[a]	Strain at AUTS	Elongation (percent)	Wires Fractured	In Gauge Length?
G11	63.09	0.98	0.0313	3.02	1	No
G86	63.77	0.99	0.0386	3.76	2	No
E35	62.86	0.98	0.0304	2.93	1	No
D38	64.17	1.00	0.0339	3.27	2	No
G62[b]	62.02	0.97	0.0266	2.53	1	No
G57	62.28	0.97	0.0281	2.70	2	No
D16	64.57	1.01	0.0436	4.25	4	No
D30	65.71	1.02	0.0505	4.95	7	No
F29	64.99	1.01	0.0361	3.50	4	No
F6	64.15	1.00	0.0332	3.20	2	No
F4	64.59	1.01	0.0346	3.36	1	No
Average[c]	64.02	1.00	0.0360	3.49	—	—
COV[c] (percent)	1.63	1.63	18.59	19.25	—	—

—No data to report.
[a]Calculated by dividing AUTS by 64.14 kip, the average AUTS of virgin strand.
[b]Shear failure in grip.
[c]Statistical calculations ignore specimens with shear failures.
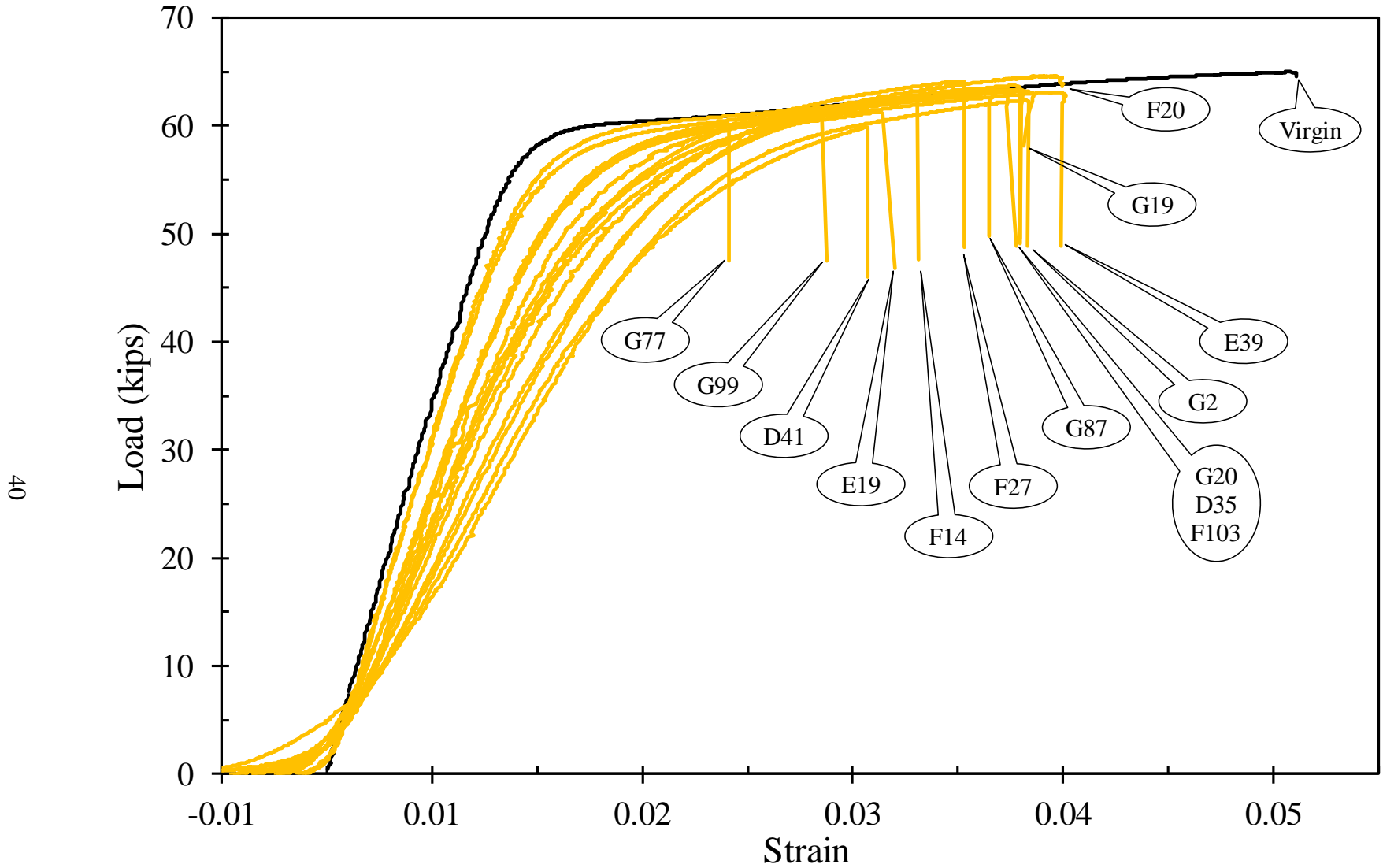
Source: FHWA.

Figure 34. Graph. Load versus strain of blast FBC strands.

40
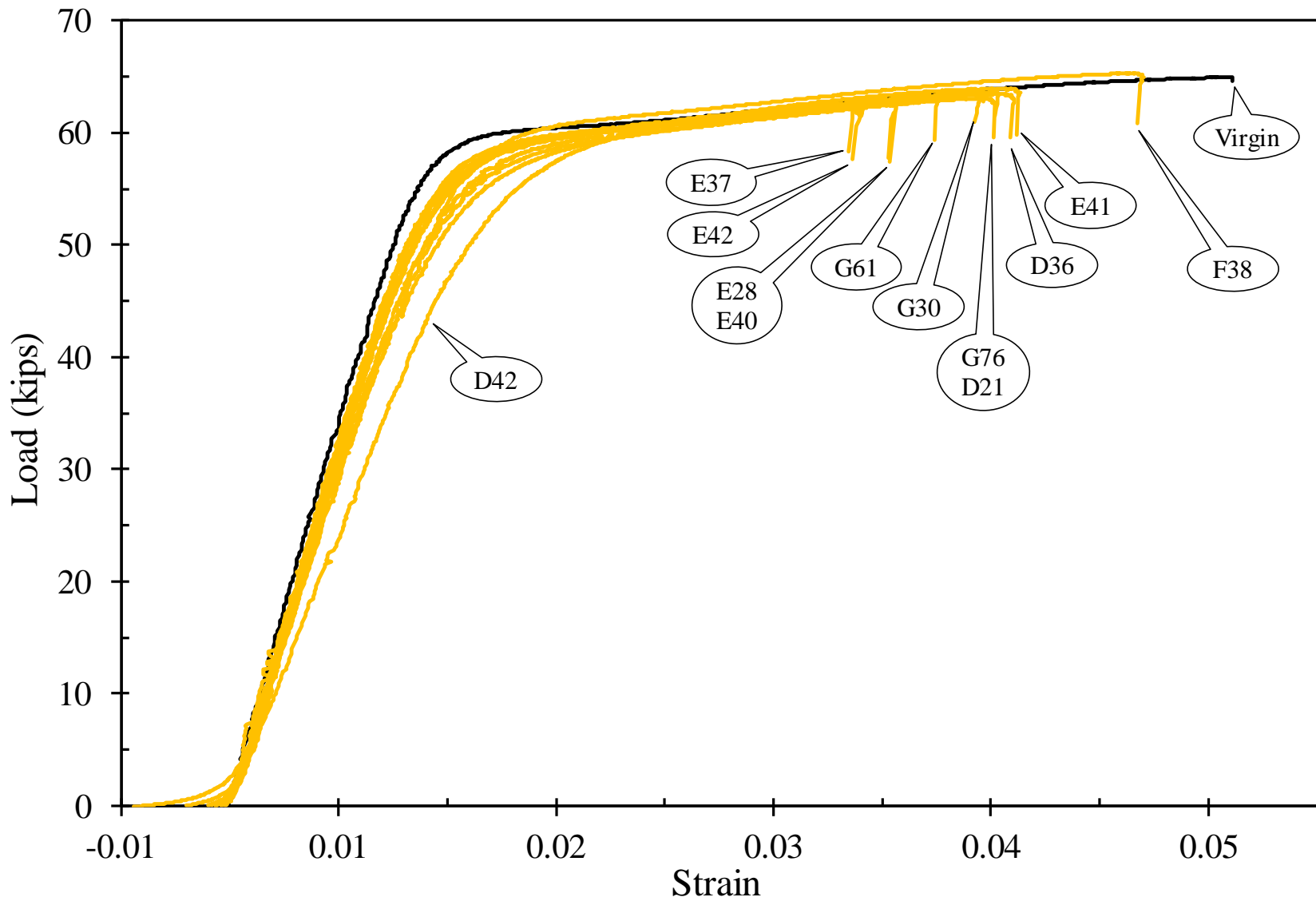
Figure 35. Graph. Load versus strain of blast IBC strands.
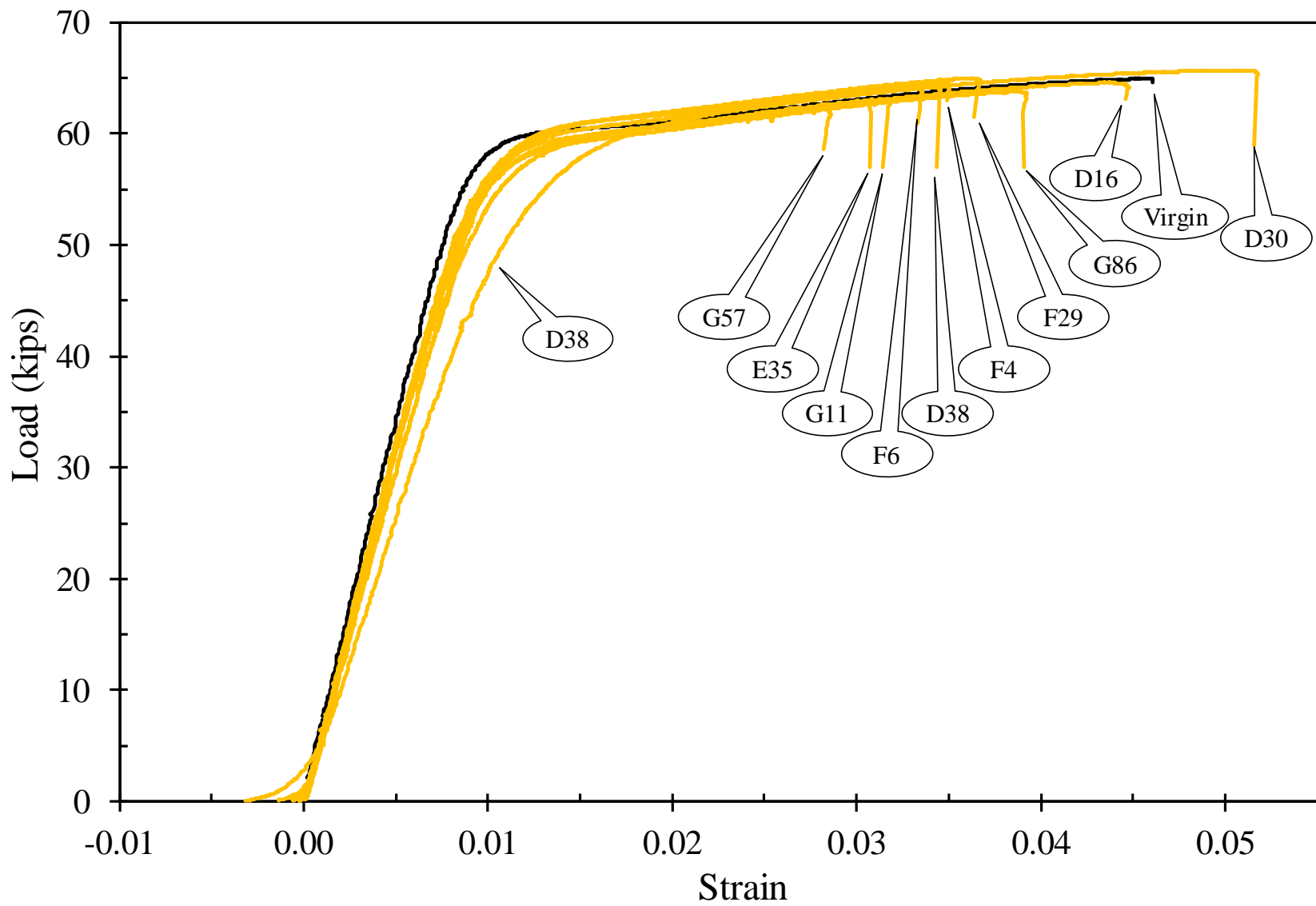
Source: FHWA.

Figure 36. Graph. Load versus strain of blast intact strands.

Figure 34 shows all the load–strain results from tension tests on FBC strands, and the soft loading response is pronounced. Generally, the load–strain behavior of these strands does not follow the reference curve of the virgin strand. The values of elastic moduli vary and show a much more gradual transition from elastic to strain hardening behavior when compared to the virgin strand curve. From the data listed in table 5 for FBC strands, all those without shear failures had AUTS ratios in excess of 92 percent; the average AUTS ratio was 98 percent. This implies, on average, the residual strength decreases about 2 percent for FBC strands. What also stands out from this batch of specimens is 8 of the 15 tested strands fractured within the gauge length of the specimen, and this did not happen in any virgin strand tests. The table footnotes indicate that for these eight strands, five of them had fractures initiated from impact damage to the strand. Impact damage is demonstrated in figure 37 from the fractured D41 strand. The arrows in the figure point to four areas where wires have impact impressions from other wires. During the blast event, strands are propelled into adjacent strands leading to these localized areas of cold work from impact. Since fractures did initiate out of these areas of impact damage, they obviously have an effect, but, on average, it is a small decrease in strength. As for the other three strands that fractured in the gauge without visual impact damage, it is possible there may have been impact damage present, but it was masked by necking of the wires near the fracture location.
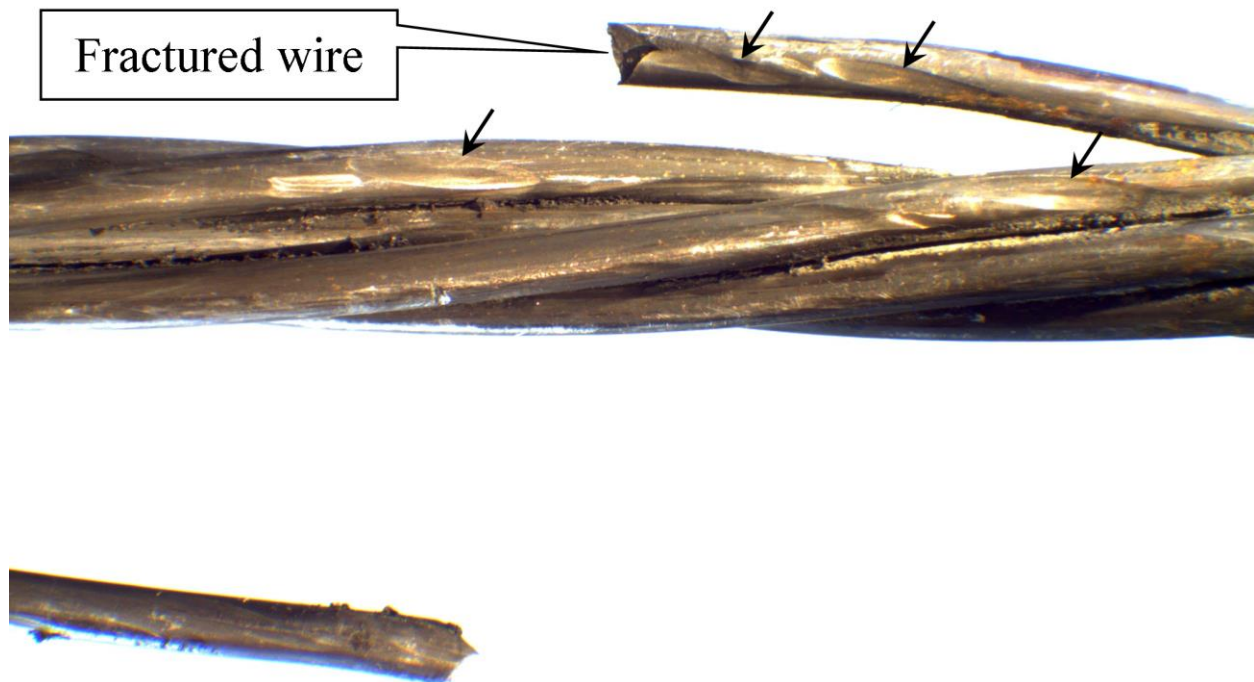
Source: FHWA.

Figure 37. Photo. Fracture D41 strand showing impact marks.

The plots of load–strain data from tests of IBC strands are shown in figure 35. The average AUTS ratio was 99 percent, and these strands on average only show a 1-percent decrease in strength. The load–strain plots of strands that were categorized as intact are shown in figure 36; the average AUTS ratio was 1.00, indicating no loss in strength. The residual tensile capacity results between IBC and intact strand tests do not differ much, and the load–strain curves follow

the virgin strand reference curve closely, with little initial soft behavior or deviation from the elastic slope. The notable exceptions in these two plots were the load–strain curves of tests on strand D38 (in figure 36) and D42 (in figure 35). Strand D42 had the largest lateral deformations of any strand tested. The soft behavior observed during the test of stand D42 corresponds to the straightening of the strand as observed in the majority of FBC strand tests. Strand D38 had one of the smallest lateral deformations but displayed soft behavior similar to strand D42. However, after reviewing the documentation photos, it was determined that strand D38 was fairly straight over the measured 24-inch-chord length. But, just beyond the chord measurement jig strand, D38 was very bent (see figure 38). Therefore, installing strand D38 in the testing machine would have caused another kink, which accounts for its soft behavior.

Source: FHWA.

Figure 38. Photo. Strand D38 documentation.

Figure 39 shows the influence of lateral deformation, vertical deformation, or birdcage diameter on the maximum load. The plot shows the average AUTS of virgin strands as a vertical dashed line to serve as the reference plane for ideal behavior. The three deformation variables are plotted relative to the virgin strength average. Looking at this plot, no discernible trend exists, as the maximum loads only vary from 60 to 66 kip over the entire range of deformations tested. Table 8 lists correlation coefficients calculated between the maximum load relative to one of the deformation variables (i.e., lateral, vertical, and diameter) and further segregated by damage type (i.e., FBC, IBC, and intact). Considering the smaller subsets of damage types, the correlation coefficients are small, indicating weak linear relationships—sometime positive and sometimes negative. Considering all the data together, there is a weak negative correlation between all the deformation variables, indicating strand strength decreases with an increase in vertical deformation, lateral deformation, or maximum diameter. Albeit, the values are nowhere near –1, indicating the poor linear fit.
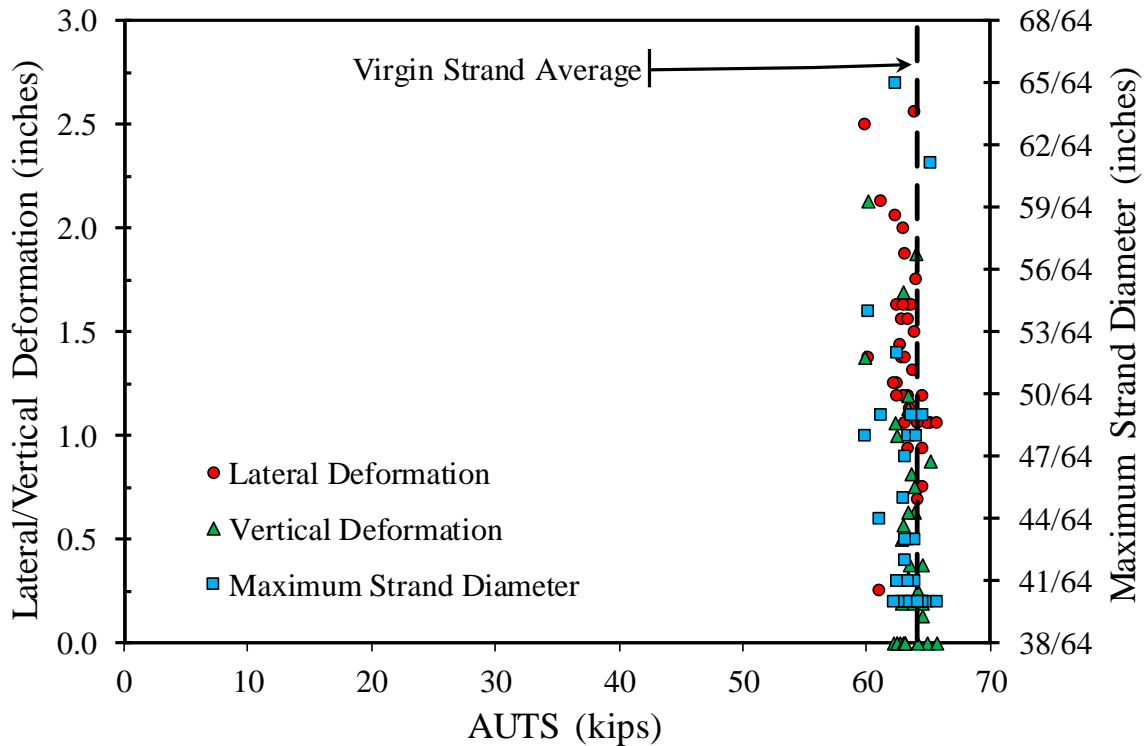
Source: FHWA.

Figure 39. Scatterplot. Relationship between maximum load and strand deformation.

Table 8. Correlation coefficients between maximum load and deformation variables.

Damage Type	Lateral Deformation	Vertical Deformation	Maximum Diameter
FBC	–0.14	–0.57	–0.18
IBC	–0.04	0.45	0.79
Intact	–0.57	–0.39	—
All	–0.32	–0.53	–0.22

—No data to report as all the diameters were the same.

BLAST WIRE TESTS

Blasted strand testing focused exclusively on strands with all wires intact, and as discussed in the prior section, the strength of the strand was reduced only a couple percent. However, there was a small population of strands that had some wires fracture during the blast event. Hypothetically, strands with broken wires likely saw the greatest level of distress during the blast event, and it was prudent to investigate the residual strength of strands with some wires fractured. To explore this realm, strands in which six wires were fractured during the blast event were focused on with the reasoning that these particular wires would have been subjected to the most extreme loading if all the neighboring wires had fractured. Based on the histograms of damage presented in the Documentation chapter, there were only 12 blast-tested strands where 1 wire was intact. These

wires were cut from their parent strand and tested in the same machine and same procedure as described in the "Virgin Wire" section.

The results of these 12 wire tests are summarized in table 9 and table 10 for outer and king wires, respectively. Load versus strain plots of the individual wires are shown in figure 40 and figure 41, for the outer and king wires, respectively. Only two blasted outer wires existed, and statistical evaluations cannot be performed on this small sample. However, from visual inspection of the load versus strain plots in figure 40, these wires could not achieve much ductility fracturing around 1.4 percent elongation. As for the king wires, eight of them were considered valid because they broke in the gauge length over a wide variety of elongations.

Each of the tables reports the AUTS ratio for each wire tested. Only 10 wires had valid results breaking in the gauge, and of those, 4 failed to meet the PTI 92 percent residual strength criterion and would be considered totally failed. However, not all the wires failed the PTI criterion, and it would be punitive to neglect the contribution of strength from strands with 6 wires cut; therefore, it was considered prudent to average the results together for the 10 valid tests. The average AUTS ratio was 0.93, indicating that strands with six wires broken have only about 7 percent reduction in strength.

Table 9. Blast outer wire results.

Strand	AUTS (kips)	AUTS Ratio[a]	Strain at AUTS	Elongation (percent)	Notes
E2	7.80	0.83	0.0139	1.41	Broke in gauge
G84	8.70	0.93	0.0144	1.45	Broke in gauge

[a]Calculated by dividing AUTS by 9.37 kip, the average AUTS of virgin outer wire.

Table 10. Blast king wire results.

Strand	AUTS (kips)	AUTS Ratio[a]	Strain at AUTS	Elongation (percent)	Notes
F107[b]	9.27	0.91	0.0181	1.83	Broke at top grip
E11	10.10	1.00	0.0453	4.66	Broke in gauge
E13[c]	8.58	0.85	0.0163	1.64	Broke at pre-necked area
F5	8.91	0.88	0.0162	1.64	Broke in gauge
E5	9.49	0.93	0.0169	1.71	Broke in gauge at impact mark
D2	9.22	0.91	0.0203	2.08	Broke in gauge
D3	9.71	0.96	0.0236	2.40	Broke in gauge
D5	8.97	0.88	0.0156	1.58	Broke in gauge
D6	9.67	0.95	0.0187	1.91	Broke in gauge
D4	10.03	0.99	0.0325	3.34	Broke in gauge
Average	9.51	0.94	0.0237	2.42	—
COV (percent)	4.73	4.74	43.70	44.34	—

—No data to report.

[a]Calculated by dividing AUTS by 10.15 kip, the average AUTS of virgin king wire.

[b]Results neglected from statistical calculations, since fracture occurred at grip.

[c]This wire had an initially necked region within the gauge length and failed at this location. The result was considered a premature failure and censored from statistical calculations.
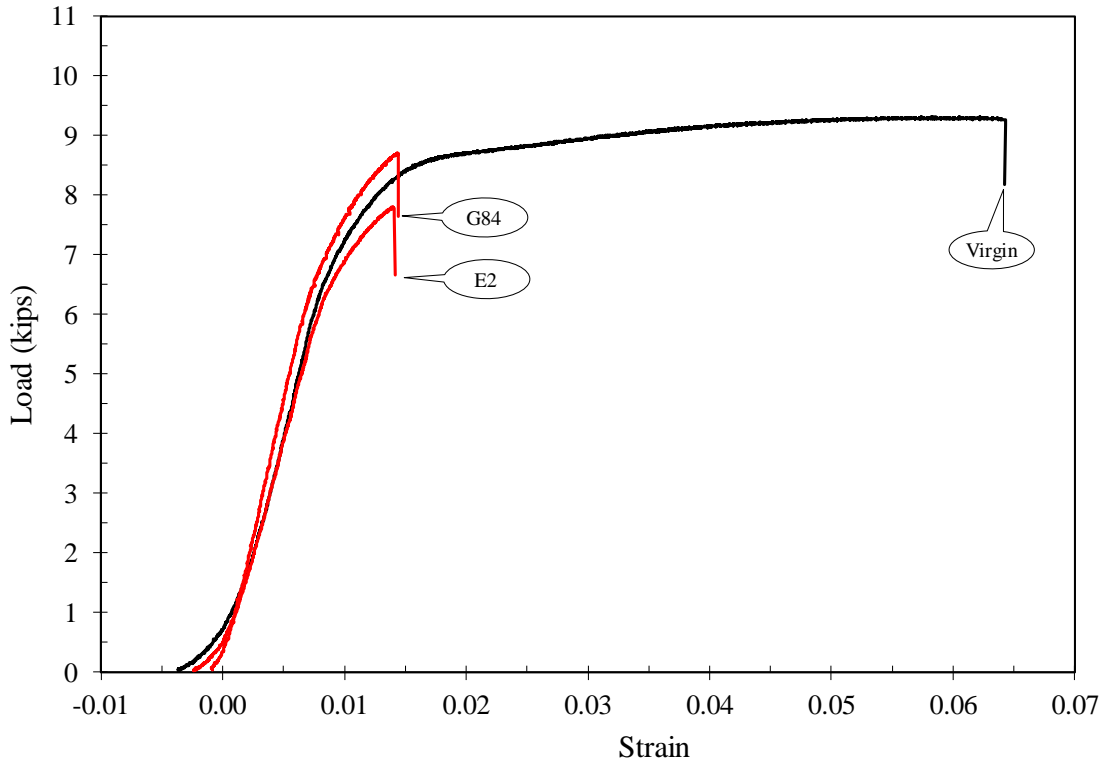
Figure 40. Graph. Load versus strain response of blast outer wires.
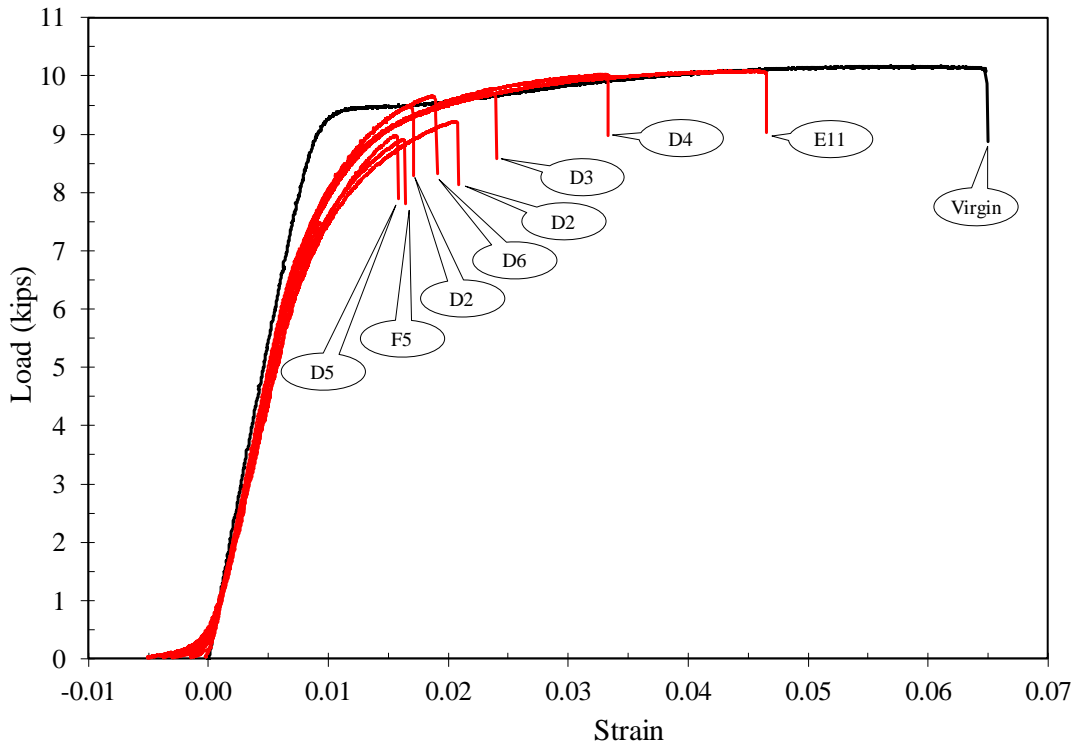
Figure 41. Graph. Load versus strain response of blast king wires.

48

INTERPRETATIONS

Going back to table 5 through table 7, FBC strands exhibited a 2-percent reduction in strength, and IBC strands exhibited a 1-percent reduction in residual maximum load. Intact strands had no reduction in residual maximum load. Null hypothesis tests were performed using a Wilcoxon rank-sum test hypothesizing there was no difference between the mean of the virgin strand and the means of FBC, IBC, or intact strands. The hypothesis was rejectable for FBC- and IBC-damaged strands even down to the two-tailed 0.01 significance level, indicating there was a statistical difference between these two damage types. The hypothesis was confirmed for the intact strands, indicating their mean strength was statistically identical to the virgin strand. Considering only FBC and IBC damage are statistically significant, it is recommended that an overall reduction factor be applied to the entire bundle to account for the reduction in strength from a blast event. Applying such a factor would alleviate the need to carefully inspect for birdcages or deformation as part of qualification.

Defining an overall blast reduction factor must also consider the notion that single wires were tested from strands with six fractured wires in this project. In this extreme example, there was only a 7-percent reduction in average strength in lieu of 2 percent for FBC strands. Considering the population of strands with zero to seven wires broken, and proportioning out a reduction in capacity between 7 and 2 percent to those populations, the overall mean blast reduction factor is 0.97. Statistics are provided in the report to account for uncertainty, but taking a more simplistic approach, a mean bundle blast reduction factor of 0.95 is recommended. This would inherently account for some uncertainty, but it is considered conservative because intact strands had no reduced capacity. The blast reduction factor should be applied to all intact wires in a qualification test. As an example, referring back to the histogram of damage for bundle G in figure 14, that bundle had 697 wires survive, though considering a blast reduction factor of 0.95, only 662 wires (i.e., 697 times 0.95) survived when comparing to the acceptance criteria, and no further work must be done to evaluate deformation or birdcaging or to account for impact damage to wires.

EFFECTS OF THERMAL EXPOSURE

Another one of the project objectives was to identify quick methods to evaluate residual strength of strands from various qualification tests of protection measures versus a physical tension test. The two simple methods of evaluation considered for this project were microstructural evaluation and hardness evaluation. Both of these were of great interest for applying to the posttest qualification results of the thermal lance cutting test. This chapter reports on work performed to evaluate the change in microstructure and hardness of a virgin strand subjected to a thermal cycle of various temperatures.

THERMOGRAVIMETRIC ANALYSIS

In the Tension Testing chapter, visual observations were made on the condition of the HDPE and grease of thermal lance strands. These simple visual observations may provide qualitative evidence as to the temperature exposure a strand may have experienced. To refine the temperature estimates, thermogravimetric analysis was performed on the HDPE and grease to understand the temperatures at which each decomposes and combusts. The test works on a small mass of material and monitors the mass loss as the temperature is increased. Tests were performed on each material in two different atmospheres: nitrogen and air. The first atmosphere of pure nitrogen created an inert atmosphere preventing combustion; therefore, the mass-loss profile represents decomposition of the material. The second atmosphere of air allowed combustion. The scenario within the actual bundle is somewhere in between the two atmospheric states depending on how easily air can enter the bundle. Combustion certainly occurs near the thermal lance, but deeper into the bundle where air flow is constrained, there is likely more decomposition in lieu of combustion. Table 11 shows the temperature where the mass-loss rate peaked and the range of temperature when 84 to 16 percent of the mass remained. This range of percent of mass loss was selected because it represents mass loss within 1 standard deviation of the mean for a normal probability distribution, which the data fit. When examining either the peak temperature or the range of temperatures, the mass changes of grease always occurred at lower temperatures than the mass changes in HDPE in both atmospheres. Therefore, due to sublimation, the temperature that a strand experiences likely never exceeds the decomposition/combustion temperature of the grease until all the grease is consumed. If grease remained on the strand, the thermogravimetric analysis data suggest the strand temperature never exceeded 800 °F. If grease was not present, the temperature likely exceeded 850 °F.

Note that the corrosion inhibiting grease and HDPE may have different compositions depending on the manufacturer, and the thermogravimetric results reported might be unique to the batch of strand tested for this project.

Table 11. Temperature of combustion and decomposition of HDPE and grease.

Atmospheric Condition	HDPE Temperature of Peak Mass Loss	Grease Temperature of Peak Mass Loss	HDPE Temperature Range[a]	Grease Temperature Range[a]
Nitrogen (decomposition)	926 °F	622 °F	877–934 °F	515–696 °F
Air (combustion)	779 °F	630 °F	717–840 °F	535–806 °F

[a]Temperature range is reported as the temperature between which 84 and 16 percent of the mass remains. The cumulative distribution of the mass-loss curves was approximately normal, and therefore this represents the ±1 standard deviation of mass loss.

MICROSTRUCTURE

A length of virgin strand was cut into approximate ¾-inch lengths for characterization of the microstructure after exposure to various temperatures. The short lengths of strand were subjected to temperatures varying between 300 and 1,500 °F in 100 °F increments in a heat treatment oven. Once the oven reached its steady-state temperature, a pair of short strand lengths was placed in it for 30 min. After 30 min, the short strand lengths were taken out and air quenched. After cooling to room temperature, the pairs of strands were mounted in epoxy for grinding, polishing, and etching to reveal microstructure in both longitudinal and transverse cross section (i.e., one ¾-inch piece became the transverse section; the other was taken apart, and each wire was exposed for a longitudinal section). The samples were etched with 2 percent Nital for 5 s to reveal the microstructure. Figure 42 through figure 69 show the longitudinal and transverse microstructures of virgin strand and at 13 different temperatures ranging from 300 to 1,500 °F. All pictures were taken using an inverted microscope at x 1,000 magnification and the same illumination settings.

At temperatures between 300 and 1,000 °F, the microstructure does not change significantly; it is ferrite/pearlite with elongated grains in the longitudinal direction as would be expected for a cold-drawn wire. The light-colored grains are the ferrite, and the darker colored grains are pearlite. At 1,100 °F, it becomes apparent that recrystallization has begun. The pearlite lamellas begin to disassociate into finer globules as the temperature progresses through 1,200 and 1,300 °F. This is most noticeable in the longitudinal sections as the directionality of the original structure begins to fade. By 1,400 °F, the structure becomes spheroidized, and by 1,500 °F, it is clear the entire structure has fully austenitized and recrystallized into a more conventional ferrite/pearlite microstructure.

Lastly, the 30-min soak at elevated temperature with an air quench was explored because this was believed to represent what strands may experience during the thermal lance cutting event. Applying the results to scenarios that may maintain temperature for longer duration or have slower/faster cooling rates requires care (e.g., sustained fire with water quenching from firefighting activities).
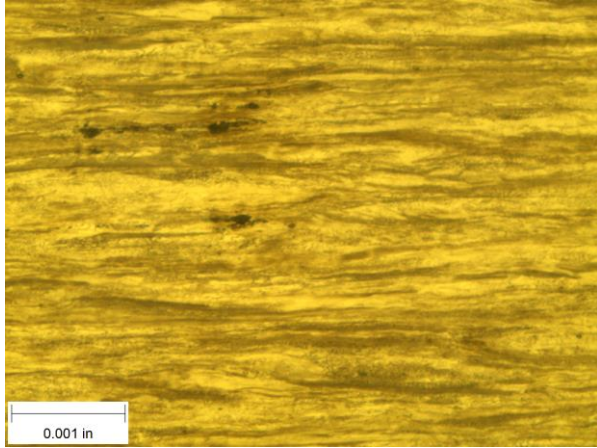
Figure 42. Photo. Longitudinal without heating.
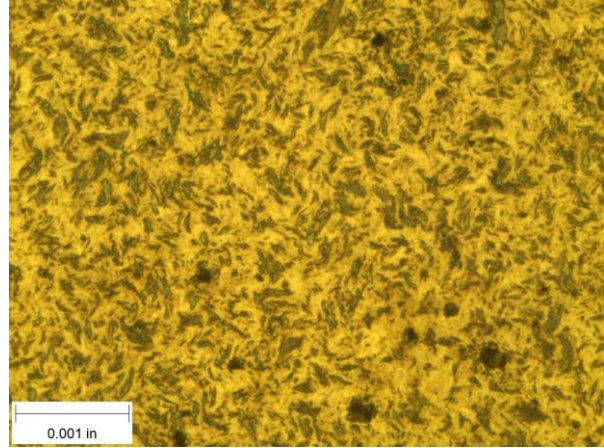
Figure 43. Photo. Transverse without heating.
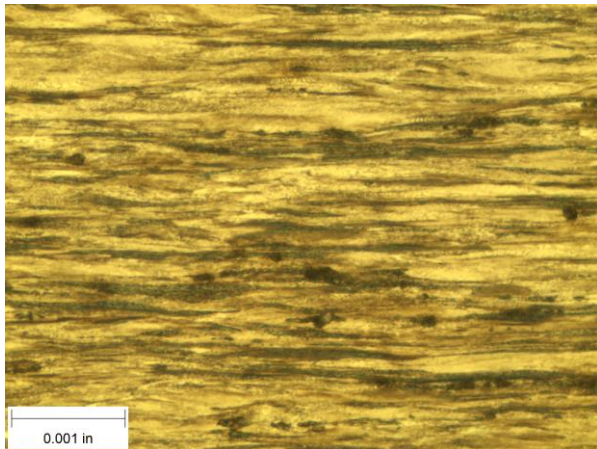
Figure 44. Photo. Longitudinal after 300 °F.
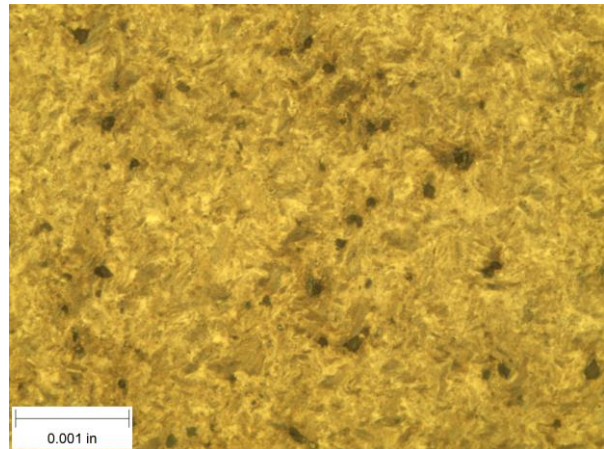
Figure 45. Photo. Transverse after 300 °F.
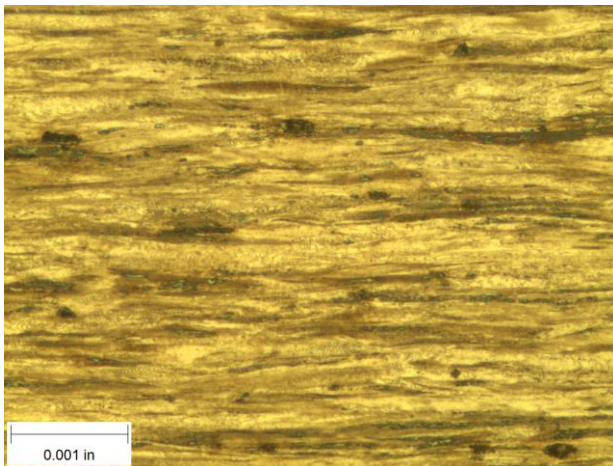
Figure 46. Photo. Longitudinal after 400 °F.
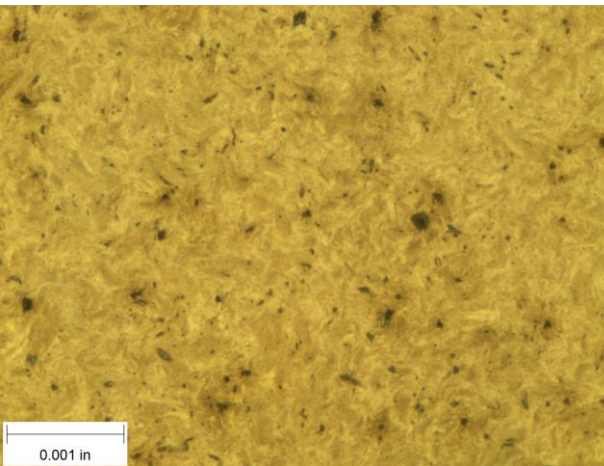
Figure 47. Photo. Transverse after 400 °F.
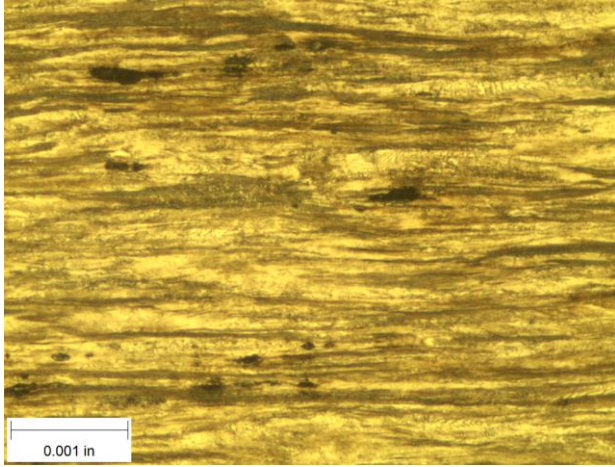
Figure 48. Photo. Longitudinal after 500 °F.
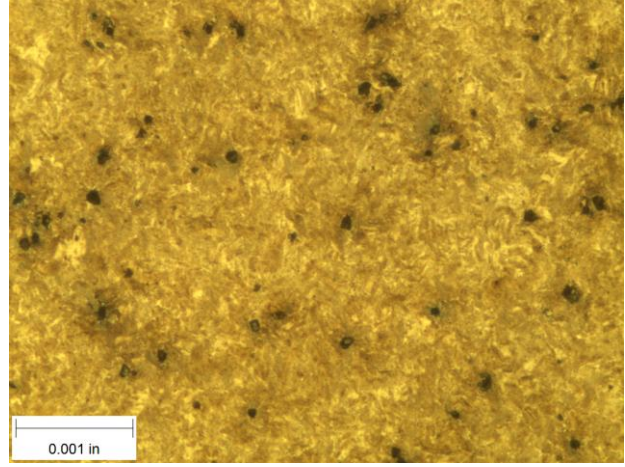
Figure 49. Photo. Transverse after 500 °F.
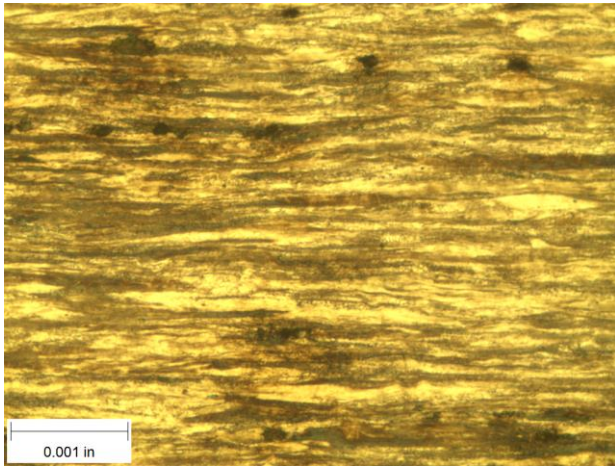
Figure 50. Photo. Longitudinal after 600 °F.
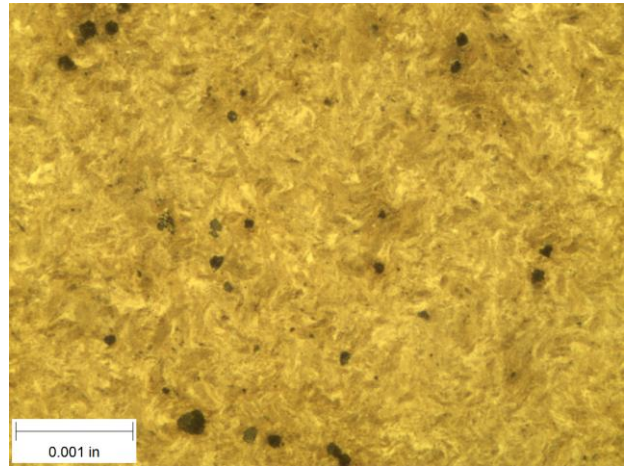
Figure 51. Photo. Transverse after 600 °F.
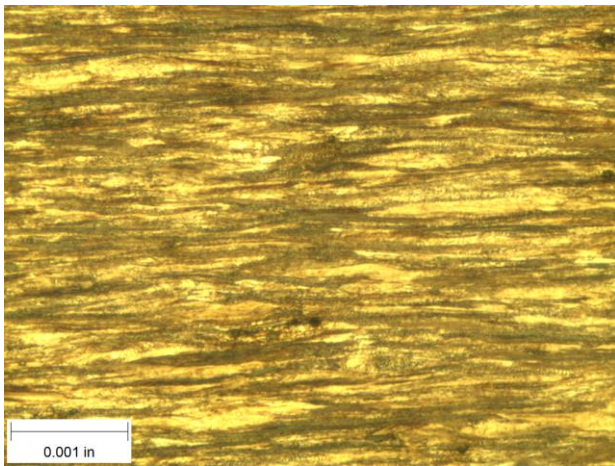
Figure 52. Photo. Longitudinal after 700 °F.
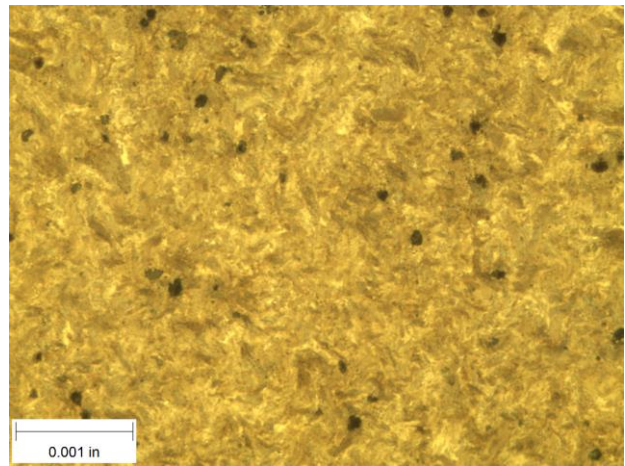
Figure 53. Photo. Transverse after 700 °F.
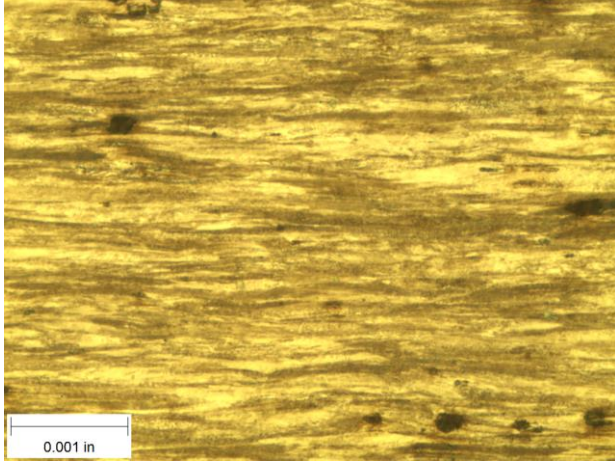
Figure 54. Photo. Longitudinal after 800 °F.
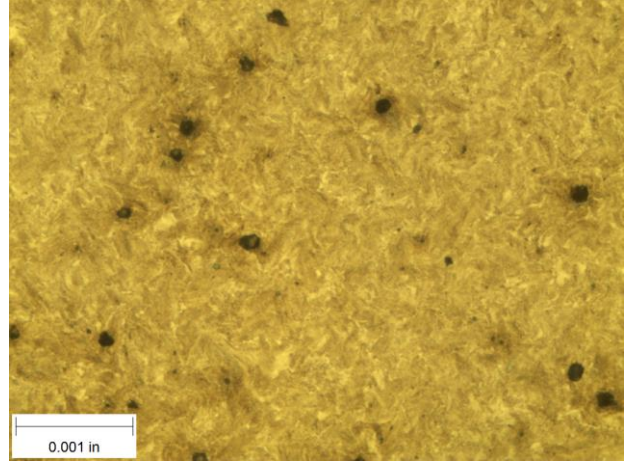
Figure 55. Photo. Transverse after 800 °F.
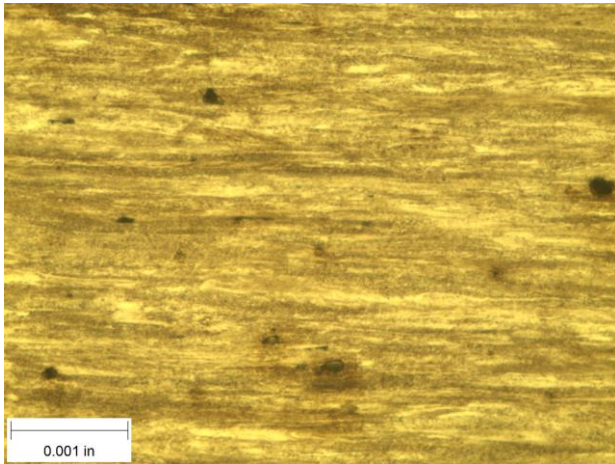
Figure 56. Photo. Longitudinal after 900 °F.
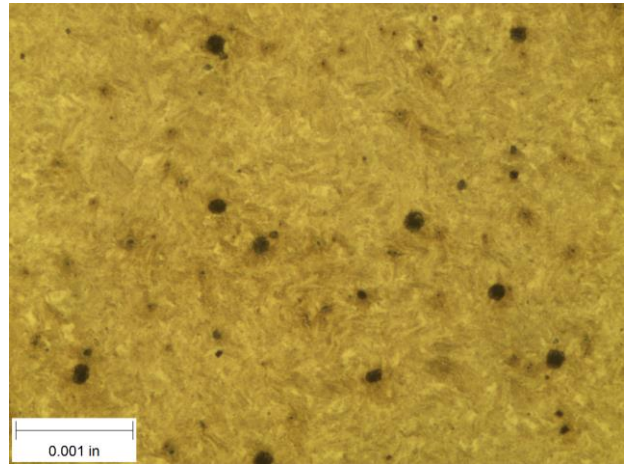
Figure 57. Photo. Transverse after 900 °F.
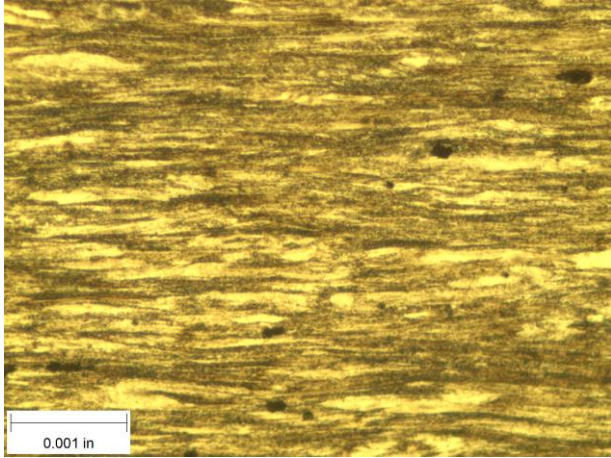
Figure 58. Photo. Longitudinal after 1,000 °F.
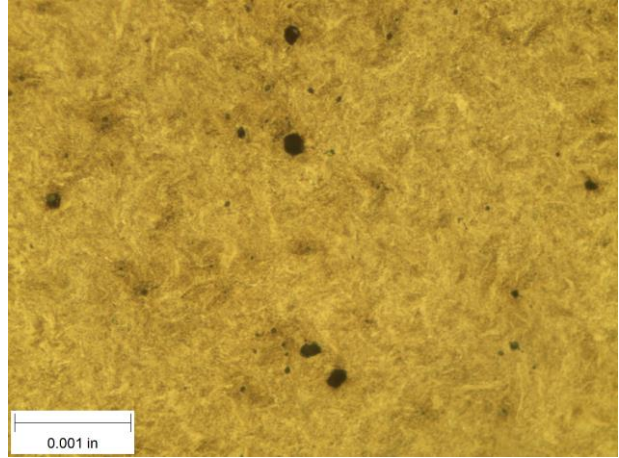
Figure 59. Photo. Transverse after 1,000 °F.
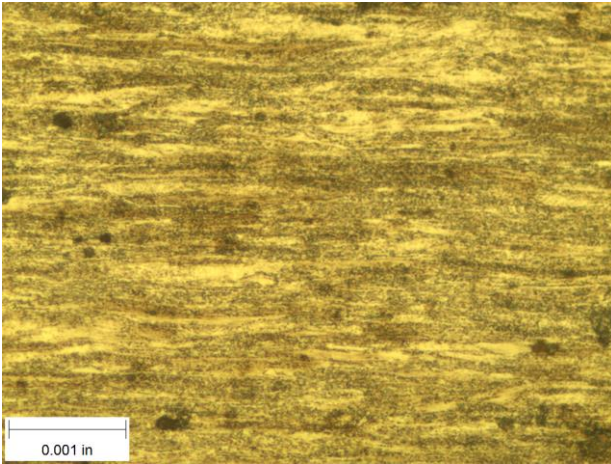
Figure 60. Photo. Longitudinal after 1,100 °F.
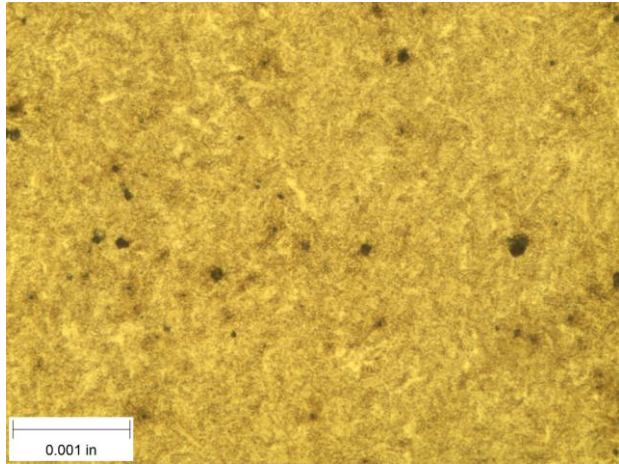
Figure 61. Photo. Transverse after 1,100 °F.
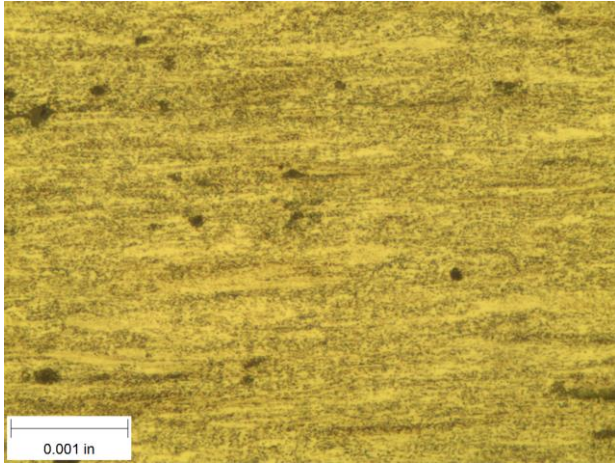
Figure 62. Photo. Longitudinal after 1,200 °F.
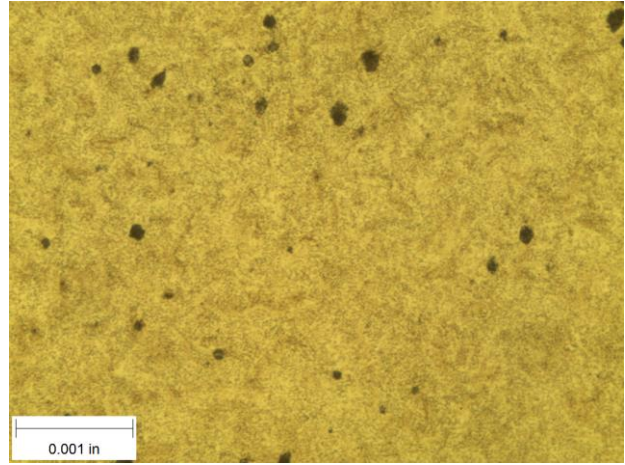
Figure 63. Photo. Transverse after 1,200 °F.
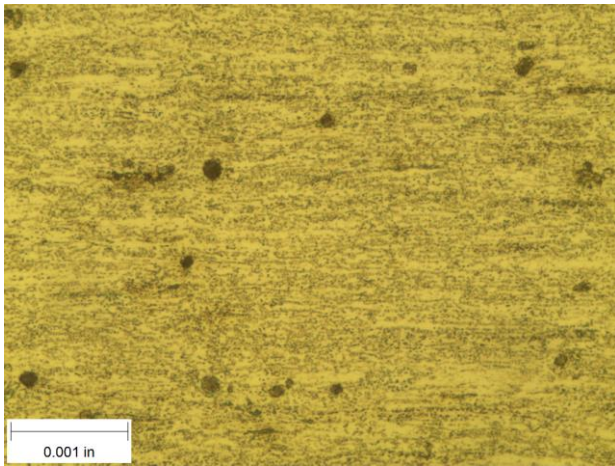
Figure 64. Photo. Longitudinal after 1,300 °F.
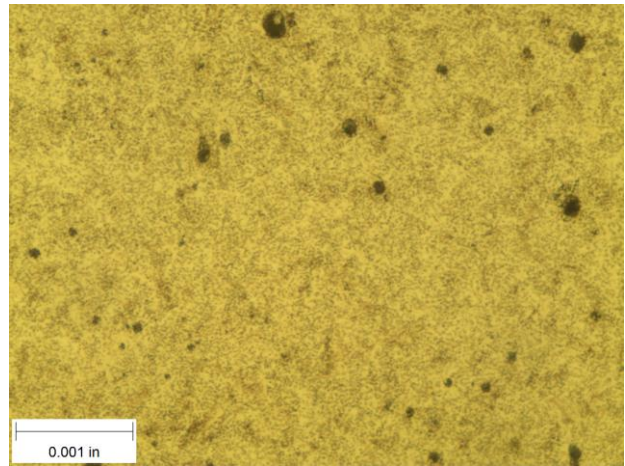
Figure 65. Photo. Transverse after 1,300 °F.
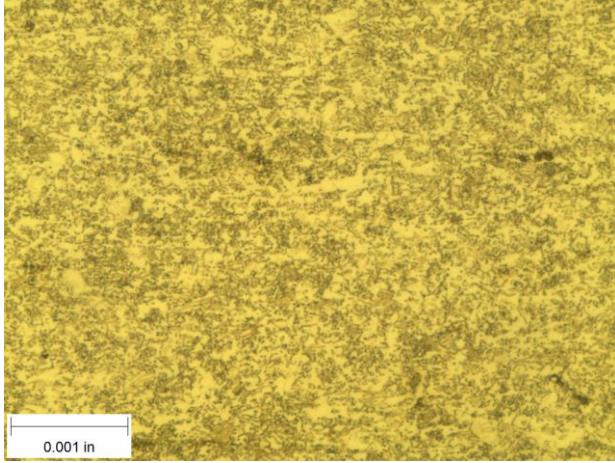
Source: FHWA.

Figure 66. Photo. Longitudinal after 1,400 °F.
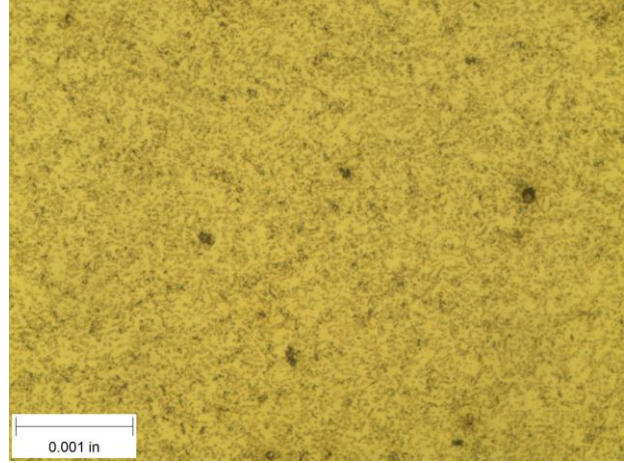
Source: FHWA.

Figure 67. Photo. Transverse after 1,400 °F.
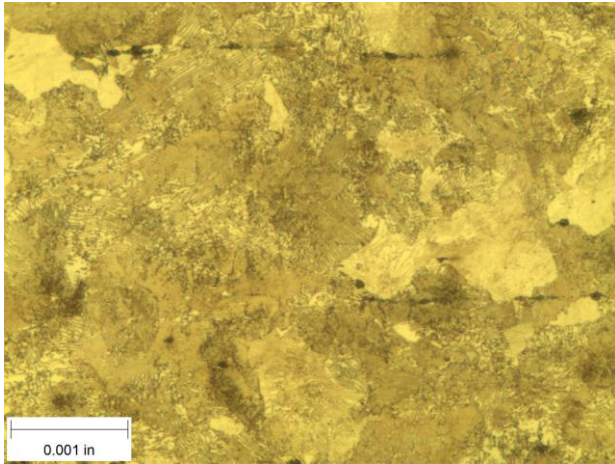
Source: FHWA.

Figure 68. Photo. Longitudinal after 1,500 °F.
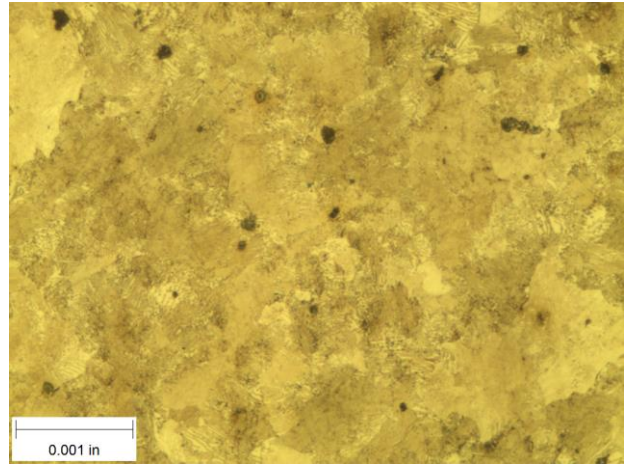
Source: FHWA.

Figure 69. Photo. Transverse after 1,500 °F.

HARDNESS

After the microstructures were evaluated, the 13 samples were repolished, and Vickers microhardness tests were performed on the transverse sections. The hardness testing conformed to ASTM E384 and used a 500-g force.[1][(6)] Figure 70 shows the pattern of 63 hardness measurements that were made on each cross section. For each wire, a local origin was established at the left edge from which the nine measurements were referenced as shown in the

---

[1]ASTM E384 is only written in metric, although 500-g force is equal to 1.102 lb.[(6)]

left side of figure 70. Within the wire, nine measurements were taken on a grid with 0.06-inch spacing in the two orthogonal directions as shown in the right portion of figure 70.
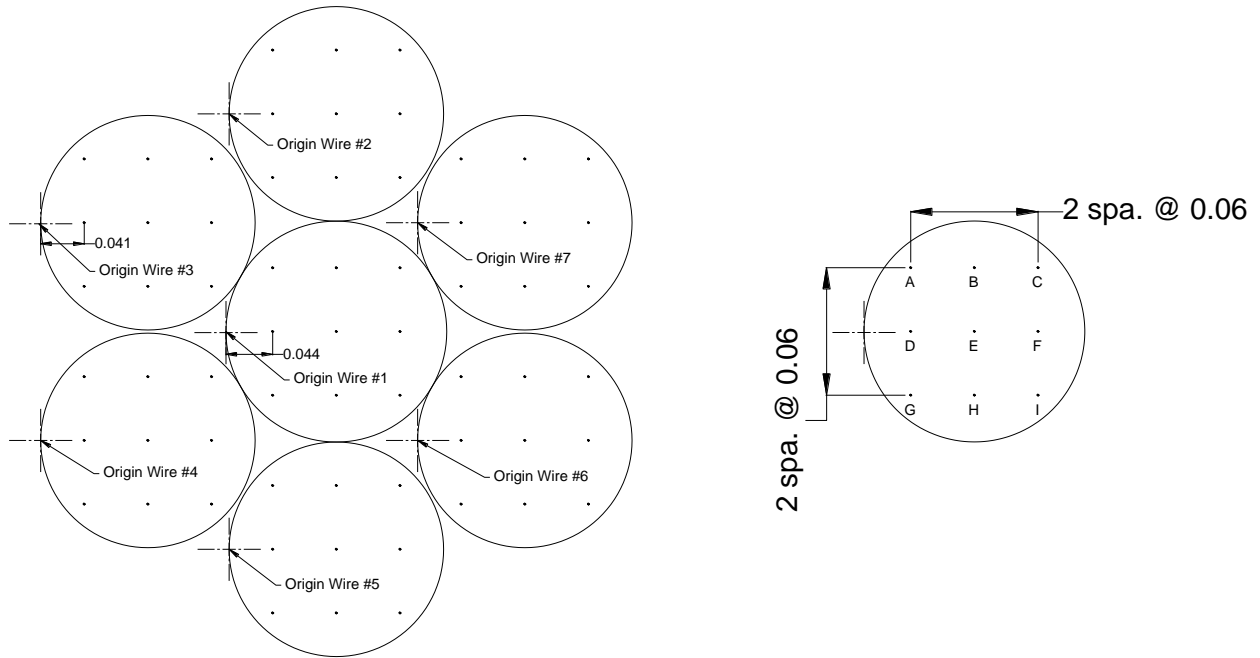
Source: FHWA.
Note: Units = inches.

Figure 70. Illustration. Measurement locations for Vickers hardness.

The microstructural evaluation showed that changes in hardness started after approximately 1,000 °F. Thus, hardness test values were recorded first on 1,500 °F specimens and hardness values measured on consecutively lower temperature specimens until they remained constant. The raw data collected from each specimen are in appendix C. No variation in hardness was observed from one wire to the next in each sample, and only the bulk statistical results are discussed. Table 12 shows a summary of the average, standard deviation, and COV for each sample. The data in table 12 are graphed and shown in figure 71 with round data points. Error bars are shown for each data point representing 2 standard deviations to each side of the data point. The average data show the hardness remains constant through 900 °F and then begins to decrease until 1,400 °F. At 1,500 °F, the hardness then increases over the value at 1,400 °F. This same behavior was also reported by Robertson et al., and their data are also shown in figure 71 but plotted against the right-hand vertical axis, as they used a different hardness scale.[7] The Robertson data were attained with a 90-min soak, though replicates were performed at 752 °F at 4- and 8-h soaks. The differences between the data are likely due to a strand lot and the hardness scale selected.

Table 12. Average hardness data for strands exposed to temperature.

Temperature (°F)	Average Hardness (HV[a])	Standard Deviation (HV[a])	COV
70	506.2	14.8	0.029
300	510.9	20.8	0.041
600	491.4	26.4	0.054
800	484.1	23.4	0.048
900	476.4	12.6	0.026
1,000	449.5	16.3	0.036
1,100	409.5	9.3	0.023
1,200	344.9	7.4	0.021
1,300	296.5	9.5	0.032
1,400	247.7	4.1	0.016
1,500	311.4	10.9	0.035

[a]HV values based on 500-g force indention load. This is equivalent to 1.102 lb.
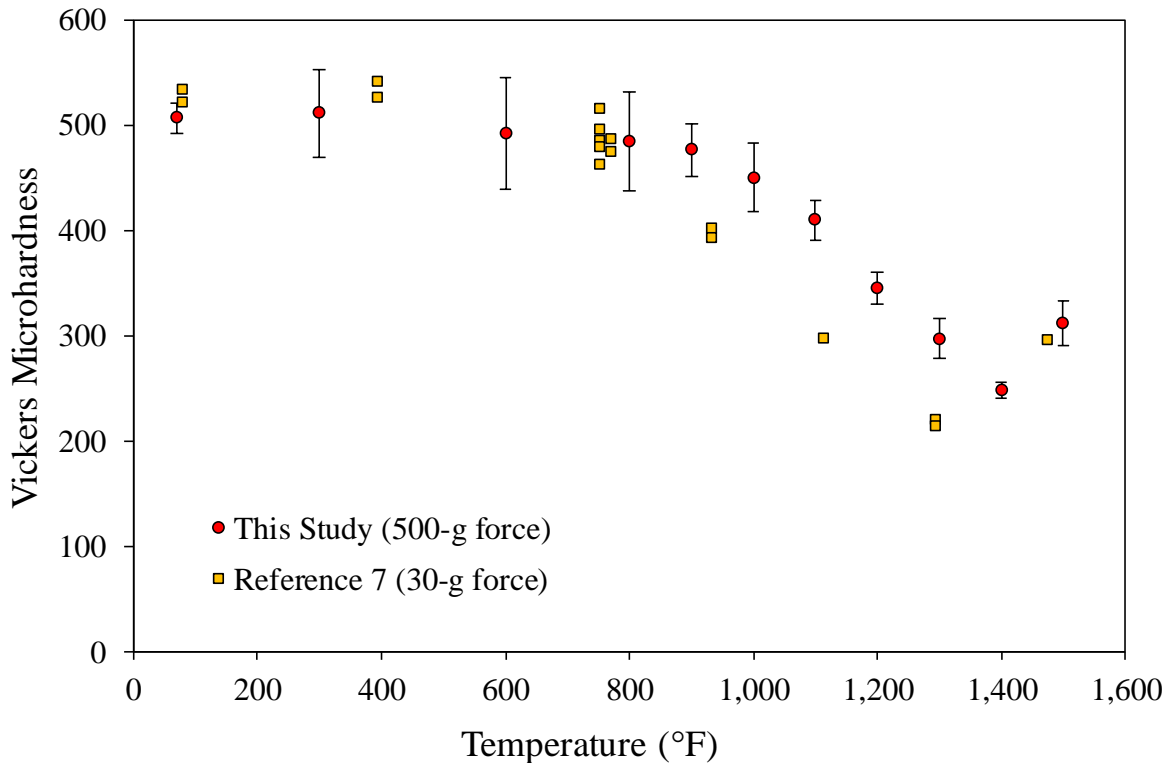
Source: FHWA.

Figure 71. Scatterplot. Variation in hardness with temperature exposure.

The other characteristic found in figure 71 is that hardness measurements are more scattered at lower temperatures but are the tightest between 1,100 and 1,400 °F. The scatter in measurements shows that hardness would only be good to assess if strands were subjected to temperatures between 1,100 and 1,400 °F, since the scatter bands in this range do not overlap with the lower temperatures. This assumption was based on an average of the 63 measurements per strand, and the graph shown in figure 72 shows the difference in scatter bands if only the center measurements in each of the seven wires are considered (shown as blue squares offset 25 °F to contrast with the red circles). This indicates that the number of measurement points could be reduced to just one within each wire, and the peak temperature between 1,100 and 1,400 °F can be uniquely identified.
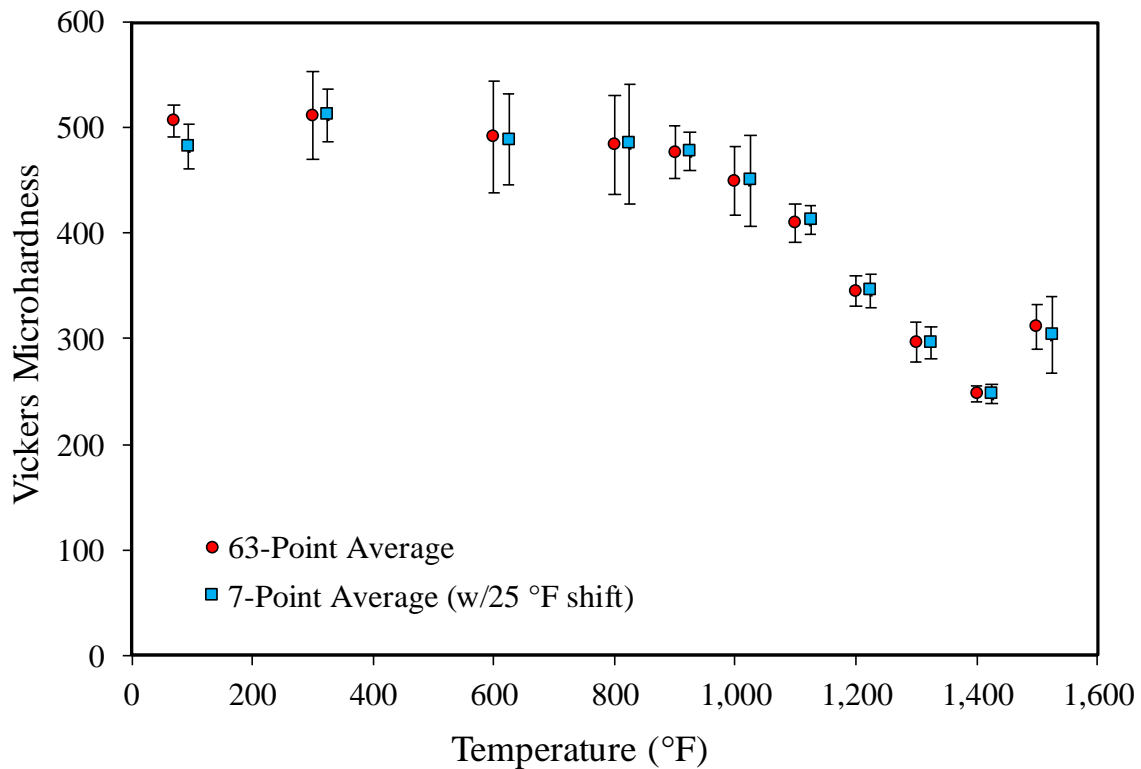
Source: FHWA.

Figure 72. Scatterplot. Variation in hardness with temperature and number of measurement points.

CHEMICAL ANALYSIS

The chemical content of steel, in particular the amount of carbon, contributes to the hardenability of the steel. Two strands were randomly selected, and from each, one outer wire and the king wire were sent out for chemical analysis. The results are reported in table 13. There are no chemical requirements for ASTM A416 strands, and this is reported strictly as informational.[2]

Table 13. Chemical composition (percent by weight).

Element	Strand A36 King Wire	Strand A36 Outer Wire	Strand B28 King Wire	Strand B28 Outer Wire
C	0.794	0.747	0.760	0.762
Mn	0.900	0.834	0.888	0.827
Si	0.763	0.748	0.738	0.741
P	0.018	0.007	0.018	0.013
S	0.010	0.011	0.006	0.011
Cr	0.117	0.049	0.116	0.067
Ni	0.031	0.038	0.029	0.038
Mo	0.009	0.009	0.007	0.009
Cu	0.067	0.105	0.067	0.108
V	0.047	0.049	0.047	0.049
Al	0.001	0.001	0.001	0.001
Ti	0.003	0.002	0.002	0.002

CORRELATION TO TEMPERATURE EXPOSURE AND STRENGTH

Some thermal lance specimens had their hardness tested after the tensile test was performed. The focus was on the specimens that were likely subjected to the highest amount of heat (i.e., those shown in figure 31) with attention given to those with the lowest breaking strengths. From each select tensile test strand, an approximate 1.5-inch portion of the strand was cut centered around any fractures in the gauge or centered around visible heat damage (burned HDPE or grease). These isolated strand sections were separated into seven individual wires and mounted transversely in epoxy. The mounts were then ground and polished to a mirror finish, and Vickers microhardness values were measured on each. A picture of each mount is shown in appendix D with the raw hardness data annotated in each picture for each wire. Generally, two hardness measurements were taken along the wire centerline, and three measurements were taken near each fracture.

Using the 63-point average line in figure 72, hardness measurements were used to estimate the temperature to which the individual wires were exposed from select thermal lanced strands. Due to the shape of the correlation in figure 72, no estimate of temperature exposure was made if the hardness exceeded approximately 490 HV. For values exceeding 490 HV, the maximum temperature reached was assumed less than 600 °F. Hardness less than approximately 300 HV would indicate temperature exposure exceeded 1,300 °F, and microstructure evaluations were required to determine if 1,400 °F was reached or exceeded. Using this approach, the data were assembled to create table 14, which reports the estimated temperature for each wire in the strand and the AUTS for the specimen. The AUTS is plotted versus the peak temperature in figure 73.

Table 14. Estimated temperatures based on hardness measurements of select thermal lance strands.

Specimen	Wire 1	Wire 2	Wire 3	Wire 4	Wire 5	Wire 6	Wire 7 (King Wire)	AUTS (kips)	HDPE Melted?
B12	1,100 °F	1,125 °F	1,075 °F	1,150 °F[a]	1,175 °F[a]	1,300 °F[a,b]	1,075 °F	42.57	Yes
A34	1,050 °F	975 °F	1,000 °F	975 °F	1,475 °F[a,c]	1,500 °F[a,c]	950 °F	44.28	Yes
A1	1,100 °F	1,075 °F	1,075 °F	1,225 °F[a]	1,100 °F[a]	1,075 °F	1,075 °F	46.92	Yes
B18	[d]	[d]	700 °F	[d]	1,175 °F[a]	1,175 °F[a]	[d]	49.50	Yes
A32	900 °F	[d]	825 °F	[d]	1,150 °F[a]	1,025 °F[a]	[d]	57.08	Yes
B6	950 °F	[d]	[d]	900 °F	[d]	1,025 °F[a]	[d]	57.37	Yes
A36	1,000 °F	950 °F	850 °F	925 °F	950 °F	900 °F	[d]	62.27	Yes
B28	875 °F	[d]	850 °F	850 °F	[d]	800 °F	[d]	64.51	Yes
B23	—	1075 °F[a]	1,000 °F	[d]	700 °F	[d]	[d]	59.42	Yes
A30	1,125 °F	1,125 °F	1,175 °F[a]	1,200 °F[a]	1,100 °F	1,075 °F	1,075 °F	45.79	Yes

—No data to report.

[a]Wire was fractured.

[b]Hardness measurements were less than 300 HV and microstructure was evaluated to be more representative to that in figure 65, therefore temperature was not expected to have exceeded 1,400 °F.

[c]Hardness measurements were less than 300 HV and microstructure was evaluated to be more representative of that in in figure 68 than figure 65, so estimated temperature was based on extrapolation of data from figure 72 between 1,400 and 1,500 °F. For Wire 6, extrapolation would predict temperature higher than 1,500 °F, and due to lack of hardness data beyond this temperature, a value of 1,500 °F was assigned.

[d]Estimated temperature was less than 600 °F.
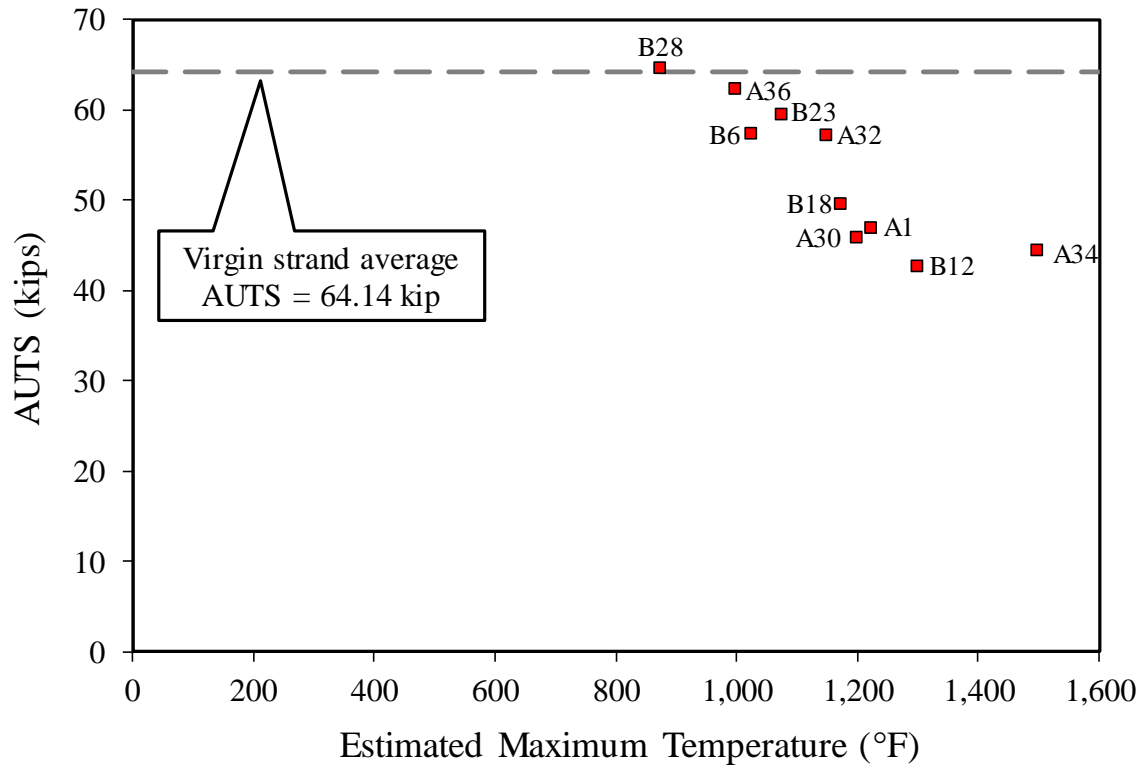
Source: FHWA.

Figure 73. Scatterplot. Correlation between estimated maximum temperature exposure and breaking load.

CONCLUSIONS AND RECOMMENDATIONS

This project was undertaken strictly to answer questions pertaining to qualification of cable-stay bundle protection measures and the acceptance criteria used. The specific question addressed was, What residual strength exists for individual strands with all wires intact (not severed) or with only one wire intact to various types of damage? This focus for the testing means the conclusions are only applicable to the qualification tests performed to enable evaluators or quality inspectors to evaluate the satisfactory acceptance of a protection system against prescribed hazards identified from an ATVA. The results were not acquired for the purpose of assessing or load rating entire cable-stay bundles that may be damaged from a hazard event on a real bridge. The following conclusions were derived from the results of this project:

- The virgin strand used to make up the qualification test bundles was in conformance with ASTM A416.[2] Since two heats of strand were used in the entire qualification test program, it is believed only one heat was characterized for virgin properties. The average results showed the virgin strand had an average yield strength of 57.53 kip, AUTS of 64.14 kip, and elongation of 3.81 percent.

- The residual mechanical properties of the thermal lance cut strands did not correlate to the proximity of strands with cut or damaged wires. That is, some strands located adjacent to others with obvious thermally cut wires were still able to achieve mechanical properties equivalent to virgin strands. The only reliable indicator of low residual strength was if the grease had been completely burned off the wires. It is recommended that, for future thermal lance cutting qualifications, strands where the grease is completely burned off all seven wires should be considered completely damaged. If strands are not greased, destructive hardness tests could be conducted on wires, and any HV readings less than 450 HV should be considered completely damaged. Low strength results were also attained when a strand had obvious gouges from the thermal lance or even fused slag. Therefore, it is recommended that any wires with thermal gouges or fused slag also be considered completely damaged.

- The residual strength of blast-tested strands had a small reduction in strength. Only strands with FBC and IBC conditions were found to have a statistically significant reduction in strength to virgin strands. This reduction in strength was approximately 2 percent for FBC strands and 1 percent for IBC strands. The reduction is attributed broadly to additional cold work imposed on the strand from the blast event through bending, untwisting, and impacts. However, no strong correlation could be identified between the amount of lateral deformation or maximum strand diameter.

- The prior conclusion was based on testing strands where all seven wires were intact. However, there was a small population of strands where between one and six wires were cut during the blast event. Wires removed from strands with six wires cut showed an average reduction in wire strength of 7 percent.

- Elongation of damaged strands can be significantly degraded while still being able to achieve maximum load requirements per ASTM A416.[2] Elongation is currently not

considered in cable-stay qualification testing. However, while specifically noted at the beginning of this section that these testing results are not applicable to assess or load rate in-service cable stays that have been damaged, it is inevitable that someone may attempt to apply the results for such a purpose. Therefore, the reduction in elongation must be highlighted, with particular focus assigned to damage states like blast impact gouges, birdcaging, and bending that has introduced additional cold-work.

RECOMMENDATIONS

Future blast qualification testing of cable bundles should abandon careful inspection of individual strands for curvature, birdcaging, and impacts. Rather, it is recommended that damage from all these forms of deformation be lumped together into an overall reduction factor applied to all surviving wires and that acceptance inspection only require counting the number of surviving wires. A reduction factor of 0.95 is recommended to be multiplied against the number of wires surviving the test to define the number of wires then compared to the acceptance criteria. This overall reduction factor accounts for the small reduction in the strength of FBC and IBC strands and the larger reduction in the strength of strands with six wires cut.

The PTI DC-45 committee should consider adding in qualification criteria for security threats to their DC45.1 specification to help unify this type of testing across the country.[5] Right now, their acceptance testing only considers corrosion resistance, anchorage fatigue, and fire resistance. As far as this work is concerned, only blast and thermal-cutting events can be addressed, and recommendations can be made only for acceptance criteria to qualify hardening systems for cable-stay bundles. The conclusions within this report regarding a mean blast bundle reduction factor and hardness limits for thermal threats are only considered starting points for deliberation.

FUTURE WORK

Working toward a national standard for qualification of hardening systems for cable-stay bundles, the following two topic areas are identified as deserving of future work:

- The acceptance criterion used for the particular bridge project that provided the mockup bundles reported herein used a 75-percent survival of wires. More work should be performed to assess if 75 percent is a good number to represent the balance between bridge safety and threat deterrence.

- This work highlighted that elongation of strands and wires can be greatly reduced as part of blast and thermal effects. Elongation is currently not considered in qualification, but additional work should be performed to see if there is a basis for including it and if the 92-percent AUTS requirement used in this report works as an appropriate surrogate.

APPENDIX A. DAMAGE OF THERMAL CUT BUNDLE

Table 15 presents raw tabular data of cut and damaged strands for the two thermal lance cuts.

Table 15. Deformation data of strands from bundle D.

Strand	Cut A Number of Wires Cut	Cut A Number of Wires Damaged	Cut B Number of Wires Cut	Cut B Number of Wires Damaged
1	0	0	7	—
2	7	—	6	0
3	5	1	7	—
4	2	2	7	—
5	2	1	7	—
6	6	1	0	0
7	7	—	4	0
8	7	—	7	—
9	7	—	7	—
10	7	—	7	—
11	7	—	7	—
12	7	—	0	0
13	7	—	1	0
14	7	—	3	3
15	7	—	7	—
16	7	—	7	—
17	7	—	5	0
18	7	—	0	0
19	6	0	0	0
20	7	—	3	0
21	7	—	6	0
22	7	—	2	0
23	7	—	0	0
24	7	—	0	0
25	7	—	0	0
26	7	—	5	0
27	7	—	2	1
28	7	—	0	0

Strand	Cut A Number of Wires Cut	Cut A Number of Wires Damaged	Cut B Number of Wires Cut	Cut B Number of Wires Damaged
29	7	—	0	0
30	0	0	0	0
31	2	0	0	0
32	0	0	0	0
33	4	0	0	0
34	0	0	0	0
35	0	1	0	0
36	0	0	0	0
37	0	0	0	0
38	0	0	0	0
39	0	0	0	0
40	0	0	0	0
41	0	0	0	0
42	0	0	0	0
43	0	0	0	0

—Not applicable. Strands with all seven wires cut did not require assessment of localize damage to wires.

APPENDIX B. DAMAGE OF BLAST BUNDLES

Table 16 through table 19 present raw tabular data of strand deformation for bundles D, E, F, and G, respectively. The data include lateral deformation, vertical deformation, strand diameter, and damage categorization.

Table 16. Deformation data of strands from bundle D.

Strand	Number of Wires Cut	Damage Category	Lateral Deformation (inches)	Vertical Deformation (inches)	Centerline Diameter (inches)	Maximum Diameter (inches)
1	7	—	—	—	—	—
2	6	—	—	—	—	—
3	6	—	—	—	—	—
4	6	—	—	—	—	—
5	6	—	—	—	—	—
6	6	—	—	—	—	—
7	5	—	—	—	—	—
8	5	—	—	—	—	—
9	5	—	—	—	—	—
10	2	—	—	—	—	—
11	0	I	5/8	3/8	40/64	40/64
12	0	I	3/8	0	40/64	40/64
13	0	I	1	1/2	40/64	40/64
14	0	I	7/8	0	40/64	40/64
15	0	I	1/8	3/8	40/64	40/64
16	0	I	15/16	3/16	40/64	40/64
17	0	IBC	15/16	1-1/8	41/64	41/64
18	0	I	1/4	7/8	40/64	40/64
19	0	IBC	1	1/4	41/64	41/64
20	0	I	1-9/16	0	40/64	40/64
21	0	IBC	1-1/8	3/8	40/64	40/64
22	0	IBC	1	1/2	41/64	41/64
23	0	I	5/16	9/16	40/64	40/64
24	0	I	1-1/8	1/2	40/64	40/64
25	0	IBC	11/16	7/16	41/64	41/64
26	0	FBC	1-1/2	0	42/64	42/64
27	0	IBC	9/16	1/8	40/64	41/64

Strand	Number of Wires Cut	Damage Category	Lateral Deformation (inches)	Vertical Deformation (inches)	Centerline Diameter (inches)	Maximum Diameter (inches)
28	0	I	11/16	1-1/8	40/64	40/64
29	0	IBC	3/4	7/16	40/64	41/64
30	0	I	1-1/16	0	40/64	40/64
31	0	IBC	1-1/16	0	40/64	41/64
32	0	I	1-1/2	1-5/8	41/64	41/64
33	0	FBC	2-9/16	0	40/64	43/64
34	0	IBC	1-5/16	0	41/64	41/64
35	0	FBC	1-3/16	1-1/8	42/64	43/64
36	0	IBC	1-9/16	1-3/16	40/64	41/64
37	0	IBC	1-5/16	3/4	41/64	42/64
38	0	I	11/16	1/4	40/64	40/64
39	0	FBC	1-3/8	1-9/16	40/64	44/64
40	0	FBC	1-11/16	3	43/64	44/64
41	0	FBC	2-1/2	1-3/8	40/64	48/64
42	0	IBC	2-9/16	3/4	40/64	43/64
43	0	FBC	1-7/8	1-3/16	41/64	42/64

—Missing data or data purposely not collected.
I = intact.

Table 17. Deformation data of strands from bundle E.

Strand	Number of Wires Cut	Damage Category	Lateral Deformation (inches)	Vertical Deformation (inches)	Centerline Diameter (inches)	Maximum Diameter (inches)
1	7	—	—	—	—	—
2	6	—	—	—	—	—
3	7	—	—	—	—	—
4	5	—	—	—	—	—
5	6	—	—	—	—	—
6	7	—	—	—	—	—
7	1	—	—	—	—	—
8	1	—	—	—	—	—
9	2	—	—	—	—	—
10	7	—	—	—	—	—
11	6	—	—	—	—	—
12	2	—	—	—	—	—
13	6	—	—	—	—	—
14	0	FBC	1-1/8	0	42/64	42/64
15	0	FBC	1-1/8	3-3/16	40/64	43/64
16	0	FBC	1-11/16	0	40/64	43/64
17	0	FBC	1-1/2	1-3/8	41/64	41/64
18	0	FBC	1-7/16	1-1/4	41/64	43/64
19	0	FBC	2-1/8	3-5/8	49/64	49/64
20	2	—	—	—	—	—
21	0	IBC	11/16	15/16	40/64	41/64
22	0	FBC	1-3/8	1/8	40/64	41/64
23	0	FBC	3/16	7/8	40/64	41/64
24	0	FBC	1-7/8	0	40/64	42/64
25	0	FBC	1-11/16	3/16	40/64	42/64
26	0	IBC	1-1/4	0	41/64	41/64
27	0	IBC	1-1/2	0	40/64	40/64
28	0	IBC	1-7/16	0	40/64	41/64
29	0	IBC	—	—	41/64	42/64
30	0	IBC	1-1/8	1	41/64	41/64
31	0	FBC	1-3/8	2-1/4	42/64	42/64

Strand	Number of Wires Cut	Damage Category	Lateral Deformation (inches)	Vertical Deformation (inches)	Centerline Diameter (inches)	Maximum Diameter (inches)
32	0	FBC	1-13/16	0	41/64	41/64
33	0	FBC	1-5/8	0	43/64	43/64
34	0	FBC	1-1/2	2-1/4	42/64	45/64
35	0	I	1-9/16	1/2	40/64	40/64
36	0	I	1-1/8	3/4	40/64	40/64
37	0	IBC	1-3/16	1	40/64	41/64
38	0	FBC	1-15/16	0	41/64	41/64
39	0	FBC	2	1-11/16	45/64	45/64
40	0	IBC	1-3/8	3/16	40/64	41/64
41	0	IBC	1-1/2	5/8	41/64	41/64
42	0	IBC	1-5/8	0	40/64	41/64
43	0	FBC	1-5/8	0	43/64	43/64

—Missing data or data purposely not collected.
I = intact.

Table 18. Deformation data of strands from bundle F.

Strand	Number of Wires Cut	Damage Category	Lateral Deformation (inches)	Vertical Deformation (inches)	Centerline Diameter (inches)	Maximum Diameter (inches)
1	0	FBC	15/16	1/8	41/64	42/64
2	0	I	3/4	1-5/8	40/64	40/64
3	0	I	0	0	40/64	40/64
4	0	I	3/4	3/8	40/64	40/64
5	6	—	—	—	—	—
6	0	I	1-1/16	0	40/64	40/64
7	0	I	1/8	0	40/64	40/64
8	0	FBC	1/16	0	41/64	42/64
9	0	FBC	1-1/4	5/8	41/64	41/64
10	0	I	7/8	15/16	40/64	40/64
11	0	IBC	1-1/16	13/16	41/64	41/64
12	0	FBC	5/8	0	40/64	41/64
13	0	IBC	7/16	5/8	41/64	41/64
14	0	FBC	1-1/4	0	50/64	52/64
15	0	FBC	1-5/8	7/8	42/64	68/64
16	0	FBC	9/16	5/16	40/64	44/64
17	0	I	9/16	3/16	40/64	40/64
18	0	IBC	7/8	1-5/8	41/64	41/64
19	0	IBC	3/4	11/16	40/64	40/64
20	0	FBC	1-3/16	1/8	44/64	49/64
21	0	I	5/8	0	40/64	40/64
22	0	I	3/4	0	41/64	41/64
23	0	I	1/4	9/16	40/64	40/64
24	0	FBC	1-5/16	2-1/2	42/64	45/64
25	0	I	7/8	3/8	40/64	40/64
26	0	FBC	5/8	1-5/8	41/64	42/64
27	0	FBC	1-3/4	1-7/8	43/64	48/64
28	1	—	—	—	—	—
29	0	I	1-1/16	0	40/64	40/64
30	0	IBC	3/8	0	40/64	41/64
31	0	I	3/16	3/8	40/64	40/64
32	0	FBC	—	—	41/64	44/64

Strand	Number of Wires Cut	Damage Category	Lateral Deformation (inches)	Vertical Deformation (inches)	Centerline Diameter (inches)	Maximum Diameter (inches)
33	0	FBC	1-7/16	1/2	40/64	47/64
34	0	I	0	0	40/64	40/64
35	0	FBC	5/16	0	45/64	44/64
36	0	IBC	7/8	0	41/64	41/64
37	0	I	1	1/4	40/64	40/64
38	0	IBC	1-1/16	7/8	40/64	43/64
39	0	I	7/8	3/8	40/64	40/64
40[a]	0	FBC	1-1/16	3/4	40/64	44/64
41	0	IBC	11/16	13/16	41/64	42/64
42	0	FBC	11/16	1/8	40/64	43/64
43	0	I	5/16	3/4	40/64	40/64
44[a]	0	I	1-1/8	11/16	41/64	41/64
45	0	IBC	11/16	9/16	41/64	42/64
46	0	I	7/16	1/8	40/64	40/64
47	0	FBC	1	5/8	43/64	44/64
48	0	FBC	1-13/16	11/16	42/64	43/64
49	0	FBC	15/16	1-1/16	41/64	43/64
50	0	I	1/2	1/8	41/64	41/64
51	0	I	1	3/4	40/64	40/64
52	0	I	1/2	7/16	40/64	40/64
53	0	I	7/8	1/2	40/64	40/64
54	0	IBC	7/16	9/16	41/64	41/64
55	0	I	15/16	0	40/64	40/64
56	0	I	0	1/2	40/64	40/64
57	0	IBC	15/16	3/16	41/64	42/64
58	0	I	15/16	1/4	40/64	40/64
59	0	I	1/4	0	41/64	41/64
60	0	I	1/8	1/2	40/64	40/64
61	0	IBC	1/2	11/16	42/64	42/64
62	0	IBC	1/16	3/16	42/64	42/64
63	0	I	1-1/8	3/16	40/64	40/64
64	0	I	1/4	3/16	40/64	40/64
65	0	FBC	1-3/16	11/16	41/64	42/64

Strand	Number of Wires Cut	Damage Category	Lateral Deformation (inches)	Vertical Deformation (inches)	Centerline Diameter (inches)	Maximum Diameter (inches)
66	0	FBC	1-5/16	7/16	42/64	42/64
67	0	I	0	5/16	40/64	40/64
68	0	IBC	0	1/4	41/64	41/64
69	0	I	7/16	3/4	40/64	40/64
70	0	IBC	1-1/4	0	40/64	41/64
71	0	FBC	1-1/16	5/8	42/64	42/64
72	0	FBC	1-1/8	1-5/8	41/64	43/64
73	0	I	7/8	5/8	41/64	41/64
74	0	IBC	7/16	1/4	41/64	41/64
75	0	IBC	3/8	1/2	41/64	41/64
76	0	IBC	5/8	0	42/64	41/64
77	0	IBC	0	0	41/64	40/64
78	0	FBC	13/16	7/16	41/64	44/64
79	0	—	1-5/16	0	—	42/64
80	0	FBC	7/8	0	41/64	44/64
81	0	IBC	13/16	1/2	41/64	41/64
82	0	I	3/4	3/8	40/64	40/64
83	0	IBC	9/16	1/2	42/64	42/64
84	0	I	1/16	1/16	40/64	40/64
85	0	I	0	1/2	40/64	40/64
86	0	IBC	7/16	5/8	41/64	41/64
87	0	FBC	1/4	0	41/64	48/64
88	0	I	1	5/16	40/64	40/64
89	0	FBC	3/8	3/4	42/64	41/64
90	0	I	3/16	9/16	40/64	40/64
91	0	I	0	0	40/64	40/64
92	0	IBC	13/16	0	41/64	41/64
93	0	I	3/4	0	40/64	40/64
94	0	I	7/8	0	40/64	40/64
95	1	—	—	—	—	—
96	0	IBC	1/2	9/16	41/64	41/64
97	0	I	7/8	1/2	40/64	40/64
98	0	I	3/16	7/16	40/64	40/64

Strand	Number of Wires Cut	Damage Category	Lateral Deformation (inches)	Vertical Deformation (inches)	Centerline Diameter (inches)	Maximum Diameter (inches)
99	0	FBC	5/8	2-1/4	42/64	47/64
100	0	I	11/16	0	41/64	41/64
101	2	—	—	—	—	—
102	1	—	—	—	—	—
103	0	FBC	1–5/8	13/16	48/64	49/64
104	0	IBC	1-1/16	0	41/64	41/64
105	0	FBC	11/16	7/8	40/64	43/64
106	1	—	—	—	—	—
107	6	—	—	—	—	—
108	7	—	—	—	—	—
109	7	—	—	—	—	—

—Missing data or data purposely not collected.
I = intact.
[a]Data are suspected to be mixed up between these two strands.

Table 19. Deformation data of strands from bundle G.

Strand	Number of Wires Cut	Damage Category	Lateral Deformation (inches)	Vertical Deformation (inches)	Centerline Diameter (inches)	Maximum Diameter (inches)
1	0	IBC	7/16	0	40/64	41/64
2	0	FBC	2-1/16	1-1/16	64/64	65/64
3	0	FBC	1/2	1-9/16	41/64	41/64
4	0	FBC	1-1/16	3/8	44/64	45/64
5	0	IBC	5/8	3/4	40/64	41/64
6	0	I	3/8	0	40/64	40/64
7	0	FBC	15/16	11/16	42/64	41/64
8	0	I	5/8	1/4	40/64	40/64
9	0	IBC	1	1/4	42/64	42/64
10	0	I	11/16	3/8	40/64	40/64
11	0	I	1-3/16	9/16	40/64	40/64
12	0	I	3/8	1/4	40/64	40/64
13	0	I	9/16	0	40/64	40/64
14	0	I	5/16	0	40/64	40/64
15	0	I	3/16	1/4	40/64	40/64
16	0	IBC	11/16	0	40/64	41/64
17	0	I	3/16	3/16	40/64	40/64
18	0	I	1/2	0	40/64	40/64
19	0	FBC	1-7/8	0	45/64	47/64
20	0	FBC	1-1/16	0	41/64	42/64
21	0	FBC	1-3/4	2-1/8	44/64	45/64
22	0	I	11/16	0	40/64	40/64
23	0	I	7/16	0	40/64	40/64
24	0	IBC	13/16	0	40/64	41/64
25	0	I	1/4	1/4	40/64	40/64
26	0	I	1/4	9/16	40/64	40/64
27	0	IBC	3/8	11/16	40/64	41/64
28	0	I	1-1/16	1/4	40/64	40/64
29	0	FBC	15/16	5/16	40/64	43/64
30	0	IBC	15/16	5/8	40/64	41/64
31	0	IBC	7/16	11/16	41/64	41/64

Strand	Number of Wires Cut	Damage Category	Lateral Deformation (inches)	Vertical Deformation (inches)	Centerline Diameter (inches)	Maximum Diameter (inches)
32	0	I	1/4	0	40/64	40/64
33	0	I	1/8	0	40/64	40/64
34	0	I	5/16	0	40/64	40/64
35	0	I	1/4	5/8	40/64	40/64
36	0	IBC	11/16	1/8	40/64	41/64
37	2	—	—	—	—	—
38	0	FBC	1-5/16	1-7/8	44/64	43/64
39	1	—	—	—	—	—
40	0	I	0	0	40/64	40/64
41	3	—	—	—	—	—
42	0	I	9/16	1/4	40/64	40/64
43	0	I	5/16	0	40/64	40/64
44	0	FBC	3/4	1-1/8	40/64	46/64
45	0	I	3/16	1/8	40/64	40/64
46	0	I	3/16	3/16	40/64	40/64
47	0	I	7/8	0	40/64	40/64
48	0	IBC	5/8	1/8	40/64	41/64
49	1	—	—	—	—	—
50	0	I	5/8	1/4	40/64	40/64
51	0	FBC	1-1/4	2-1/2	40/64	44/64
52	0	FBC	2-1/2	2-1/2	52/64	55/64
53	0	FBC	13/16	0	40/64	41/64
54	5	—	—	—	—	—
55	0	IBC	5/16	7/8	41/64	41/64
56	0	I	1/4	3/16	40/64	40/64
57	0	I	1-1/4	0	40/64	40/64
58	1	—	—	—	—	—
59	0	FBC	1-1/16	3/4	42/64	44/64
60	1	—	—	—	—	—
61	0	IBC	1-3/8	0	42/64	43/64
62	0	I	1-1/4	1/2	40/64	40/64
63	0	I	1/4	3/16	40/64	40/64
64	0	I	1/4	0	40/64	40/64

Strand	Number of Wires Cut	Damage Category	Lateral Deformation (inches)	Vertical Deformation (inches)	Centerline Diameter (inches)	Maximum Diameter (inches)
65	0	I	7/16	1/2	40/64	40/64
66	0	FBC	1-3/8	0	40/64	44/64
67	0	I	7/16	5/8	40/64	40/64
68	0	IBC	7/8	1/8	40/64	41/64
69	0	I	3/16	3/8	40/64	40/64
70[a]	—	—	—	—	—	—
71[a]	—	—	—	—	—	—
72	0	IBC	1/2	0	40/64	41/64
73	0	I	7/16	1/2	40/64	40/64
74	0	FBC	1-9/16	3-1/4	40/64	43/64
75	0	IBC	3/4	0	40/64	41/64
76	0	IBC	1-5/8	0	40/64	41/64
77	0	FBC	1-3/8	2-1/8	40/64	54/64
78	0	I	1-3/16	11/16	40/64	40/64
79	0	I	1/2	3/8	40/64	40/64
80	0	IBC	1-1/4	1/8	40/64	43/64
81	0	I	13/16	1/4	40/64	40/64
82	0	I	3/8	0	40/64	40/64
83	0	I	13/16	3/16	40/64	40/64
84	6	—	—	—	—	—
85	0	FBC	1-1/2	11/16	43/64	44/64
86	0	I	1-5/16	3/16	40/64	40/64
87	0	FBC	1-5/8	5/16	42/64	48/64
88	7	—	—	—	—	—
89	7	—	—	—	—	—
90	7	—	—	—	—	—
91	0	FBC	1-3/16	1	41/64	42/64
92	0	IBC	3/8	0	41/64	41/64
93	0	I	1-1/8	3/4	40/64	40/64
94	0	I	7/8	0	40/64	40/64
95	0	FBC	1-9/16	1	42/64	45/64
96	0	IBC	1-1/4	0	41/64	42/64
97	0	I	3/16	1/2	40/64	40/64

Strand	Number of Wires Cut	Damage Category	Lateral Deformation (inches)	Vertical Deformation (inches)	Centerline Diameter (inches)	Maximum Diameter (inches)
98	0	I	3/4	9/16	40/64	40/64
99	0	FBC	1/4	3-1/16	42/64	44/64
100	0	FBC	15/16	1	40/64	45/64
101	0	I	15/16	1/4	40/64	40/64
102	0	I	1/4	3/16	40/64	40/64
103	0	IBC	1/4	0	40/64	41/64
104	0	IBC	5/8	1/8	40/64	40/64
105	0	I	1/4	0	40/64	40/64
106	0	FBC	1-1/4	1-7/8	40/64	43/64
107	5	—	—	—	—	—
108	0	I	3/16	3/8	40/64	40/64
109	0	FBC	15/16	5/16	40/64	44/64

—Missing data or data purposely not collected.
I = intact.
[a]These strands could not be located.

APPENDIX C. HARDNESS MEASUREMENT RAW DATA

Table 20 through table 30 report raw HV measurements on strand segments subjected to different temperatures for 30 min. Each column in the table reports nine individual measurements made within each wire as depicted in figure 70.

Table 20. HV measurements for 1,500 °F.

Wire	A	B	C	D	E	F	G	H	I
1	311.6	305.3	298.7	305.9	276.7	309.1	296.2	304.2	305.7
2	326.4	318.0	308.2	301.3	326.6	301.6	311.3	306.4	296.1
3	314.8	332.9	306.3	316.9	302.3	306.8	309.4	301.0	304.7
4	325.5	314.9	311.8	329.1	290.4	314.4	320.9	314.0	307.5
5	312.4	312.1	309.4	324.7	288.6	309.2	327.8	323.4	319.0
6	322.1	302.1	303.4	322.4	327.8	322.8	294.0	323.7	314.8
7	305.8	310.8	325.3	312.4	313.0	316.2	317.8	305.2	319.5

Table 21. HV measurements for 1,400 °F.

Wire	A	B	C	D	E	F	G	H	I
1	253.5	251	254.8	249.9	251.2	247.9	244.3	253.2	249.5
2	Epoxy	Epoxy	Epoxy	Epoxy	Epoxy	Epoxy	Epoxy	Epoxy	Epoxy
3	253	247.4	251.4	251.5	236.4	251.1	245.3	243.4	245.9
4	248.5	253.1	248.6	254.2	248.1	249.6	251.5	243.6	246
5	246.2	242.3	239.9	242.3	244.5	248.6	244.6	244.8	249.9
6	242.5	244.1	245.2	245.9	248.2	238.5	249.7	248.6	247
7	251.1	248.5	247.5	242.4	250.1	251.7	250.6	244.3	252.3

Note: Epoxy indicates the wire was not exposed through polishing and remained covered with mounting epoxy, therefore measurement could not be made.

Table 22. HV measurements for 1,300 °F.

Wire	A	B	C	D	E	F	G	H	I
1	303.6	325.8	319.4	314.4	305.9	309.7	309.8	315.4	310.9
2	299.1	303.0	304.2	300.0	302.2	305.0	300.0	302.7	297.6
3	293.6	292.2	292.9	294.0	321.8	294.5	292.1	290.8	294.6
4	292.0	287.1	286.9	293.6	287.8	295.5	289.2	287.6	288.5
5	291.8	290.8	288.8	286.8	303.8	291.4	283.9	289.7	291.4
6	298.8	299.5	293.7	295.3	296.4	285.8	293.4	292.5	288.9
7	285.1	286.5	292.8	287.3	303.1	294.3	290.9	287.2	283.9

Table 23. HV measurements for 1,200 °F.

Wire	A	B	C	D	E	F	G	H	I
1	362.8	360.9	360.9	363.0	351.5	361.6	353.6	358.6	357.3
2	345.1	335.4	334.3	342.4	345.5	340.9	342.2	343.2	341.7
3	344.1	344.9	346.6	339.6	341.9	346.8	341.6	346.4	345.6
4	342.2	343.2	342.9	339.8	343.1	338.4	346.1	341.5	334.4
5	339.4	339.6	339.7	347.9	328.6	339.5	338.9	340.2	346.0
6	350.1	339.7	339.0	343.3	332.5	339.1	344.5	338.0	339.4
7	350.5	346.5	344.8	343.5	353.8	352.7	348.1	347.6	345.9

Table 24. HV measurements for 1,100 °F.

Wire	A	B	C	D	E	F	G	H	I
1	424.9	423.9	425.6	423.4	406.3	424.2	419.8	418.8	423.8
2	407.9	408.7	417.8	409.5	420.5	399.8	402.3	402.3	416.3
3	422.4	390.4	402.5	407.4	411.4	412.5	402.6	403.1	414.1
4	398.9	411.1	408.9	409.5	376.0	409.9	420.0	406.2	406.8
5	403.8	406.4	409.0	412.9	384.1	410.5	399.8	403.2	410.1
6	411.8	406.4	403.6	410.2	414.3	414.3	409.4	396.3	414.4
7	411.6	409.8	408.5	411.2	397.6	414.8	402.6	415.9	414.6

Table 25. HV measurements for 1,000 °F.

Wire	A	B	C	D	E	F	G	H	I
1	478.3	416.2	444.5	438.4	438.5	474.5	445.3	465.6	464.2
2	450.2	452.9	454.0	449.5	451.1	443.1	448.1	457.7	444.3
3	451.7	424.5	472.9	431.5	445.0	447.5	453.3	509.4	437.6
4	451.9	468.9	446.0	443.7	445.9	408.7	449.1	450.6	445.2
5	445.8	454.5	444.6	415.5	441.4	456.8	447.7	442.8	448.9
6	450.1	439.2	448.5	443.1	444.1	440.6	442.3	445.4	454.0
7	435.5	463.5	449.7	455.0	501.1	478.3	445.3	441.0	444.2

Table 26. HV measurements for 900 °F.

Wire	A	B	C	D	E	F	G	H	I
1	488.5	490.0	498.5	483.9	473.6	488.9	498.9	495.4	494.7
2	468.0	476.3	489.5	487.0	495.3	476.9	477.5	464.4	476.2
3	472.3	471.1	485.8	473.9	523.4	463.9	479.5	466.5	466.4
4	480.3	485.0	481.6	485.6	440.0	491.8	479.9	481.9	462.7
5	473.9	463.6	457.6	474.5	474.7	473.6	481.8	475.8	481.4
6	473.2	473.9	474.1	476.0	459.0	472.9	476.4	472.2	468.9
7	466.4	458.6	465.0	460.0	467.6	471.8	473.9	466.1	466.4

Table 27. HV measurements for 800 °F.

Wire	A	B	C	D	E	F	G	H	I
1	514.8	505.7	503.6	509.0	496.7	482.9	512.4	515.2	497.8
2	478.3	488.4	494.2	488.4	485.6	463.5	513.5	487.5	467.0
3	497.8	477.3	478.2	491.3	482.9	480.1	508.0	498.4	492.8
4	501.1	493.4	487.6	500.8	505.0	489.6	477.4	479.6	472.3
5	493.2	474.7	483.8	490.8	519.3	494.4	494.2	483.5	496.8
6	489.1	463.6	430.1	481.4	431.6	441.0	495.2	479.8	463.6
7	482.1	433.0	416.4	462.7	426.5	539.8	457.4	463.5	490.1

Table 28. HV measurements for 600 °F.

Wire	A	B	C	D	E	F	G	H	I
1	471.1	484.8	520.1	502.2	486.4	510.5	515.4	524.8	535.9
2	498.8	502.1	504.7	491.8	472.9	498.1	485.7	495.0	511.1
3	440.9	439.0	458.2	436.3	442.0	446.6	455.1	455.2	446.3
4	436.1	449.6	477.5	463.1	459.0	468.0	506.1	506.0	507.6
5	497.8	493.4	501.5	496.0	488.7	490.7	523.3	517.0	514.5
6	512.3	494.7	512.0	511.1	485.0	508.4	530.6	509.1	520.9
7	507.6	494.2	521.0	492.1	479.8	498.3	512.3	515.4	529.5

Table 29. HV measurements for 300 °F.

Wire	A	B	C	D	E	F	G	H	I
1	519.2	526.6	541.0	533.8	532.0	527.4	524.5	528.0	553.8
2	525.7	509.6	528.3	513.9	483.7	496.0	511.6	505.1	506.8
3	565.2	510.2	521.4	515.5	483.9	513.8	560.5	493.6	516.5
4	524.6	508.9	531.1	509.9	521.5	509.2	502.8	514.6	499.9
5	498.1	490.6	508.3	491.5	466.4	494.0	453.5	483.9	503.3
6	513.3	512.9	500.9	497.7	483.0	527.3	501.7	528.2	526.8
7	524.3	478.8	epoxy	497.5	465.5	517.3	523.0	504.9	515.7

Table 30. HV measurements for 70 °F.

Wire	A	B	C	D	E	F	G	H	I
1	521.8	524.8	538.0	523.0	481.6	513.0	522.6	501.9	517.0
2	508.3	483.9	509.6	499.6	502.6	515.2	531.1	483.4	517.7
3	508.5	510.8	507.6	512.8	486.0	508.4	532.8	486.4	501.6
4	495.2	491.6	504.0	497.8	483.7	492.7	517.7	498.0	519.0
5	512.1	503.3	494.5	507.0	469.6	515.1	508.9	503.2	512.3
6	516.4	482.8	525.5	519.3	468.9	498.6	511.4	512.6	512.2
7	507.0	497.3	522.6	502.6	483.9	530.1	508.0	503.4	512.6

APPENDIX D. HARDNESS DATA OF SELECT THERMAL LANCE SPECIMENS

Figure 74 through figure 83 show pictures of transverse mounts of wires removed from strands A1, A32, A30, A34, A36, B6, B12, B18, B23, and B28, respectively. Each figure depicts various hardness measurements that were taken and an estimate of the temperature exposure based on the correlation presented in figure 71.
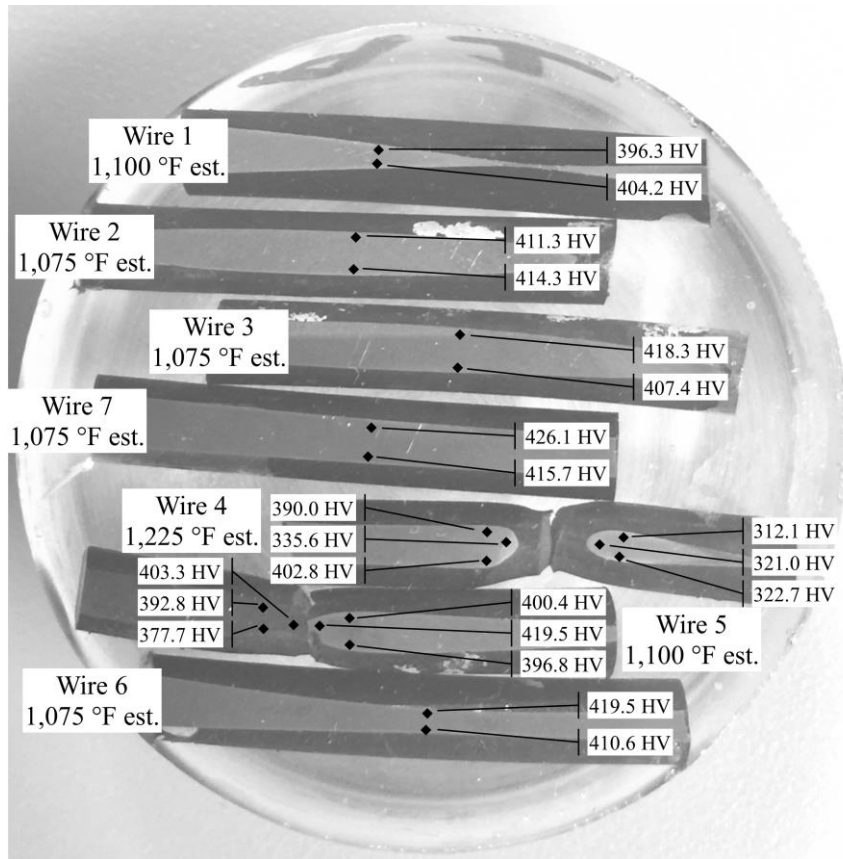
Source: FHWA.

Figure 74. Photo. Hardness results of wires of strand A1.
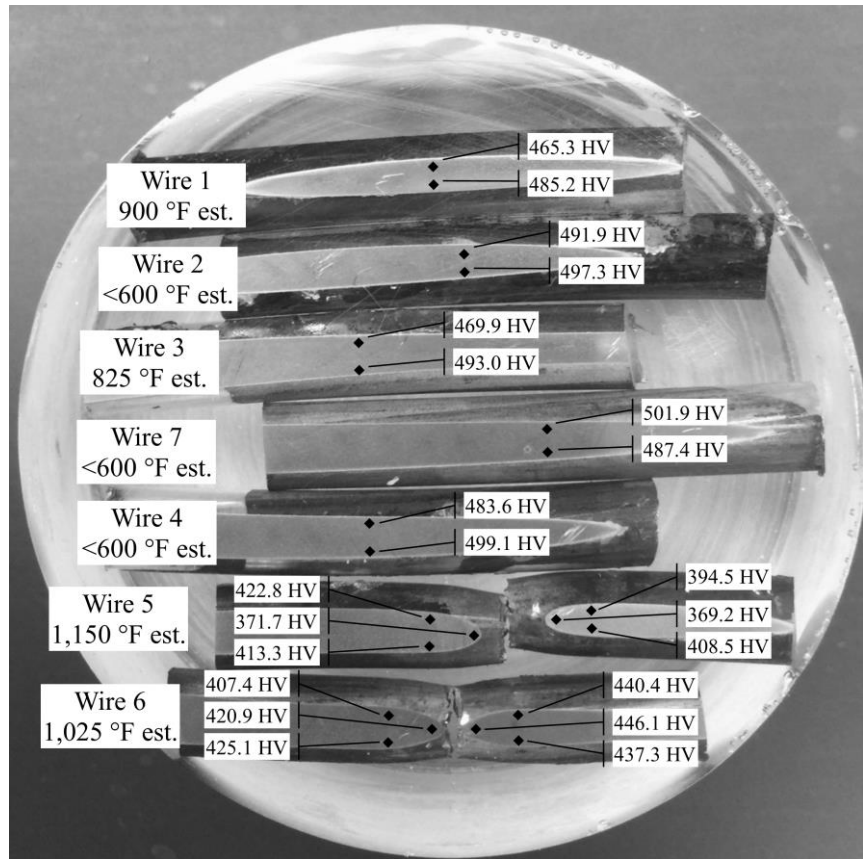
Source: FHWA.

Figure 75. Photo. Hardness results of wires of strand A32.
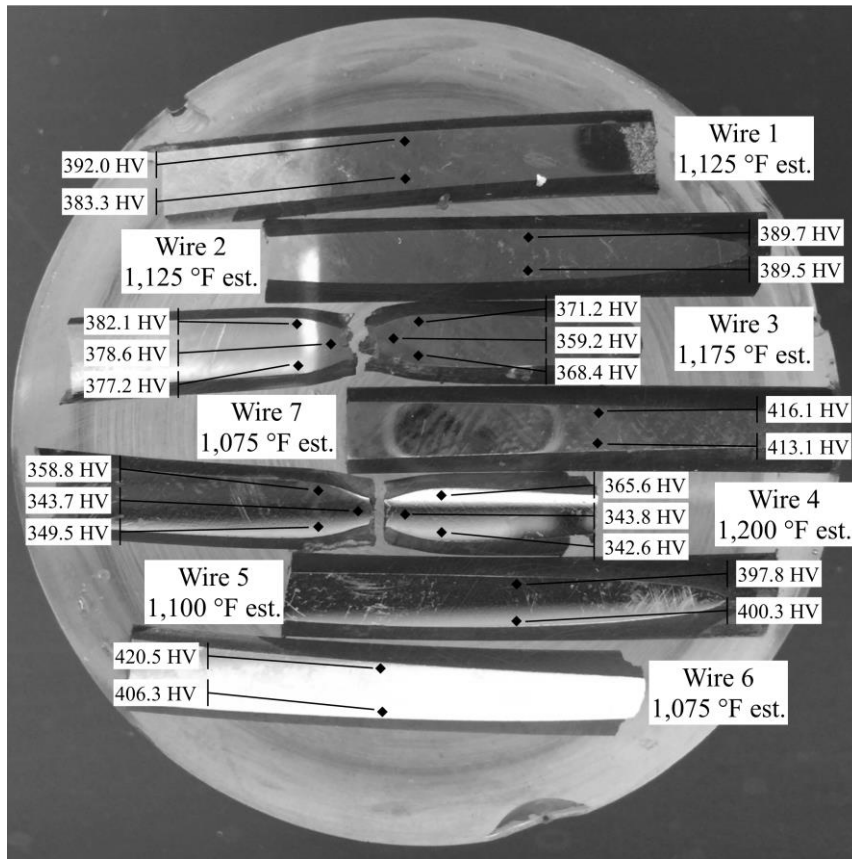
Source: FHWA.

**Figure 76. Photo. Hardness results of wires of strand A30.**
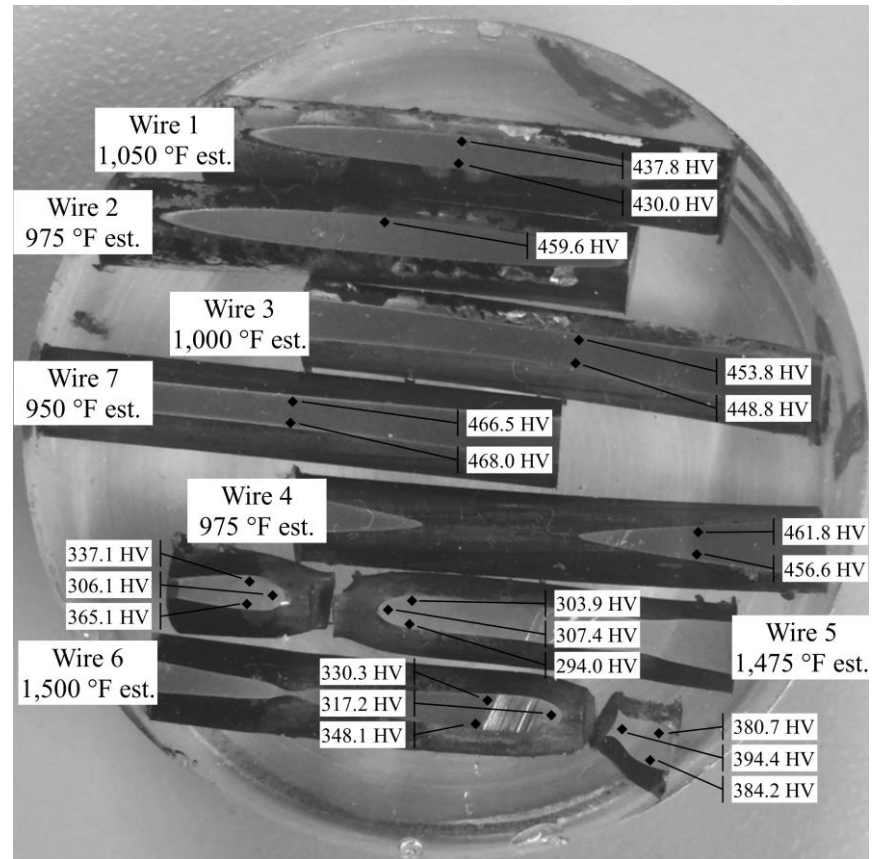
Source: FHWA.

Figure 77. Photo. Hardness results of wires of strand A34.
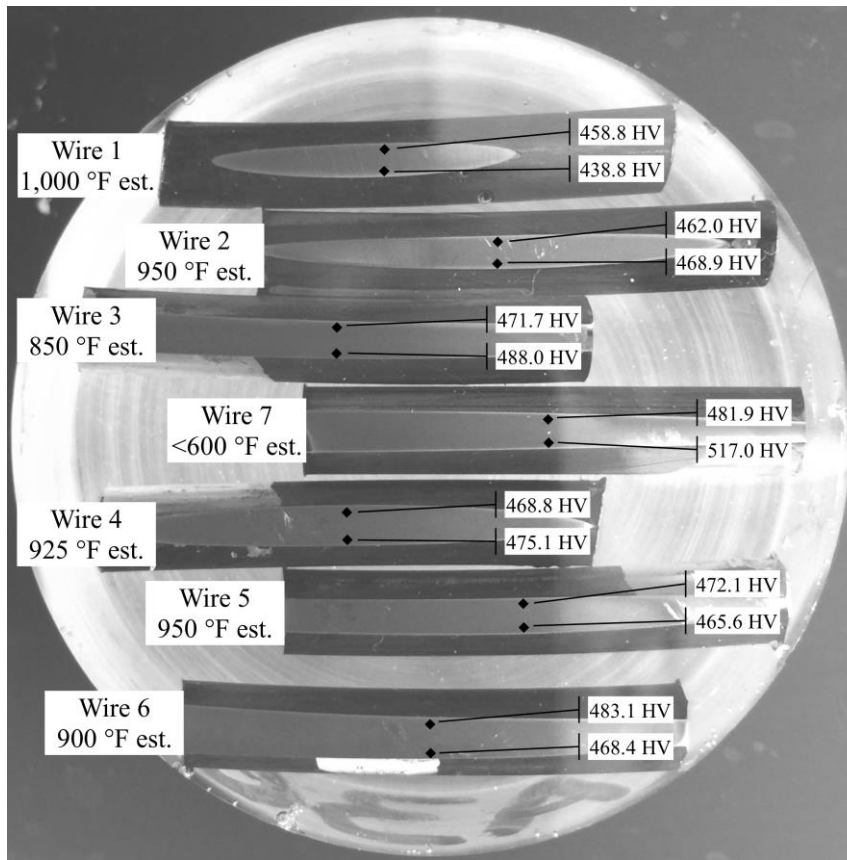
Source: FHWA.

Figure 78. Photo. Hardness results of wires of strand A36.
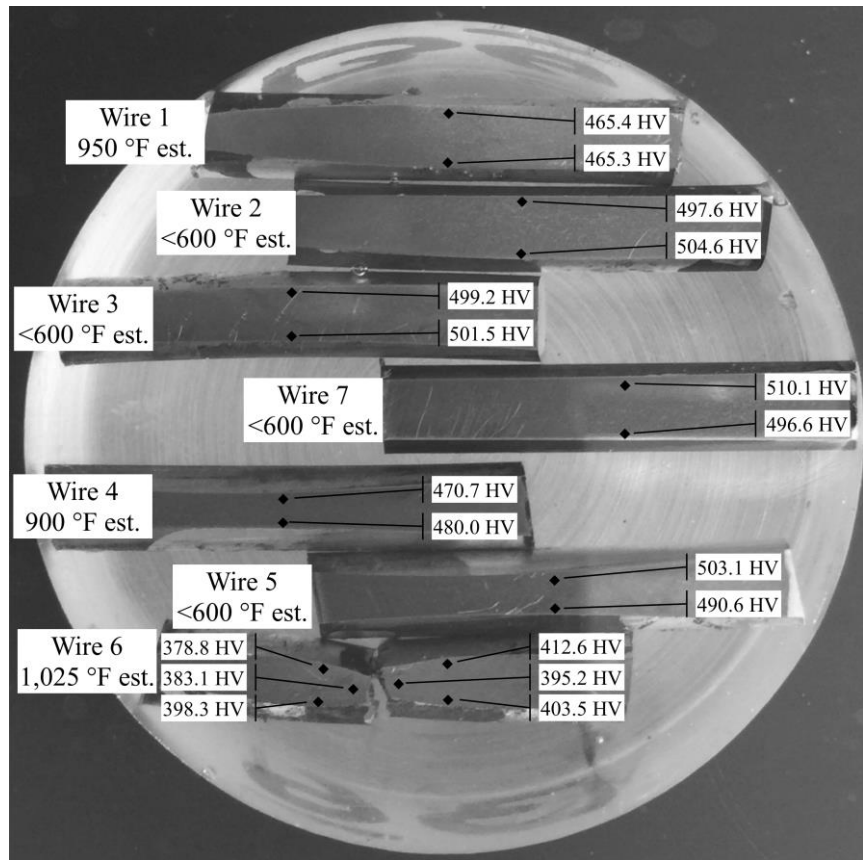
Source: FHWA.

Figure 79. Photo. Hardness results of wires of strand B6.
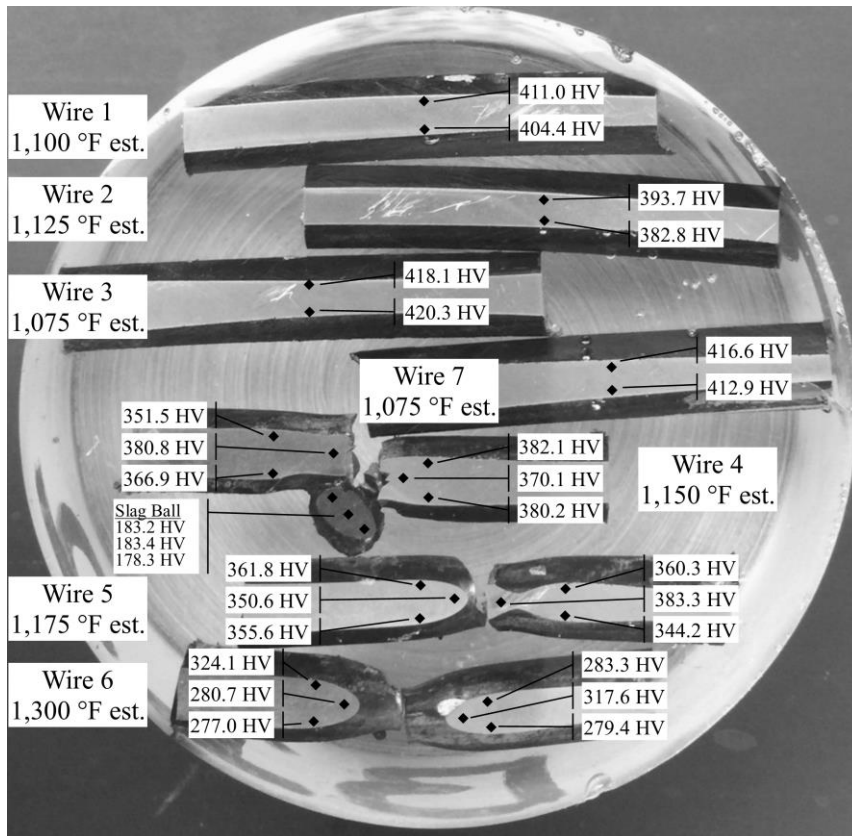
Source: FHWA.

Figure 80. Photo. Hardness results of wires of strand B12.
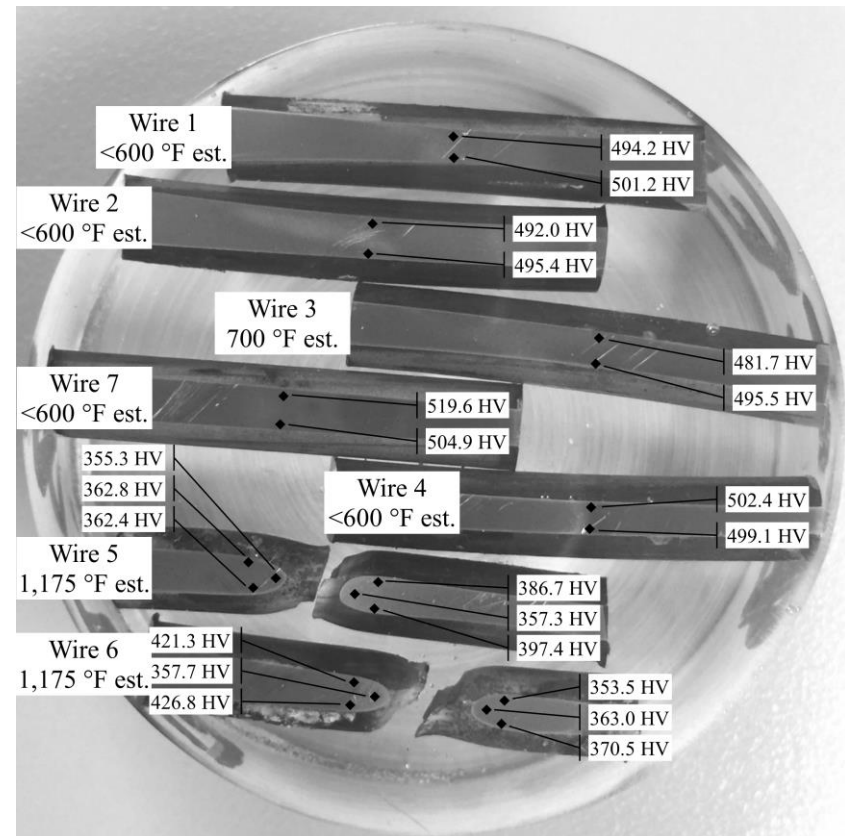
Source: FHWA.

Figure 81. Photo. Hardness results of wires of strand B18.
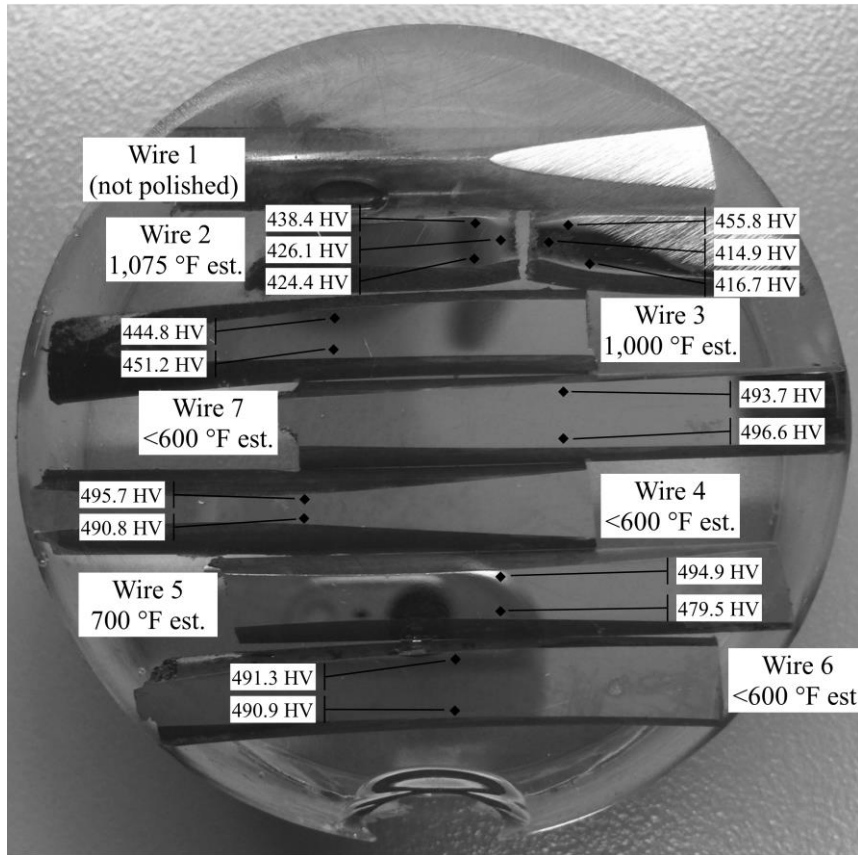
Source: FHWA.

Figure 82. Photo. Hardness results of wires of strand B23.
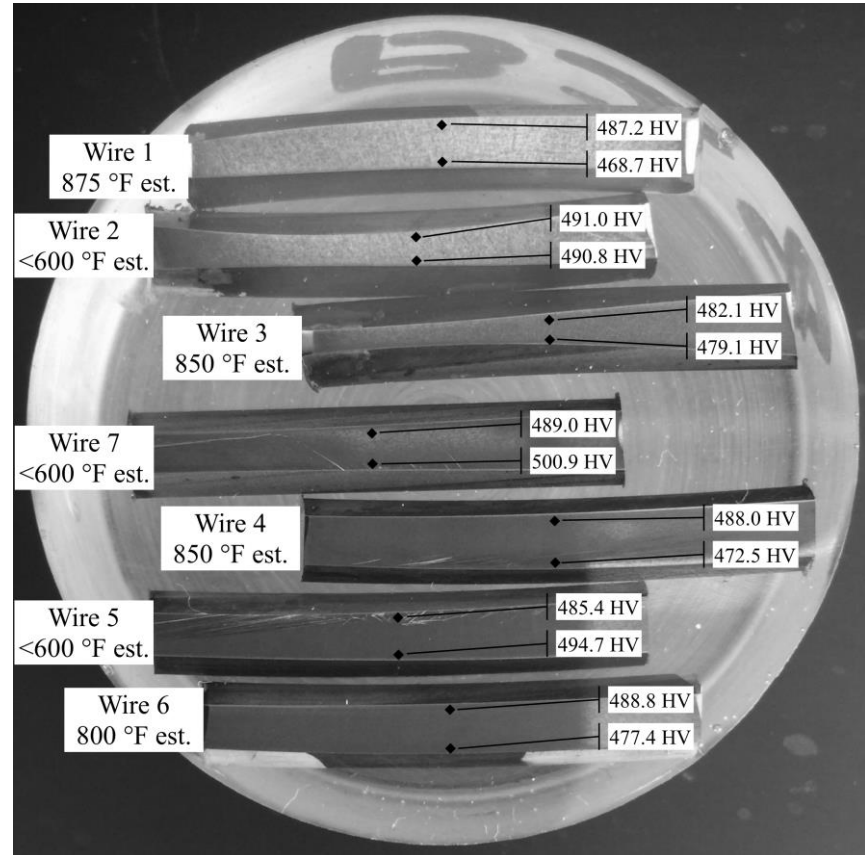
Source: FHWA.

Figure 83. Photo. Hardness results of wires of strand B28.

REFERENCES

1. FHWA. (2003). *Recommendations for Bridge and Tunnel Security,* Report No. FHWA-IF-03-036, Federal Highway Administration, Washington DC.

2. ASTM A416/A416M. (2016). "Standard Specification for Low-Relaxation, Seven-Wire Steel Strand for Prestressed Concrete." *Book of Standards Volume 01.04*. ASTM International, West Conshohocken, PA.

3. ASTM A1061/A1061M. (2016). "Standard Test Methods for Testing Multi-Wire Steel Prestressing Strand." *Book of Standards Volume 01.04*. ASTM International, West Conshohocken, PA.

4. ASTM E8/E8M. (2016). "Standard Test Methods for Tension Testing of Metallic Materials." *Book of Standards Volume 03.01*, ASTM International, West Conshohocken, PA.

5. PTI. (2012). "Recommendations for Stay Cable Design, Testing, and Installation." PTI DC45.1. Post-Tensioning Institute, Farmington Hills, MI.

6. ASTM E384. (2016). "Standard Test Method for Microindentation Hardness of Materials." *Book of Standards Volume 03.01*. ASTM International, West Conshohocken, PA.

7. Robertson, L., Dundorova, Z., Gales, J., Vega, E., Smith, H., Stratford, T., Blackford, J., and Bisby, L. (2013). *"Microstructural and Mechanical Characterization of Post-Tensioning Strands Following Elevated Temperature Exposure."* Presented at the Application of Structural Fire Engineering Conference, Prague, Czech Republic.